Experiments on the Response of Arch-Supported Membrane Shelters to Snow and Wind Loading

by

David Marc Carradine

Thesis submitted to the Faculty of the

Virginia Polytechnic Institute and State University

in partial fulfillment of the requirements for the degree of

Master of Science

in

Civil Engineering

APPROVED:

____
R. H. Plaut, Chairman

____
W. S. Easterling

____
R. K. Kapania

April, 1998

Blacksburg, Virginia

Keywords: Scale Models, Pneumatic Structures, Snow Loads, Wind Loads, Structural Collapse, Pressurized Arches

Experiments on the Response of Arch-Supported Membrane Shelters to Snow and Wind Loading

by

David Marc Carradine

R. H. Plaut, Chairman

Civil Engineering

(ABSTRACT)

For many years, inflatable structures and membrane enclosed structures have proved useful for a variety of purposes, such as athletic pavilions, exhibition spaces, coliseums, and kiosks. More recently, structures that combine highly pressurized inflatable arch members with light fabric membrane coverings have been considered for use as a variation of such structural systems. The United States Army has begun to investigate pressurized arch-supported membrane shelters that would be large, lightweight, and easily erected in a short amount of time. These shelters are proposed for a variety of purposes, including aircraft hangars, vehicle maintenance shelters, and medical aid stations.

The specific contribution of this study was the creation and testing of scale models to obtain a better understanding of how these structures behave under wind and snow loading conditions. Three models were constructed, one at a scale of 1:100 and two at a scale of 1:50. The 1:100 scale model represented a proposed prototypical structure 200 ft

long, 75 ft wide, and 50 ft tall, with multiple arches. Of the 1:50 scale models, one model represented a structure with the same dimensions as the 1:100 scale model and the other represented a single arch from one of the proposed prototypical structures. Both of the full structural models were wind and snow load tested. The single arch model was tested under full and partial snow loading. Data from the testing were collected, tabulated, and evaluated. The experimental results are discussed, conclusions are drawn, and recommendations for further research are presented.

Acknowledgments

I would like to thank Dr. Easterling, Dr. Kapania and Dr. Plaut for serving as my committee members and for participating with this research project. I would especially like to thank Dr. Plaut for giving me the opportunity to perform this research and for his enthusiasm regarding the project.

I would like to thank Professor Robert Schubert and Bill Sevebeck from the College of Architecture for providing access to and assistance with the low-speed wind tunnel. I would like to thank Dr. Roger Simpson from the Aerospace and Ocean Engineering Department for the information regarding wind tunnel testing and for the use of the open-throat return subsonic wind tunnel. I would also like to thank Dr. Thomas Brandon of the Geotechnical Engineering Program Area for providing access to the laboratory in which I conducted my snow load testing.

I am extremely grateful to the United States Army Research Office for the financial support provided for this research under Grant No. DAAH04-95-1-0175.

I would especially like to thank my wife, Ann. Her editing and sewing skills were greatly appreciated, and her constant encouragement helped me keep everything in perspective and enjoy this project. I can’t thank her enough for all of her help and support.

Table of Contents

List of Figures ix

List of Tables.. xii

Chapter 1. Introduction... 1

Chapter 2. Literature Review 3

2.1 Introduction 3

2.2 Air-Supported Structures.. 3

2.2.1 Experimental Methods 4

2.2.2 Analytical Methods 7

2.3 Fabric Membrane Structures 11

2.3.1 Experimental Methods 11

2.3.2 Analytical Methods 12

2.4 Pressurized Arch-Supported Membrane Structures 13

2.4.1 Experimental Methods 14

2.4.2 Analytical Methods 16

2.5 Conclusions 17

Chapter 3. Experimental Methods **18**

3.1 Introduction 18

3.1.1 1:100 Scale Model 18

3.1.2 1:50 Scale Model 19

3.2 Procedure 20

3.2.1 1:100 Scale Model 20

Materials 21

Construction 21

Wind Tunnel Testing 24

Snow Load Testing 26

3.2.2 1:50 Scale Model 31

Materials 32

Construction 32

Wind Tunnel Testing 33

Snow Load Testing 36

3.2.3 1:50 Scale Single Arch Model 40

Materials 40

Construction 40

Snow Load Testing 42

Chapter 4. Results **45**

4.1 Introduction 45

4.2 1:100 Scale Model 45

4.2.1 Wind Tunnel Testing 45

4.2.2 Snow Load Testing 52

4.3 1:50 Scale Model 63

4.3.1 Wind Tunnel Testing 63

4.3.2 Snow Load Testing 66

4.4 1:50 Scale Single Arch Model 75

4.4.1 Snow Load Testing 75

Chapter 5. Conclusions **91**

5.1 Introduction 91

5.2 1:100 Scale Model 91

5.2.1 Wind Tunnel Testing 91

5.2.2 Snow Load Testing 91

5.3 1:50 Scale Model 92

5.3.1 Wind Tunnel Testing 92

5.3.2 Snow Load Testing 93

5.4 1:50 Scale Single Arch Model 94

5.5 General Conclusions and Recommendations 95

Bibliography **96**

Appendix A **103**

Vita.. **107**

List of Figures

Figure 3.1. 1:100 Scale Model 20

Figure 3.2. Bases for the 1:100 Scale Model 22

Figure 3.3. Plan View of the Open-Throat Return Subsonic Wind Tunnel 25

Figure 3.4. 1:100 Scale Model in Wind Tunnel During Trial 3 25

Figure 3.5. Overhead View of 1:100 Scale Model with Node Locations 27

Figure 3.6. 1:100 Scale Model with Monofilament Strand Deflection Markers 28

Figure 3.7. 1:50 Scale Model 34

Figure 3.8. 1:50 Scale Model in Wind Tunnel During Trial 1 35

Figure 3.9. Overhead View of 1:50 Scale Model with Node Locations 37

Figure 3.10. 1:50 Scale Model with Monofilament Strand Deflection Markers 38

Figure 3.11. 1:50 Scale Single Arch Model with Partial Load Apparatus 41

Figure 3.12. 1:50 Scale Single Arch Model with Loading Apparatus 44

Figure 4.1. 1:100 Scale Model Wind Tunnel Test Trial 4 53

Figure 4.2. 1:100 Scale Model Wind Tunnel Test Trial 3 53

Figure 4.3. 1:100 Scale Model Node Layout 57

Figure 4.4. 1:100 Scale Model Membrane Deflections at Load Increments 0, 1, 6, 13, and 17 Between Nodes 1 and 25 58

Figure 4.5. 1:100 Scale Model Membrane Deflections at Load Increments 0, 1, 6, 13, and 17 Between Nodes 2 and 26 59

Figure 4.6. 1:100 Scale Model Membrane Deflections at Load Increments 0, 1, 6, 13, and 17 Between Nodes 3 and 27 60

Figure 4.7. 1:100 Scale Model Snow Load Testing at Load Increment 5 62

Figure 4.8. 1:100 Scale Model Snow Load Testing After Failure 62

Figure 4.9. 1:50 Scale Model Membrane Deflections at Load Increments 0, 1, 2a, 2b, and 3 Between Nodes 4 and 37 69

Figure 4.10. 1:50 Scale Model Membrane Deflections at Load Increments 0, 1, 2a, 2b, and 3 Between Nodes 5 and 38 70

Figure 4.11. 1:50 Scale Model Membrane Deflections at Load Increments 0, 1, 2a, 2b, and 3 Between Nodes 3 and 39 71

Figure 4.12. 1:50 Scale Model Load Vs. Arch Apex Deflections for Arches B, C, D, and E 72

Figure 4.13. 1:50 Scale Model Snow Load Testing After Failure (End View) 73

Figure 4.14. 1:50 Scale Model Snow Load Testing After Failure (End View) 74

Figure 4.15. 1:50 Scale Single Arch Model Snow Load Deflected Shapes: Trial 1 76

Figure 4.16. 1:50 Scale Single Arch Model Snow Load Deflected Shapes: Trial 2 77

Figure 4.17. 1:50 Scale Single Arch Model Snow Load Deflected Shapes: Trial 3 78

Figure 4.18. 1:50 Scale Single Arch Model Snow Load Deflected Shapes: Trial 4 79

Figure 4.19. 1:50 Scale Single Arch Model Snow Load Deflected Shapes: Trial 6 80

Figure 4.20. 1:50 Scale Single Arch Model Snow Load Deflected Shapes: Trial 8 81

Figure 4.21. 1:50 Scale Single Arch Model After Failure: Trial 7 83

Figure 4.22. 1:50 Scale Single Arch Model After Failure: Trial 3 83

Figure 4.23. 1:50 Scale Single Arch Model: Trial 4 85

Figure 4.24. Load Vs. Horizontal Arch Apex Deflection for Trial 8 86

Figure 4.25. 1:50 Scale Single Arch Model Load Vs. Arch Apex Deflections: Trial 3...... 87

Figure 4.26: 1:50 Scale Single Arch Model Load Vs. Arch Apex Deflections: Trial 7...... 88

Figure 4.27. 1:50 Scale Single Arch Model With Twist: Trial 3 89

Figure 4.28. 1:50 Scale Single Arch Model After Shifting Load Apparatus: Trial 8 90

Figure A.1. Stress Vs. Strain: Test 1 104

Figure A.2. Stress Vs. Strain: Test 2 105

Figure A.3. Stress Vs. Strain: Test 3 106

List of Tables

Table 3.1. Weights and Averages of Lead Impregnated Putty Tape 30

Table 3.2. Weights and Averages of Lead Coated Duct Tape 30

Table 4.1. 1:100 Scale Model Wind Tunnel Test Data Table: Trial 1 46

Table 4.2. 1:100 Scale Model Wind Tunnel Test Data Table: Trial 2 47

Table 4.3. 1:100 Scale Model Wind Tunnel Test Data Table: Trial 3 48

Table 4.4. 1:100 Scale Model Wind Tunnel Test Data Table: Trial 4 49

Table 4.5. 1:100 Scale Model Wind Tunnel Test Data Table: Trial 5 50

Table 4.6. 1:100 Scale Model Snow Load Testing Data Table 54

Table 4.7a. 1:100 Scale Model Snow Load Testing Deflection Table 55

Table 4.7b. 1:100 Scale Model Snow Load Testing Deflection Table 56

Table 4.8. 1:50 Scale Model Wind Tunnel Testing Data Table: Trial 1 64

Table 4.9. 1:50 Scale Model Wind Tunnel Testing Data Table: Trial 2 64

Table 4.10. 1:50 Scale Model Wind Tunnel Testing Data Table: Trial 3 65

Table 4.11. 1:50 Scale Model Wind Tunnel Testing Data Table: Trial 4 65

Table 4.12. 1:50 Scale Model Wind Tunnel Testing Data Table: Trial 5 66

Table 4.13. 1:50 Scale Model Snow Load Testing Data Table 67

Table 4.14a. 1:50 Scale Model Snow Load Testing Deflection Table 67

Table 4.14b. 1:50 Scale Model Snow Load Testing Deflection Table 68

Table 4.15. 1:50 Scale Single Arch Model Snow Load Testing: Trial 1 76

Table 4.16. 1:50 Scale Single Arch Model Snow Load Testing: Trial 2 77

Table 4.17. 1:50 Scale Single Arch Model Snow Load Testing: Trial 3 78

Table 4.18. 1:50 Scale Single Arch Model Snow Load Testing: Trial 4 79

Table 4.19. 1:50 Scale Single Arch Model Snow Load Testing: Trial 6 80

Table 4.20. 1:50 Scale Single Arch Model Snow Load Testing: Trial 7 81

Table 4.21. 1:50 Scale Single Arch Model Snow Load Testing: Trial 5 82

Table 4.22. 1:50 Scale Single Arch Model Snow Load Testing: Trial 8 82

Table 4.23. 1:50 Scale Model and Single Arch Model Failure Loads 84

Chapter 1. Introduction

Inflatable structures and membrane enclosed structures utilize advanced technology that enables large structures to be lightweight and easily deployable. For many years such structures have proved useful for a variety of purposes, such as athletic pavilions, exhibition spaces, coliseums, and kiosks. More recently, structures that combine highly pressurized inflatable arch members with light fabric membrane coverings have been considered as a variation of such structural systems. In particular, the United States Army has begun to investigate arch-supported membrane shelters that would be large, lightweight, and easily erected in a short amount of time. These shelters are proposed for a variety of purposes, including aircraft hangars, vehicle maintenance shelters, and medical aid stations. Because of the crucial nature of the uses of these structures, it is very important to have a complete and accurate understanding of how they behave under various weather conditions. An understanding of the behavior of these structures subjected to various loading conditions may facilitate more efficient and accurate design procedures.

The objective of the present research, funded by the United States Army, is to develop procedures for accurate and efficient analysis and design of tent structures supported by pressurized arches. The specific contribution of this study is the creation and testing of scale models to obtain a better understanding of how these structures behave under wind and snow loading conditions. In addition, because the development of design procedures for these structures is in an early phase, modes of failure and controlling limit states will be investigated. The qualitative observations and quantitative measurements of the behavior of the models can be used to supplement future design procedures and serve as a basis for analytical comparison.

For the present research, three models were constructed, one at a scale of 1:100 and two at a scale of 1:50. The 1:100 scale model represented a proposed prototypical structure 200 ft long, 75 ft wide, and 50 ft tall, with multiple arches. Of the 1:50 scale models, one model represented a structure with the same dimensions as the 1:100 scale model and the other represented a single arch from one of the proposed prototypical structures. Both of the full structural models were wind and snow load tested. The single arch model was tested under full and partial snow loading.

Data from the testing were collected, tabulated, and evaluated. The experimental results are discussed, conclusions are drawn, and recommendations for further research are presented. The data from the model testing should be compared and analyzed with data from computer analyses of the same types of structures under various loading conditions in the future. Using these methods of research, it is intended that procedures for designing these structures more efficiently and effectively will be developed.

Chapter 2. Literature Review

2.1 Introduction

The structures under investigation consist of pressurized arches that support fabric membranes. This type of structure combines the technologies of inflated structures and fabric membrane structures. There are large bodies of research that have focused on both of these building types, using experimental and numerical methodologies. A dearth of experimental research has been performed regarding snow loads on both of these structural types, although wind effects have been thoroughly researched using wind tunnel tests and numerical procedures. Examples of research can be found on pressurized arch and beam structures, although these building types have not been researched to the extent that inflatable and fabric membrane structures have.

Presented here are examples of research conducted on inflated structures, fabric membrane structures, and pressurized arch and beam structures. Various research methods have been used and different aspects of the structures have been considered. The research presented is intended to elucidate the need for further analysis and investigation of pressurized arch supported membrane structures.

2.2 Air-Supported Structures

Inflatable structures have been in use for many years. The technology has advanced such that large, lightweight, and easily deployable shelters can be created using air-supported structures (Kronenburg, 1996). The majority of these structures consist of a thin membrane that is held aloft by a constant, but rather low, pressure. This building type has been extensively researched (e.g., Srivastava, Turkkan, and Dickey, 1984; Beger and Macher, 1967; Kassem and Novak, 1992). Efforts to understand the structural characteristics of these enclosures have been undertaken using experimental and analytical methods. Research has also been conducted concerning the appropriate design methodology for these structures.

2.2.1 Experimental Methods

Due to the light and flexible nature of air-supported structures, understanding the response to wind loading is highly important for this field of research. In order to make any predictions about the behavior of semi-cylindrically shaped buildings, the distribution of pressure as wind passes across them must be studied.

Srivastava, Turkkan and Dickey (1984) performed wind tunnel tests on both rigid and flexible hemispherical models and found the distribution of pressure and the displacements as functions of the internal pressure (p_i) and the dynamic wind pressure (q). The rigid model produced results that were consistent with the Canadian Building Code. The flexible models behaved very much like the rigid models at higher values of the ratio p_i/q, but not at lower values. They advocate doing more testing, especially with flexible models of various shapes in order to find more definite conclusions.

Kawamura and Kiuchi (1986a) also performed wind tunnel testing on rigid and flexible models of low-rise and high-rise profile scale models. In addition, they built a much larger flexible model and recorded the deflections of the model under naturally occurring wind situations while varying the internal pressure of the model. From the experiments conducted, they developed pressure coefficient distributions for the models and developed schemes for the design of pneumatic structures. Kawamura and Kiuchi (1986b) elaborated upon the results of these tests by integrating dynamic membrane characteristics with the design schemes to create specific design criteria for wind loaded inflatable structures.

A model of a low-profile, cable-reinforced, air-supported dome was created by Fukao, Isawa, Mataki, and Okada (1986) and its behavior was analyzed as the model was subjected to a naturally occurring typhoon. Roof deflections, cable tension, and internal pressure were recorded and these results were compared with the findings of a static loading test simulation of the wind testing done on the same model. Analytical methods that determined cable tension and roof deflection were developed based on the results of these experiments.

It is also fundamental to have an understanding of the manner in which an air-supported structure deforms as a result of wind loading. Wind tunnel tests were performed by Beger and Macher (1967) on three different shaped inflatable models. They tested a hemisphere, a semi-cylinder, and a three-quarter sphere in a low-speed wind tunnel. Observations of the deformations and measurements of the pressure distributions were recorded as the wind velocity and the internal pressures of the models were varied. The authors felt that due to the minimal influence of Reynolds number on the responses of the structural models, the findings of the study would be applicable to larger structures.

Kassem and Novak (1992) wind tunnel tested an inflated hemisphere and the roof response and internal pressure fluctuations were monitored as the exposure, internal pressure, gradient wind speed, and enclosure volume were manipulated. They were concerned with how the structure and the wind would affect one another under turbulent wind conditions. From rigid model tests and analytical methods, they formulated a numerical prediction of the behavior of the model that compared well with the experimental results.

A different type of model testing was performed by Bohme and Rontsch (1967) with the intention of gaining a more exact understanding than previous wind tunnel tests had provided, regarding the deformations and strains that inflatable structures undergo during snow and wind loading situations. The internal pressure of the model and the external snow and wind loads were simulated using a set of concentrated loads. Using the wind pressure distributions from previous wind tunnel tests, displacements were determined for the different load cases. The snow loading cases considered fully distributed and partially distributed loading on the top of the structure.

It is important when perusing the literature on wind tunnel studies to have a notion of how experimental data obtained in this way correlate to real world structural situations. In one effort to understand this comparison, models of different scales were tested in the same wind tunnel, one model was tested in different wind tunnels, and these sets of data were compared to a full-scale canopy roof building that was tested in an outdoor situation (Moran and Robertson, 1986). All of the situations measured pressure distributions as wind loads were applied to the structure. Significant differences were found among all of the cases tested, but the general trend was that, "wind tunnel results underestimate the magnitude of external suctions over the windward roof slope and ridge for a wind normal to the ridge, yet overestimate the suctions at the ridge for winds at 45° or more from normal to the ridge" (Moran and Robertson, 1986, p. 123). The authors suggested that visualization experiments be conducted to further establish the causes of the discrepancies, which may be attributable to differences in Reynolds number effects.

2.2.2 Analytical Methods

In addition to experimental testing, there has also been a great deal of research executed using numerical models to understand and predict the responses of loaded air-supported structures. Often these methods can be optimized using computers to create efficient and accurate design strategies for a wide range of building applications.

One way of analyzing pressurized structures is to consider a building long enough to be treated as a two-dimensional cross section that may be generalized to the building as a whole. This is the approach that Uemura (1972) took in trying to determine the membrane tension and deformations of a cylindrical inflatable model subjected to wind acting normal to its longitudinal axis. In the analysis, the author used the finite deformation membrane theory and manipulated wind velocity, inflation pressure, cylinder radius, wind pressure distribution, and membrane extensional rigidity in order to predict the membrane tension and displacements. Wind tunnel tests were also conducted for comparison with the numerical analysis and it was found that the observable deformations were in agreement, but the membrane tensions were not measured on the model.

Kunieda (1975) also utilized the fact that for a large length/width ratio, a curved membrane roof could be analyzed in a two-dimensional configuration in order to simplify the calculations. In this research, a numerical analysis for determining the critical wind velocity parallel to the longitudinal axis that would induce a dangerous fluttering of the membrane was conducted. This critical velocity determination was intended to be generalized to roofs constructed of any material at any size that had a curvature within a specified range of the study. The author acknowledged the importance of a more complete understanding of the interaction between a structure and the wind stream acting on it.

A two-dimensional analysis approach for inflatable structures was also taken by Newman and Goland (1982) in their development of a theory for predicting the membrane tension for inflatable structures under wind loads. They determined the membrane tension as a function of the wind velocity, the terrain in which the structure was located, the roughness of the membrane, and the internal pressure. Wind tunnel tests were performed and provided a fair agreement with the theory predicted values of tension in the membrane.

Han and Olson (1987) did separate three-dimensional analyses for the wind and for an inflatable structure, as a means of modeling the behavior of the wind loaded structure. The flow of the wind was modeled using a boundary element procedure and the structure was analyzed using a finite element method. "These two numerical techniques are then coupled to capture the interaction effects in the analysis" (Han and Olson, 1987, p. 699). Upon comparison with the behavior of an existing structure and with wind tunnel tests, good agreement was reached using this analysis technique.

Dynamic excitation was investigated by Sygulski (1996), using boundary element and finite element methods. Numerical analyses of aerodynamic damping and flutter vibrations were conducted and compared to wind tunnel tests, with satisfactory agreement. Further wind tunnel tests on models of different shapes were suggested to "enable better knowledge and understanding of flutter vibrations for pneumatic structures" (Sygulski, 1996, p. 961).

The problem of how to analyze the deformed shape of these flexible structures has also been addressed using analytical methods. Spinelli (1983) studied the complex determination of responses corresponding to a time interval as the structure undergoes dynamic behavior due to wind. By using a particular version of Newmark's β method, the author established some determinations of dynamic response by direct integration of the equation of motion, where the geometric and kinematic quantities are updated continuously at the end of each time interval. This takes into account the changing shape of the flexible membrane. A good rate of convergence and a strong stability of this method were demonstrated.

In conjunction with wind tunnel experiments that determined experimental wind pressure distributions and displacements, Srivastava et al. (1983) developed a numerical approach using a network method to analyze a hemispherical membrane and its responses to wind loading. The analysis was performed in such a manner that it could be easily adapted to use by a computer and, like the wind tunnel tests, displacements and pressure distributions were determined for different internal pressures (p_i) and dynamic wind pressures (q). The theoretical distributions closely matched the experimental ones for higher values of the ratio p_i/q. The theoretical radial deformations came close to experimental ones at lower p_i/q values, but differed considerably at higher p_i/q values.

Both experiments and numerical analyses are performed in efforts to comprehend how inflatable structures will react when loaded in various ways. Once there is a solid behavioral understanding, it naturally follows that investigations would be done regarding the design of these types of structures.

Some of the fundamental factors involved in designing air-supported structures were provided by Rudolf (1967). This research provided some approximate formulas for determining the internal forces of the membrane as well as the deformed shape under wind loading. Taken into account for these calculations were the suppositions that tensile stresses can only occur in two perpendicular directions in the membrane and that the internal pressure of the enclosure changes as the membrane deforms. Different snow and wind loading cases were evaluated and a wind loaded hemisphere was provided as an example of how to calculate the approximate stresses. Once the stresses within the fabric are known, the membrane can be designed. In another study, it was suggested that the allowable stress of the fabric be on the order of one-fourth to one-tenth of the ultimate strength of the membrane (Uemura, 1971).

These are some examples of the investigations that have been done on the behavior and design of air-supported structures. These structures usually have airlocks for access to the inside, which would not work for an enclosing function such as a hangar or a vehicle maintenance shelter, where large vehicles must be able to pass through large openings in the exterior shell of the building (Kronenburg, 1996). For this reason and other constructional and logistical criteria, the Army has turned their attention toward structures that have pressurized arches as their primary structural elements.

2.3 Fabric Membrane Structures

Fabric membrane structures have been in use for thousands of years. These structures consist of a membrane that is attached or stretched over a stiff framework, thus enclosing the space inside the framework. Tents are the oldest example of this type of structure and are one of the earliest building types known to man (Berger, 1996). The technology of designing and constructing these structures has advanced to a point where "membrane structures now benefit from modern materials that have higher strength characteristics than steel" (Kronenburg, 1995, p. 11). Like inflatable structures, fabric membrane structures are light-weight, easily transportable, and can be used to enclose large spaces effectively. Efforts to understand the structural characteristics of these enclosures have been undertaken using experimental and analytical methods, and some are described here. In addition, some research concerning the appropriate design methodology for these structures is described.

2.3.1 Experimental Methods

Much like air-supported structures, the light and flexible nature of fabric membrane structures necessitates a thorough understanding of the responses to wind loading. Wind tunnel tests have proven useful as a means of furthering the behavioral understanding of these structures, as well as leading to design criteria.

Rigid models of membrane structures were wind tunnel tested by Sykes (1994) to obtain pressure distributions on irregularly shaped pavilion enclosures. The results were used to design the structures, "for which code-based loading data was not available"

(Sykes, 1994, p. 383). Swami, Seetharamulu, and Chaudhary (1988) also wind tunnel tested a rigid model. An inverted, asymmetric cone shaped model was constructed and tested at various orientations with respect to the wind flow. Pressure distributions were obtained and it was concluded that "suction or positive pressures are predominant. As a result, when dead loads and live loads are considered the net loading effect on the shell surface is reduced." (Swami, Seetharamulu, and Chaudhary, 1988, p. 853). More wind tunnel testing was advocated to obtain a better understanding of the behavior of these types of structures.

Daw and Davenport (1989) tested a flexible, semi-cylindrical shell model in a wind tunnel while also subjecting the model to asymmetric vibrations. Observations were made of the effects that the deformed structure under wind loading had on the wind flow around the structure. They concluded that aeroelastic coefficients, which are based on the motion of the structure, are "dependent upon the structure shape and are linearly related to amplitude, for small amplitudes" (Daw and Davenport, 1989, p. 91).

Snow loading behavior of a lightweight suspended tent roof structure was considered by Oiger and Parts (1988). Observations were made of the forces within the fabric subjected to full and partial snow loads. Maintenance conditions and duration of loading were concluded to be essential design considerations and a numerical scheme was derived from the experiments conducted.

2.3.2 Analytical Methods

In addition to experimental testing, research has been conducted using numerical models to understand and predict the responses of loaded membrane structures. Often these methods can be optimized using computers to create efficient and accurate design strategies for a wide range of building applications.

A common method of numerical analysis for membrane structures is the finite element method. Shugar, Brittan, and Hsu (1985) developed a two phase, nonlinear finite element approach to analyze a hypothetical aircraft hangar. "The analysis procedure is organized around a phase-I analysis to compute an initial configuration and a phase-II analysis to compute the structural response to in-service loads relative to the initial configuration." (Shugar et al., 1985, p. 25). Membrane stresses and displacements were determined and provided "an illuminating and detailed understanding of structural behavior" (Shugar et al., 1985, p. 25).

Ikemoto, Mizoguchi, Fujikake, Kojima, and Hirota (1986) also performed a nonlinear finite element analysis and developed a series of computer algorithms and graphic interfaces that could be used to design membrane structures. They incorporated wrinkling into the design procedures and conducted wind tunnel studies to confirm their results.

2.4 Pressurized Arch-Supported Membrane Structures

Air-supported structures usually consist of a relatively airtight membrane that creates an enclosure by being held in a particular shape by a constant, low (0.1 psi) air pressure (Kronenburg, 1996). Pressurized arch structures are made up of inflated, small diameter (4 inch to 24 inch) tubes with pressures ranging from 4 psi to 100 psi and formed into arches. These arches "are normally individually inflated units over which the covering material of the building is tensioned" (Reffell, 1967, p. 64). The covering can be manipulated to allow for access into the shelter by either personnel or vehicles of various sizes, due to the fact that the overall enclosure is not pressurized and does not need to be kept airtight. As with air-supported structures and fabric membrane structures, these constructs need to be experimentally and numerically researched in order to be efficiently and accurately designed.

2.4.1 Experimental Methods

Experiments have been conducted on various components and configurations of pressurized arch-supported membrane structures in order to obtain a more complete understanding of the behavior of these structures.

Steeves (1975b) investigated the behavior of pressurized beams, as a step in the process of understanding pressurized arches. The beams were tested for bending, and the materials used for the beams were tested for elastic modulus and shear modulus values. These experimental results were compared to previously obtained theoretical results, which were determined to be "adequate for the prediction of the deformation and load carrying capacity of pressure stabilized beams" (Steeves, 1975b, p. 23).

Hajek and Holub (1967) experimentally established that for membranes to be used as pressurized members it was necessary to test them in a manner more consistent with their application as such, rather than the typical tensile strip test. Also considered were the effects of weather and natural aging on inflated fabric members. In addition to material properties, the authors investigated the stability of simply-supported inflated beams of different internal pressures subjected to three different concentrated loads. The results exemplified that the deflections of the beams did not vary linearly and led to the conclusion that, “it seems that the most reliable criterion for judging the stability of an inflated beam at present is still the experiment. At least we shall hardly succeed by applying some of the classical methods of analysis that are used with conventional construction materials” (Hajek and Holub, 1967, p. 162).

Research on inflated beams and arches made with prestressed fabric skins, conducted by Kawaguchi, et al. (1972), indicated that “prestressed fabric skins present quite different behaviors from those of membranes” (Kawaguchi et al., 1972, p. 458). The major behavioral difference was a significant increase in bending stiffness of the fabric skin members as the internal pressure was increased, and was attributed to the weft and the warp in the fabric skins.

Dietz, Proffitt, Chabot, and Moak (1969) performed wind tunnel tests on a wide array of inflatable models and inflatable arch models. Various structural configurations were tested. Deflections and internal pressures were monitored during the experiments and design criteria based on these factors were developed. It was noted that the design of pressurized arch structures “should not allow wrinkling, even for the severest of the design loads,” and also that “deformation becomes excessive almost immediately after wrinkling begins” (Dietz et al, 1969, p. 117).

Research was conducted on pressurized arches and documented by Reffell (1967). Tests were done using an arch that spanned 45 feet, was 10 inches in diameter, and had an internal pressure of 100 psi. Using four “engined transport aircraft”, the arch was found to be able to withstand 70 mph winds and remained stable. This arch was also tested under “monsoon” rain load conditions, and was found to effectively shed water, as long as its initial parabolic form was maintained. At the time of that study, some of the proposed applications of these structures included a motorway construction shelter, a marine storage and cleaning device, an air cushion support device, solar heated railway structures, and various sea markers and buoyant radar reflectors.

2.4.2 Analytical Methods

Analytical methods have been applied to pressurized arches and to pressurized beams in order to gain a better understanding of structural behavior under loading and to be able to develop design strategies for these building components.

Steeves (1975a, 1978b, and 1979) conducted research that analyzed various aspects of pressurized beam behavior and design. One investigation (Steeves, 1975a) used numerical methods to predict wrinkling loads for static concentrated loading cases as a function of internal pressure, the geometry of the beam, and properties of the material. Another study (Steeves, 1978b) resulted in the development of a specific finite element for use with a finite element computer program. The developed finite element "provides a means for carrying out design analysis of pressure-stabilized frame-supported tents under general loading" (Steeves, 1978b, p. 20). Optimization of beam weight was the subject of the third study on beams (Steeves, 1979). The results indicated that "the minimum weight is obtained with large values of inflation pressure, small values of cross-section radius and, not surprisingly, low values of fabric density" (Steeves, 1979, p. 17).

Lukasiewicz and Balas (1988) investigated the formation of "pneumatic hinges" that occur in inflatable arches upon wrinkling of the membrane. Numerical methods were developed and then confirmed with experiments on inflatable arches, resulting in load-displacement relationships based on the radius of the cross section, the radius of the arch, the internal pressure, and the portion of a circle, in degrees, that the arch forms.

A computer program was developed by Steeves (1978a) that provided the amount of load that an inflatable arch can withstand before wrinkling begins and the amount of deformation of the arch under loading. The program was compared with previous experimental work and the comparison “establishes the (program) theory as being adequate for the prediction of the deformation and load-carrying capability of pressure-stabilized arches. Thus the study can provide a rational basis for the structural design of shelters using pressure-stabilized arches” (Steeves, 1978a. p. 70).

2.5 Conclusions

Research indicates that there is a distinct need for further studies of the structural characteristics of inflatable structures (Srivastava et al., 1984; Moran and Robertson, 1986; and Kunieda, 1984). More specifically there is a need for research of pressurized arch-supported membrane structures that consider the structure as an integrated whole, and not as a grouping of separately analyzed structural components. In regard to presently accepted building codes and the uniqueness of the structures under investigation, it is important to note that, “codes give safe upper bound values for the majority of structures but the level of uncertainty increases as the building’s configuration deviates from the codified norms” (Blackmore, 1997). By subjecting scale models of pressurized arch structures to wind loading and snow loading simulations, a more thorough understanding of the behavioral responses of them will be pursued.

Chapter 3. Experimental Methods

3.1 Introduction

Two models were constructed, one at a scale of 1:100 to a proposed prototypical structure, and another at a scale of 1:50 to a similar prototype. The models represented variations of structures that consist of pressurized arches that support fabric membranes. The structures represented by the models were 200 ft long, 75 ft wide, and 50 ft high, with five vertical arches, each spaced 25 ft apart, creating four bays in between, and three angled arches on each end. The diameter of the circular cross section of the arches in the represented structures was 2 ft. In addition to scale differences, the shapes of the arches differed in that the smaller model (1:100 scale) used a parabolic function for the curvature of the arches and the larger model (1:50 scale) had more circularly shaped arches. The scale for the smaller model was partly dictated by the dimensions of the wind tunnel used for the testing. The smaller model used essentially rigid arches made of copper tubing, while the larger model used more flexible arches made from polyethylene tubing. Both models were tested for wind and snow loading. Besides these two models of the structures, a single arch model with polyethylene tubing was constructed at a scale of 1:50 and was only load tested.

3.1.1 1:100 Scale Model

The smaller model was wind tunnel tested in the open-throat return, subsonic wind tunnel, located in Randolph Hall and owned by the Aerospace and Ocean Engineering (AOE) Department of Virginia Polytechnic Institute and State University. This wind tunnel was constructed by Virginia Tech faculty and is used mostly for student instruction and experimentation. The wind tunnel testing investigated the deflected shape of the model at various wind speeds and angles of the model with respect to the wind direction. Observational data regarding the fluttering of the membrane and the possibility of excessive membrane flutter was gathered.

This model was snow load tested in the Geotechnical Laboratory in Patton Hall. The snow load testing consisted of recording incremental measurements of the deflected shape of the membrane as the load intensity was increased to failure of the structure.

3.1.2 1:50 Scale Model

The larger model was wind tunnel tested in the low speed, boundary layer wind tunnel located at the Environmental Systems Laboratory and owned by the College of Architecture and Urban Studies at Virginia Polytechnic Institute and State University. Because of its large size, this model could not be tested in the open-throat return, subsonic wind tunnel. Observations of the flow interaction between the wind and the structure at various wind speeds and wind directions were made during the wind tunnel testing. Flutter in the membrane was visually monitored, but because of the low wind speeds, none was observed.

The snow load testing consisted of recording incremental measurements of the deflected shape of the membrane as the load intensity was increased to structural failure.

Snow loading was also performed on the 1:50 scale single arch model, using 8 different arches and 4 different loading conditions. All of the single arch tests were also continued until structural failure occurred.

3.2 Procedure

3.2.1 1:100 Scale Model

The dimensions of the 1:100 scale model constructed were 24 in. long, 9 in. wide, and 6 in. high, with five vertical arches, each spaced 3 in. apart. The cross sections of the arches in the model had an outside diameter of 0.25 in. Figure 3.1 shows the constructed model.

Figure 3.1: 1:100 Scale Model

Each end of the modeled structure was comprised of three arches, all with common base points. Each arch was rotated, in plane, 30° with respect to the adjacent arches. The plane of the final arch was oriented horizontally. Therefore, the three end arches created a quarter of a paraboloid. The shape of each arch was formulated using the following parabolic function:

$$y = \frac{x^2}{28.125}$$

The model was constructed using the same arch orientations and curvatures as the structure represented.

Materials

The materials for the model were chosen to approximate as closely as possible the types of materials used in the structures represented, as well as for practicality in construction of the model. Two bases were used for the model and are shown in Figure 3.2. Both were made from 0.5 in. thick plywood. The bases could be attached to each other with 5 bolts and wing nuts. The lower of the two bases was rectangular in shape and attached to brackets on the wind tunnel framework. The upper base was circular and the model was attached directly to it.

The arches were made of soft copper tubing having an outside diameter of 0.25 in. and a thickness of 0.03 in. The membrane was a flexible plastic material designed for landscaping that was 0.004 in. thick with a grainy texture and black in color. Tension tests on the membrane material estimated its modulus of elasticity as 3.6 ksi (see Appendix A).

Construction

The larger, rectangular base was 34 in. long and 51 in. wide. The smaller, circular base had a diameter of 32 in. and was mounted onto the larger base at its center and at four points near the outer edge of the circle. The circular base could be rotated

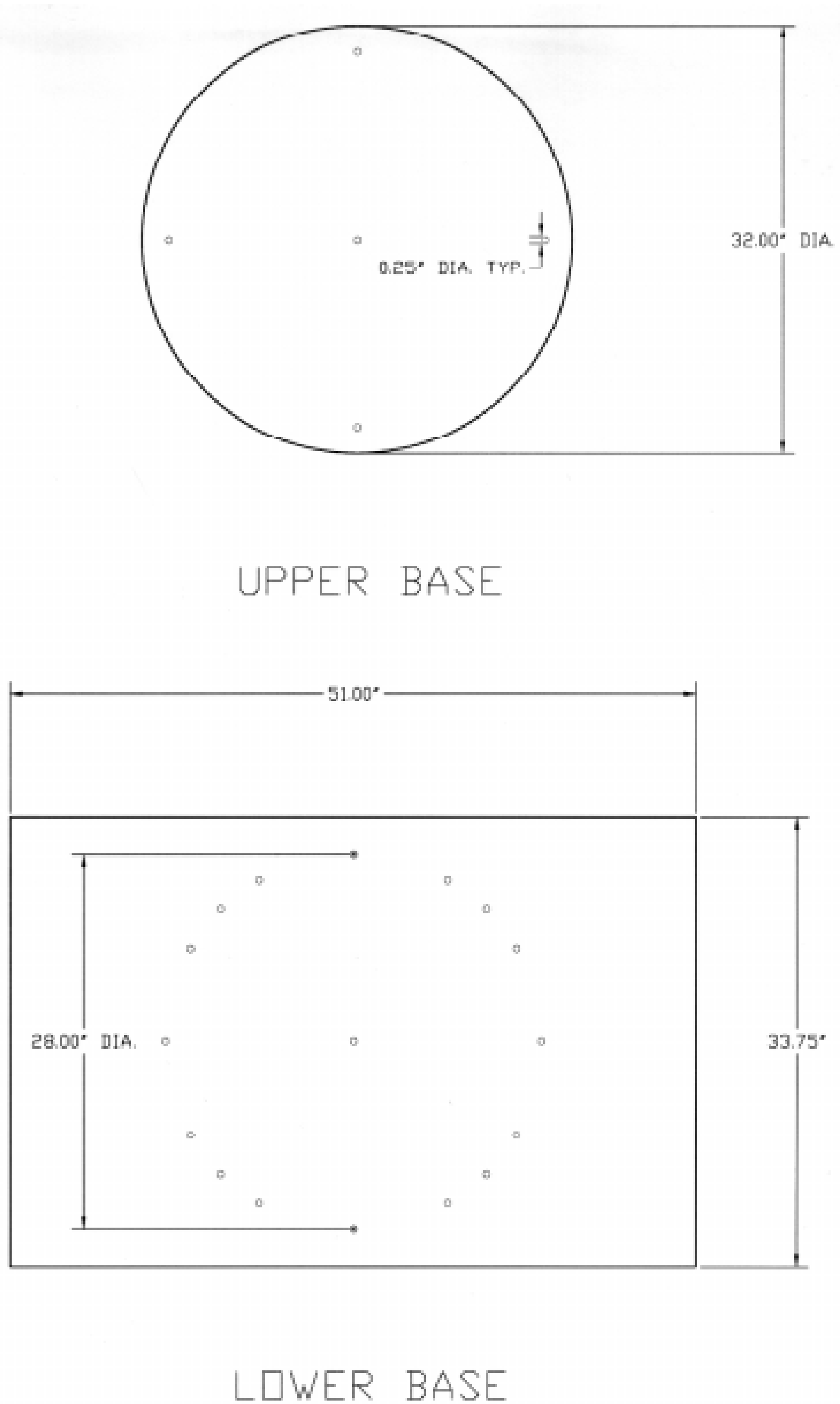

Figure 3.2: Bases for the 1:100 Scale Model

about its center and secured at different orientations in relation to the lower base.

The copper tube arches were formed by pressing the tubing into a plywood mold containing the specified parabolic arch shape. The curve was maintained after the tubes were removed from the forms. Ten 0.3125 in. diameter holes were drilled into the circular base at a 69.25° angle to horizontal, and the bases of the vertical arches were placed into the holes and secured with epoxy. In this way the arches of the model mounted firmly to the base and a fixed connection was provided at the base of each arch. The two leaning arches on each end of the model were fixed, with screws, to wooden blocks that attached securely to the base. The horizontal arch on either end was screwed directly to the base in several places, with small washers between the copper tubing and the base. Sections of copper tubing were also fixed horizontally onto the base, between each set of vertical arches, thus creating a band of tubing around the entire base perimeter of the model.

The membrane was formed by machine sewing sections of the material together to form an outer casing for the model that fit smoothly over the framework created by the arches. The sections were created using patterns derived from the shapes between the vertical and leaning arches. At the seams of the sections, the material was doubled along the arch lengths. Using the same material, a drawstring channel was machine sewn around the lower edge of the casing, and a strand of monofilament was inserted to hold the membrane onto the band of copper tubing around the base perimeter of model. The casing was positioned over the arched framework of the model and was hand stitched to each vertical arch, along the length of the arches. The monofilament channel was also hand stitched to the copper tubing perimeter around the model. The casing was not hand sewn to the arches that were positioned at 30° and 60° to the vertical plane.

Wind Tunnel Testing

The wind tunnel used for the 1:100 scale model wind loading was the open-throat return, subsonic wind tunnel and is shown in Figure 3.3 (taken from the AOE home page). The wind speed in the tunnel was obtained from a pitot-static tube mounted on the outflow of the open section of the wind tunnel. The pressure was recorded on a differential manometer and was read in inches of water. These pressure readings were converted to velocities after the testing. The wind tunnel was equipped with a valve that could be opened during operation in order to get a more even wind stream, but which resulted in lower maximum wind speeds. All of the tests were conducted with this valve in the fully open position.

The rectangular model base was attached directly to brackets on the wind tunnel framework and was placed 5 in. below the centerline of the circular opening of the wind tunnel by means of four 6 in. long bolts and four 5 in. long, 1 in. square aluminum tubing sections as spacers. This was done in an effort to minimize the blockage of air flow caused by the model itself. Figure 3.4 shows the model placed within the wind tunnel.

Five separate trials were conducted for the wind tunnel testing. Each trial consisted of placing the model at a specific orientation with respect to the wind direction and gradually, incrementally increasing the wind speed in the tunnel until the maximum speed was reached. The different angles tested were 0°, 30°, 45°, 60°, and 90° relative to

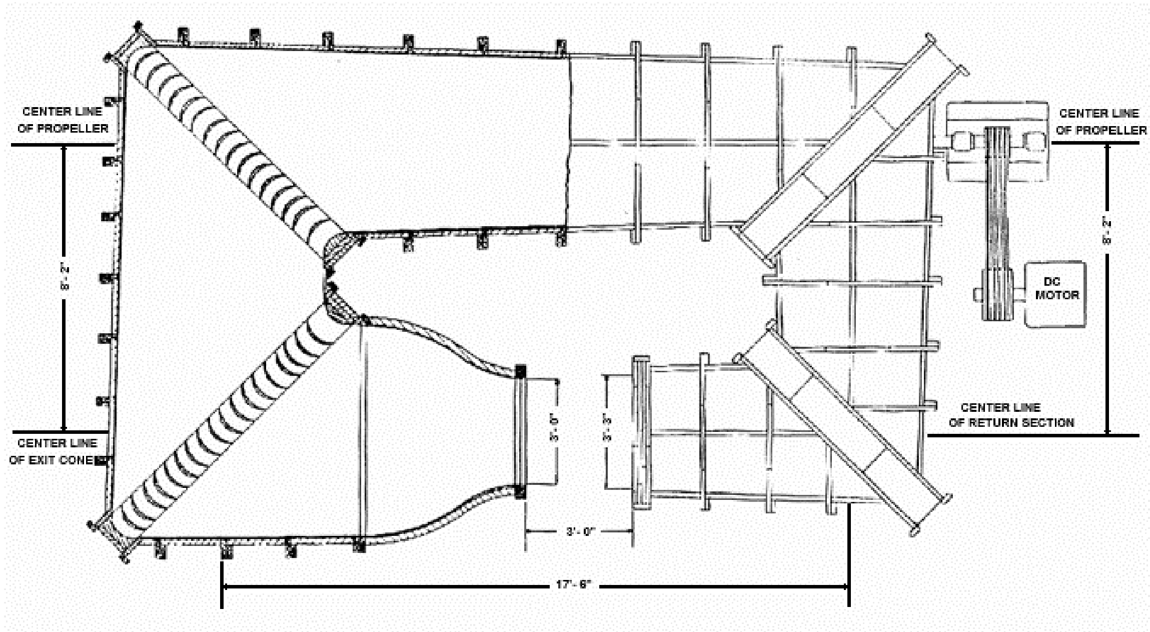

Figure 3.3: Plan View of the Open-Throat Return Subsonic Wind Tunnel

Figure 3.4: 1:100 Scale Model in Wind Tunnel During Trial 3

the direction of the wind flow. Each trial was videotaped and photographs were taken intermittently throughout the various trials.

During each trial for the wind tunnel testing, various measurements were recorded. In an effort to maintain some consistency across the trials, the number of revolutions per minute of the fan motor was used as the method of gauging the increase in wind. The 1:100 Scale Model Wind Tunnel Testing Data Tables in Chapter 4 list the increments used. The temperature during each trial was recorded using a digital thermometer mounted on the wind tunnel. The barometric pressure was obtained from the National Weather Service and was taken three hours before the testing began. A tare measurement of the inches of water registered by the differential manometer attached to the pitot-static tube leads was recorded at the beginning of each trial. Manometer measurements were taken for each increase in the revolutions per minute of the fan motor. Behavioral observations were noted as comments at various times during the testing. All of the data have been tabulated in the 1:100 Scale Model Wind Tunnel Testing Data Tables in Chapter 4.

Snow Load Testing

The snow load testing for the 1:100 scale model was conducted in the Geotechnical Laboratory located in Patton Hall. It was assumed that no snow would accumulate on any areas of the membrane that had more than a 30° angle with the horizontal. The area loaded was a strip down the center of the model that measured 2 in. along the curve of the arch, and spanned between the two leaning arches on each end of the model that were angled at 60° to horizontal. On the represented structure, this strip would measure 16.83 ft wide and 150.00 ft long. For measuring deflections, nine nodes were used between each arch, and one node at the top of each arch was used. Only one quarter of the model was used for deflection measurement, assuming that the structure would behave symmetrically. The locations of the nodes on the model are shown in Figure 3.5.

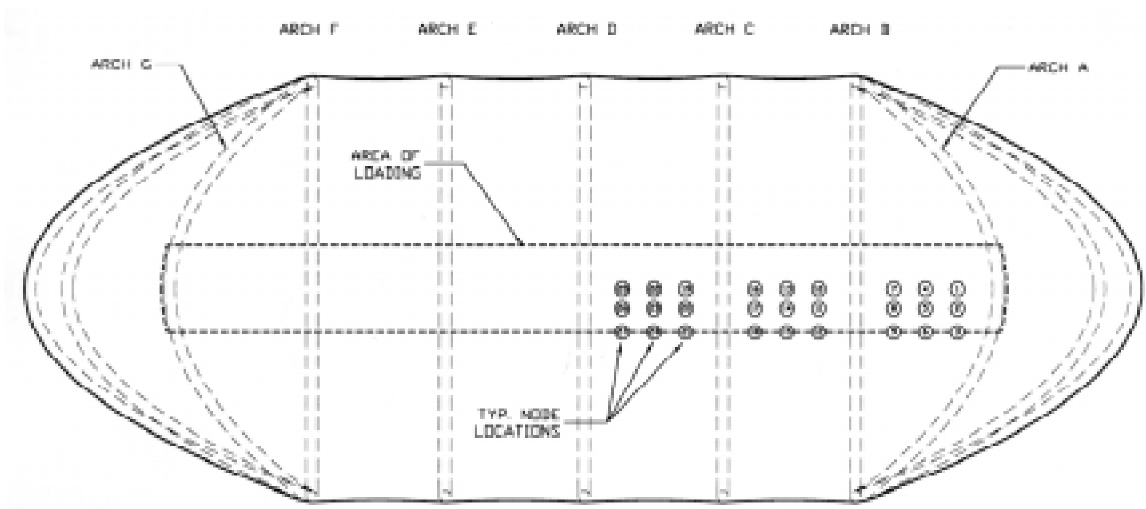

Figure 3.5: Overhead View of 1:100 Scale Model with Node Locations

A portion of the circular base located beneath the area of the model that was to be loaded was removed without affecting the arches or the membrane, with enough extra room to facilitate easy access to the inside of the model. The portion was removed in order to install the deflection-measuring monofilament strands. A sheet of 1/8” thick masonite was placed over the hole in the model base and was screwed to the underside of the base. In this masonite, 5/64 in. diameter holes were drilled at locations directly under the nodes on the model. Segments of 10 lb test, 0.012 in. diameter, monofilament penetrated the membrane at the nodes and were knotted on top of the membrane. The monofilament was kept from pushing through the membrane by stringing it through small pieces of masking tape, approximately 0.25 in. by 0.25 in., that were placed between the membrane and the knots in the end of the monofilament. At the arch tops, the monofilament was tied directly to the arches at the proper locations. All strands then went through the appropriate holes in the masonite and were marked at the lower end with the node numbers written on pieces of masking tape that were attached to the ends of the monofilament. These markers also served to keep the strands hanging vertically, without causing any deflection to the membrane, and are shown in Figure 3.6.

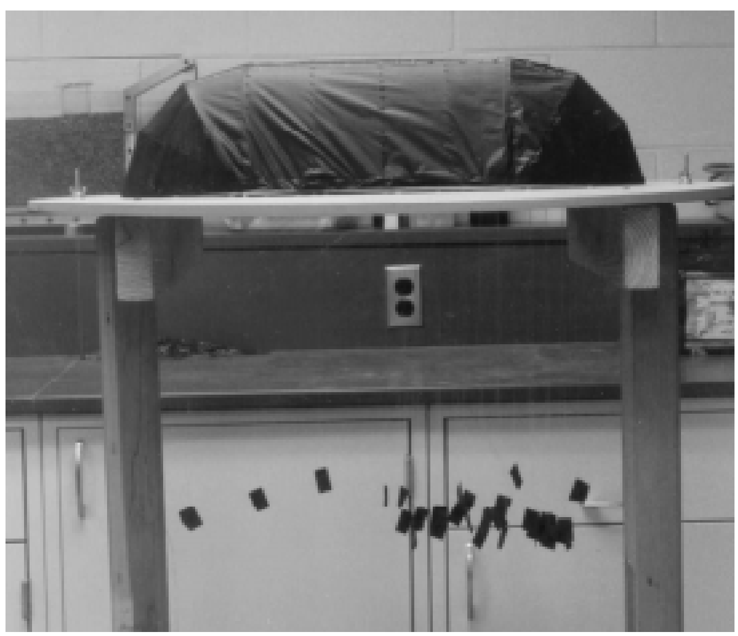

Figure 3.6: 1:100 Scale Model with Monofilament Strand Deflection Markers

Three different types of weights were added to simulate the snow load. Each load type was placed in full layers, directly on top of the previous type. The first type of weight consisted of 3/4 in. wide putty tape, a material typically used to seal openings around windows and doors in mobile homes, cut into 2 in. strips. It was then impregnated with a single layer of #2 (0.15 in. diameter) lead shot on one side. The side without lead was placed directly on the membrane in order to keep the loads from sliding off of the model. The second weight type was the same as the first, except that both sides of the putty tape were impregnated with the lead shot. This type of weight was very time consuming to make and became unstable on top of the structure. Therefore, the third type of weight was created by coating 2 in. wide by 3 in. long sheets of duct tape with the #2 lead shot and then placing a second 2 in. by 3 in. sheet of duct tape over the exposed lead shot. This weight type was easy to make and proved to be very stable on the structure. Several strips of each weight type were weighed, thus providing an average weight per strip to be used in calculating accumulated loads on the model. During the experiment, the points at which the weight types were changed were noted in the 1:100 Scale Model Snow Loading Data Tables in Chapter 4. The sample weights that were recorded, and the average weights, can be found in Tables 3.1 and 3.2.

The strands of monofilament that were used to record the deflections hung vertically from the holes in the sheet of masonite that was attached to the bottom of the model base. The point on each monofilament strand as it exited the masonite was used as the marking point for the deflections. As the load on the model was increased, marks were made on the strands as a record of the deformed shape of the model.

Table 3.1: Weights and Averages of Lead Impregnated Putty Tape

Single Side Impregnated with #2 Lead Shot			Both Sides Impregnated with #2 Lead Shot		
Segment Length (in.)	Weight (lb)	Weight per Length (lb/in.)	Segment Length (in.)	Weight (lb)	Weight per Length (lb/in.)
1	0.03	0.03	1	0.05	0.05
2	0.06	0.03	2	0.10	0.05
3	0.09	0.03	3	0.13	0.04
4	0.11	0.03	4	0.20	0.05
5	0.14	0.03	5	0.24	0.05
6	0.15	0.03	6	0.27	0.05
1	0.03	0.03	2	0.10	0.05
1	0.03	0.03	2	0.10	0.05
1	0.03	0.03	2	0.10	0.05
Average Weight per Length = 0.03 lb/in.			Average Weight per Length = 0.05 lb/in.		

Table 3.2: Weights and Averages of Lead Coated Duct Tape

All segments were 3 in. long and 2 in. wide	
Segment	Weight (lb)
1	0.19
2	0.20
3	0.21
4	0.20
5	0.20
6	0.21
7	0.20
8	0.19
9	0.20
10	0.20
Average weight = 0.20 lb	

The testing began by marking all of the monofilament strands and then applying the first layer of single sided, lead impregnated putty tape. It was observed that the putty tape strips exceeded the boundaries of the intended loading, although for calculation purposes, the area of weight coverage was assumed to be 2 in. wide.

Load increments 2 through 7 were added using the double sided, lead impregnated putty tape and deflections were recorded for selected increments. Trials 8 through 18 were added using the #2 lead shot coated duct tape strips and deflections were again recorded for selected increments. The criteria used to determine at which load increments the deflections were recorded were based on the amount of deformation caused by a particular load increment.

Loads were added across the entire loading area for each load increment. Deflections were not marked on all of the strands for every load increment where the deflections were too small to accurately record. The loads and the marks made were recorded in the 1:100 Scale Model Snow Loading Data Table in Chapter 4, as well as comments regarding the behavior of the model during the testing. Loads were added until the membrane failed due to tearing in two bays of the model.

3.2.2 1:50 Scale Model

The dimensions of the 1:50 scale model constructed were 48 in. long, 18 in. wide, and 12 in. high, with five vertical arches, each spaced 6 in. apart. The cross sections of the arches in the model had an outside diameter of 0.50 in.

Each end of the modeled structure was comprised of three arches, all with common base points. Each arch was rotated, in plane, 30° with respect to the adjacent arches. The plane of the final arch was oriented horizontally. Therefore, the three end arches created a quarter of a sphere-like shape. The shape of each arch was formed by allowing the tubes that comprise the arches to take the most natural shape when the width, height, and base angle of the arches were fixed. The model was constructed using the same arch orientations and curvatures as the structure represented.

Materials

The materials for the model were chosen to approximate as closely as possible the types of materials used in the structures represented, as well as for practicality in construction of the model. The base for the model was made from 0.5 in. thick plywood. The arches were made of translucent polyethylene tubing, having an outside diameter of 0.50 in. and a thickness of 0.0625 in. The membrane was a flexible plastic material designed for landscaping that was 0.004 in. thick with a grainy texture and black in color. Tension tests on the membrane material estimated its modulus of elasticity as 3.6 ksi (see Appendix A).

Construction

The base was 48 in. long and 18 in. wide. The middle 24 in. of the base was rectangular, but on each end it was cut to the shape of the arches and was routed on the bottom to a radius of 0.25 in. This simulated a horizontal arch on each end of the model. Notches were cut in the base to accept the ends of each of the five vertical arches.

The polyethylene arches were formed by attaching, with two screws on each end, the tubing to a block of wood on each side of the base that was 1.45 in. tall and beveled inward at 81° from horizontal. This 81° angle was continued by the 0.50 in. wide notches in the base that the arches fit into. By fixing the tubing to these blocks and keeping the arches vertical and 12 in. high, the curve was the same for all of the arches. The curve taken by the arches was neither circular nor parabolic, although it more closely resembled a circle. The two leaning arches on each end of the model were fixed, with two screws on each end, to wooden blocks that attached securely to the base, and were also fixed at the initial 81° angle. The final arch on either end was formed by the base. By routing a 0.50 in. diameter curve on the underside perimeter of the base, it served as a band around the model, much like the band of copper tubing on the 1:100 scale model.

The membrane was formed by machine sewing sections of the material together to form an outer casing for the model that fit tightly over the framework created by the arches. The sections were created using patterns derived from the shapes between the arches. At the seams of the sections, the material was doubled along the arch lengths. Using the same material, an extra flap was machine sewn around the lower edge of the casing, and this flap was securely attached to the underside of the model with duct tape. Once the casing was positioned over the arched framework of the model, it was hand stitched to each vertical arch and to the two arches that were at 60° to horizontal, along the length of the arches. The casing was not hand sewn to the arches that were positioned at 30° to the horizontal plane. The constructed model is shown in Figure 3.7.

Wind Tunnel Testing

The wind tunnel used for the 1:50 scale model wind loading was the low-speed boundary layer wind tunnel, located at the Environmental Systems Laboratory. The wind

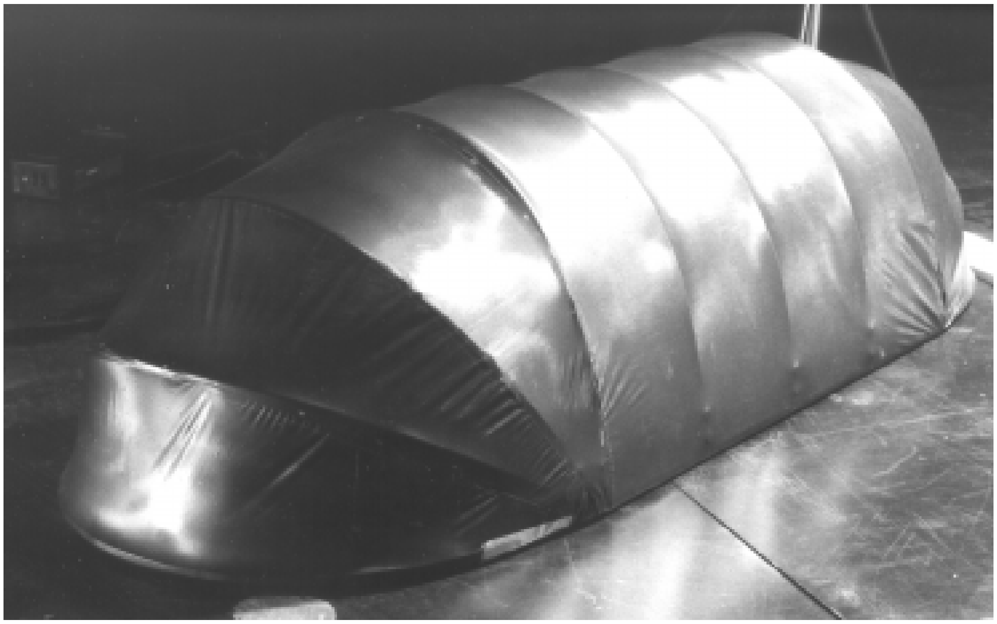

Figure 3.7: 1:50 Scale Model

speed in the tunnel was obtained from a plot located in the wind tunnel of fan frequency in Hertz versus either miles per hour or feet per second. All of the trials were conducted using the same increases in fan frequency in order to maintain consistency across the trials. The wind tunnel was equipped with a smoke generator, and an auxiliary smoke generating device was used for two of the trials.

The model was placed directly on the horizontal working surface of the wind tunnel, centered from side to side, and between the fans and the intake openings. A strip of wood, 0.75 in. by 3.50 in. by 8 ft, was placed across the work surface, along the leeward side of the model, to insure that there was no movement of the model during the testing. The model within the low-speed can be seen in Figure 3.8.

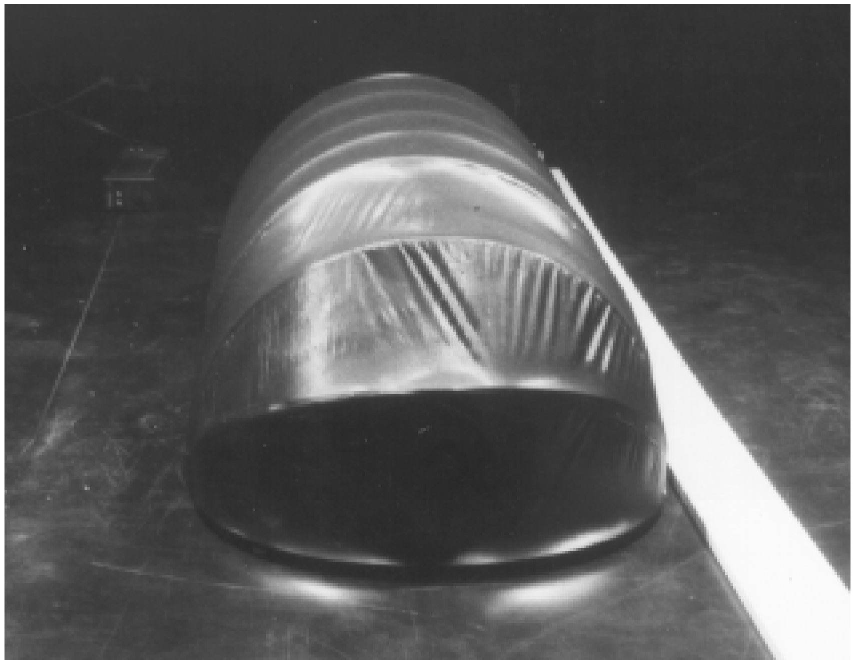

Figure 3.8: 1:50 Scale Model in Wind Tunnel During Trial 1

Five separate trials were conducted for the wind tunnel testing. Each trial consisted of placing the model at a specific orientation with respect to the wind direction and gradually, incrementally increasing the wind speed in the tunnel until the maximum speed was reached. The different angles tested were 0°, 30°, 45°, 60°, and 90° relative to the direction of the wind flow. Each trial was videotaped and photographs were taken intermittently throughout the various trials.

During each trial for the wind tunnel testing, the frequency of the fans, the miles per hour, and the feet per second velocities of the wind were recorded. In an effort to maintain some consistency across the trials, the increments used for increasing the wind velocity were kept consistent for all of the trials. The 1:50 Scale Model Wind Tunnel Testing Data Tables list the increments used. Some qualitative observations were noted as comments at various times during the testing. All of the data have been tabulated in the 1:50 Scale Model Wind Tunnel Testing Data Tables in Chapter 4.

Snow Load Testing

The snow load testing for the 1:50 scale model was conducted in the Geotechnical Laboratory located in Patton Hall. It was assumed that no snow would accumulate on any areas of the membrane that had more than a 30° angle with the horizontal plane. The area that was loaded was a strip down the center of the model that measured 10 in. wide along the curve of the arch, and spanned between the two leaning arches on each end of the model that were angled at 60° to horizontal. On the represented structure, this strip would measure 41.67 ft wide and 150.00 ft long. For measuring deflections, a total of 44 nodes was used, and these are shown in Figure 3.9. Only one quarter of the model was used for deflection measurement, assuming that the structure would behave symmetrically. In addition to the quarter of the structure, some deflections were measured along the arches that were outside of the quarter, in order to test the assumption of symmetry.

A portion of the circular base located beneath the area of the model that was to be loaded was removed without affecting the arches or the membrane, with enough extra room to facilitate easy access to the inside of the model. The portion was removed in

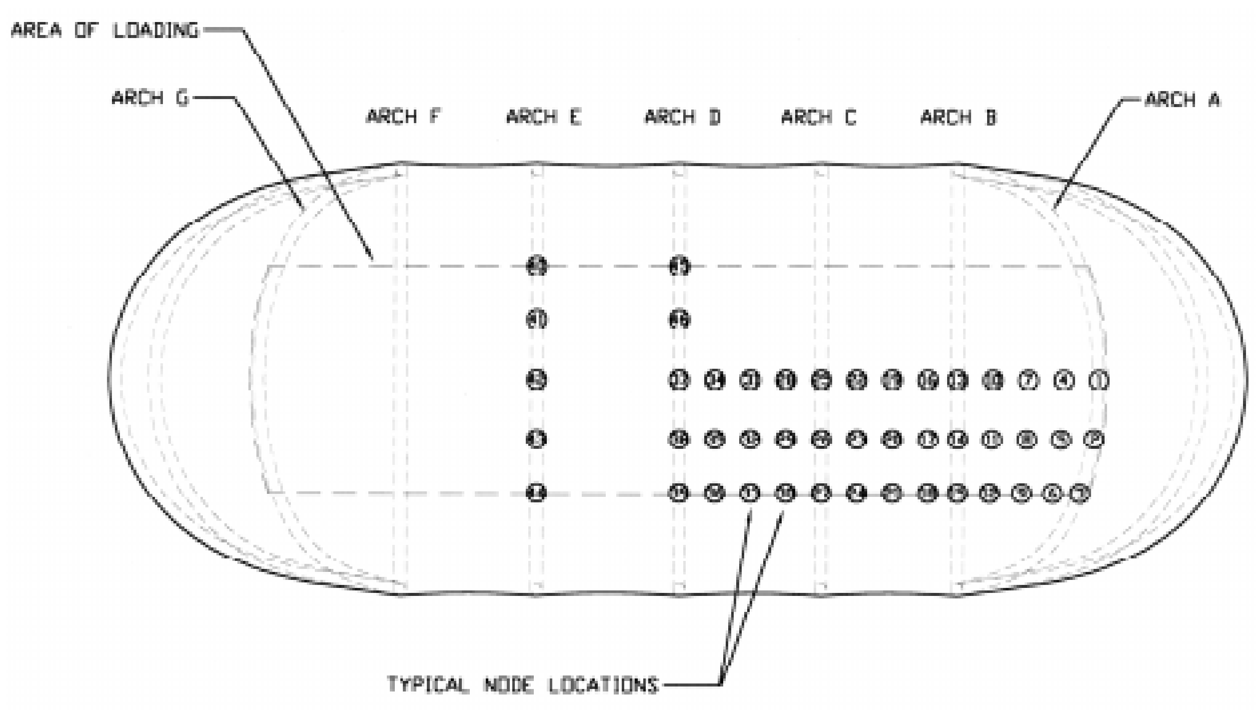

Figure 3.9: Overhead View of 1:50 Scale Model with Node Locations

order to install the deflection measuring monofilament strands. A sheet of 1/8 in. thick masonite was placed over the hole in the model base and was screwed to the underside of the base. In this masonite sheet, 5/64 in. diameter holes were drilled at locations directly under the nodes on the model. Segments of 10 lb. test, 0.012 in. diameter, monofilament penetrated the membrane at the nodes and were knotted on top of the membrane. The monofilament was kept from pushing through the membrane by stringing it through small pieces of masking tape, approximately 0.25 in. by 0.25 in, that were placed between the membrane and the knots in the end of the monofilament. All of these strands then went through the appropriate holes in the masonite and were marked at the lower end with the node numbers written on pieces of masking tape that were attached to the ends of the monofilament. These markers also served to keep the strands hanging vertically, without deflecting the membrane and are shown in Figure 3.10.

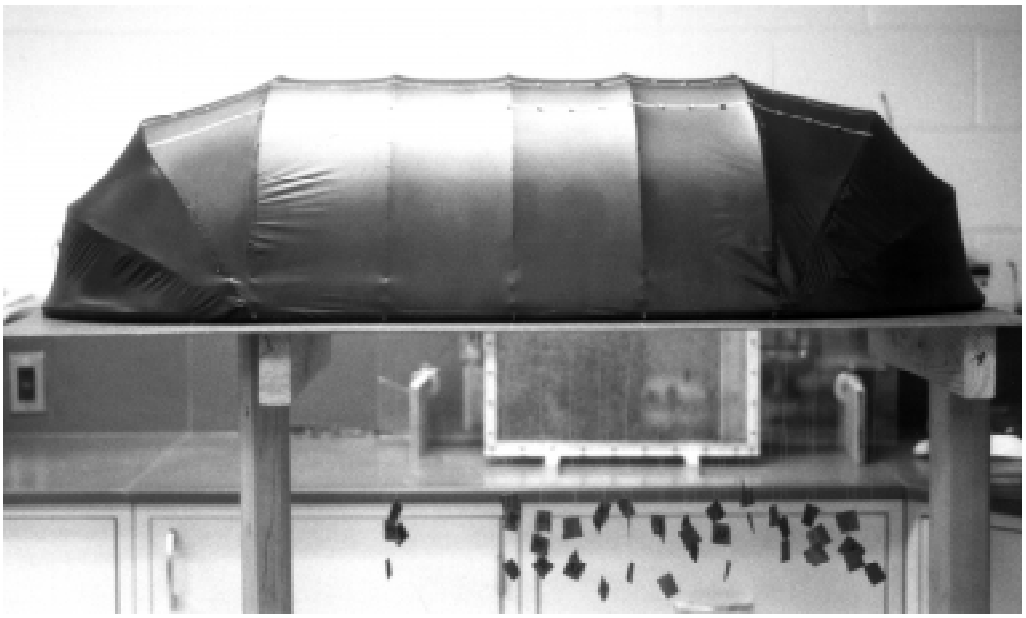

Figure 3.10: 1:50 Scale Model with Monofilament Strand Deflection Markers

The snow loading for the 1:50 scale model was done using variations of a single weight type. The weights were varied as a result of making use of the weights that were used for the 1:100 scale model snow loading. All of the load strips were held together using strips of duct tape, 2 in. wide and 10 in. long. The first load increment recycled the lead impregnated putty tape segments from the 1:100 scale model snow loading, by sandwiching several pieces of it between two 10 in. strips of duct tape. The composite strips varied in weight, but all of them weighed between 0.80 pounds and 0.95 pounds.

The entire layer of load was weighed and an average weight per strip was used for the load determinations. The second load increment used the 2 in. by 3 in. strips of lead shot and duct tape used for the 1:100 scale model snow loading by connecting three of the 3 in. segments together with two 10 in. strips of duct tape. This load layer was also weighed and an average weight per strip was assumed. The third load increment was created by coating 2 in. wide by 10 in. long sheets of duct tape with #7½ (0.095 in. diameter) lead shot and then placing a second 2 in. by 10 in. sheet of duct tape over the exposed lead shot.

The strands of monofilament that were used to record the deflections hung vertically from the holes in the sheet of masonite that was attached to the bottom of the model base. The point on each monofilament strand as it exited the masonite was used as the marking point for the deflections. The testing began by marking all of the monofilament strands and then applying the first layer of weights. Each load layer was added in such a manner as to load the model symmetrically. This was accomplished by starting at either end of the model and adding the load by bays, alternating from one end to the other, towards the center bay of the model. After marks were made on the monofilament strands, the next layer of loads was added. Between the second and third load increments, two marks were made on each strand of monofilament. The first mark was made immediately after the application of the second load. The second mark was made 2 hours after the load was added, immediately prior to addition of the third load increment, and measured the amount of deformation due to sustained loading, or creep. Loads were added across the entire loading area for each load increment. Deflections were recorded on all of the strands for every load increment due to the large deflections at each loading. The loads and the marks made, as well as comments regarding the behavior of the model during the testing, were recorded in the 1:50 Scale Model Snow Loading Data Table in Chapter 4. Loads were added until the model failed due to simultaneous collapse of the loaded arches.

3.2.3 1:50 Scale Single Arch Model

The arch represented by the single arch model built at a 1:50 scale was 75 ft wide and 50 ft high, with a 2 ft diameter tube. Therefore the model dimensions were 18 in. wide and 12 in. high, and the cross sections of the arches in the model had an outside diameter of 0.50 in. The shape of each arch was created by allowing the tubes that comprise the arches to take the most natural shape when the width, height, and base angle of the arches were fixed. The constructed model is shown in Figure 3.11.

Materials

The base for the model was made from 0.5 in. thick plywood. The arches were made of translucent polyethylene tubing, having an outside diameter of 0.50 in. and a thickness of 0.0625 in.

Construction

The base was 14 in. long and 18 in. wide. Notches were cut into the base to accept the ends of the arch.

The polyethylene arch was formed by attaching, with two screws on each end, the tubing to a block of wood on each side of the base. The blocks were 2.13 in. tall and beveled inward at 81° from horizontal. This 81° angle was continued in the 0.50 in. wide

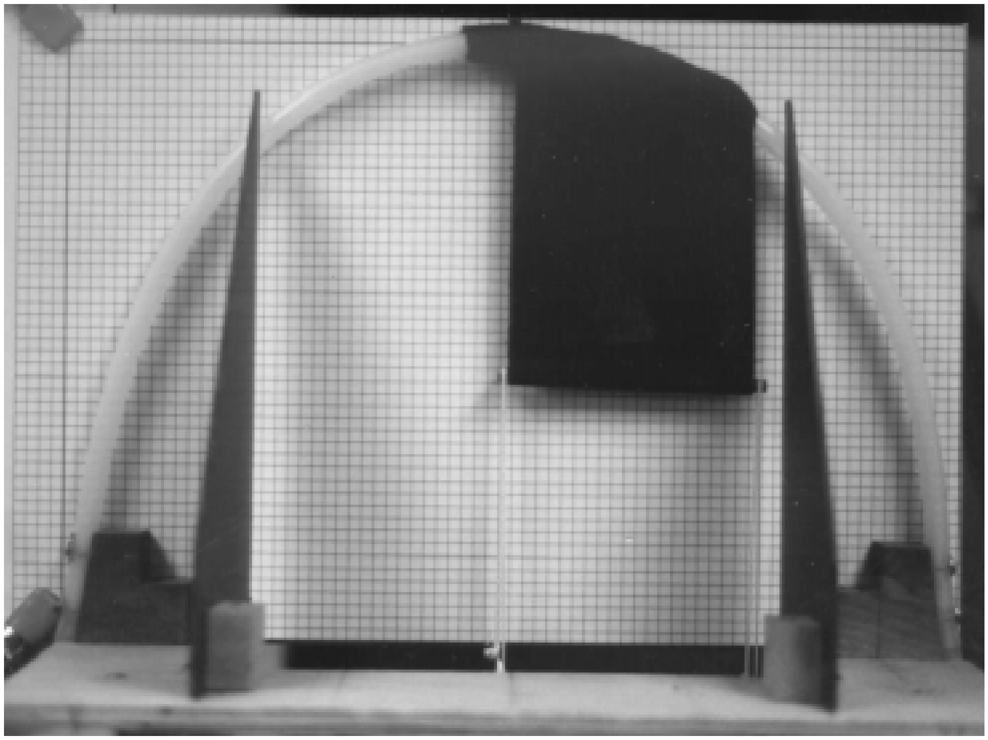

Figure 3.11: 1:50 Scale Single Arch Model with Partial Load Apparatus

notches in the base that the arch ends fit into. The curve taken by the arch was neither circular nor parabolic, although it more closely resembled a circle. For each of the eight trials that were conducted, a new piece of tubing was used.

It was necessary for most of the snow loading trials to have the arch restrained from deflecting out of the plane of the arch excessively. On one side of the arch, restraint was accomplished by a 12 in. by 18 in. piece of masonite, positioned parallel to the plane of the arch, 0.25 in. away from the arch. This masonite was also there as a backing for the sheets of gridded paper that were used to mark the deflected shapes of the arch. On the other side of the arch, two pieces of masonite, 11.00 in. high, were placed perpendicular to the plane of the arch, each at 5.25 in. from the arch center. The edges of the masonite pieces were also 0.25 in. away from the arch. These restraints were removable to allow for unrestrained trials as well.

Snow Load Testing

The snow load testing for the 1:50 scale single arch model was conducted in the Geotechnical Laboratory located in Patton Hall. Trials were done for full snow loading and partial snow loading. The full snow load was such that 10 in. along the curve of the arch was subjected to a uniformly distributed load. On the represented structure, this strip would measure 41.67 ft along the arch. The partial snow load was such that 5 in. along the curve of the arch, beginning at the arch center, was subjected to a uniformly distributed load. On the represented structure, this strip would measure 20.83 ft along the arch.

The shapes taken by each arch during a given trial were recorded by scribing lines along the top of each arch after the load increment had been added. These lines were drawn directly onto a sheet of paper with a 0.25 in. grid throughout. Care was taken to ensure that the lines accurately rendered the shapes of the loaded arches.

The full snow loading of the single arch was accomplished by using a 9.50 in. wide by 7.00 in. long, double layered fabric sheet that was sewn together to form fabric tubes along the two 9.50 in. long edges. The top edge was shaped to the curvature of the arch, so that the fabric tube fit snugly around the cross section of the arch. A 5/16 in. diameter, 10.50 in. long hollow brass tube was slid through the tube in the lower edge of the fabric sheet and had small notches cut near each end. The partial snow loading had the same setup, except that the fabric was cut in half and a small screw was placed through the fabric into the arch at the top of the curve to keep the sleeve from sliding off of the arch. The brass tube was also cut, to 5 in. long, with the notches added on each end. A 6 in. by 12 in. portion of the base was removed from the center of the base without affecting the arch, so that the apparatus for adding the load to the arch could be installed. This apparatus consisted of two small plastic buckets that were suspended by strings, fit into the notches in the brass tube, and hung through the opening in the model base. Increments of #2 lead shot were then weighed and placed in the suspended buckets. The shape of the arch was outlined along its top edge, depending on the amount of deflection the arch underwent. Care was taken to ensure that the scribed lines accurately represented the deformed arches. Certain increments were not outlined if the deflections were too close to those from the previous load increment. Loading combinations were varied in order to expand the understanding of the behavior of the loaded arches. The model with the load apparatus attached is shown in Figure 3.12.

The loads and comments made during the testing were recorded in the 1:50 Scale Single Arch Model Snow Loading Data Tables. The deflected shapes were digitized and are presented with the Data Tables in Chapter 4. A total of eight trials was performed, three trials with the full snow load, laterally restrained, two trials with the full snow load, laterally unrestrained, two trials with the partial snow load, laterally restrained, and one trial with the partial snow load, laterally unrestrained. Loads were added until each arch failed due to snap-through, or until the deflections became so excessive that the loading apparatus was bearing on some part of the model or model base.

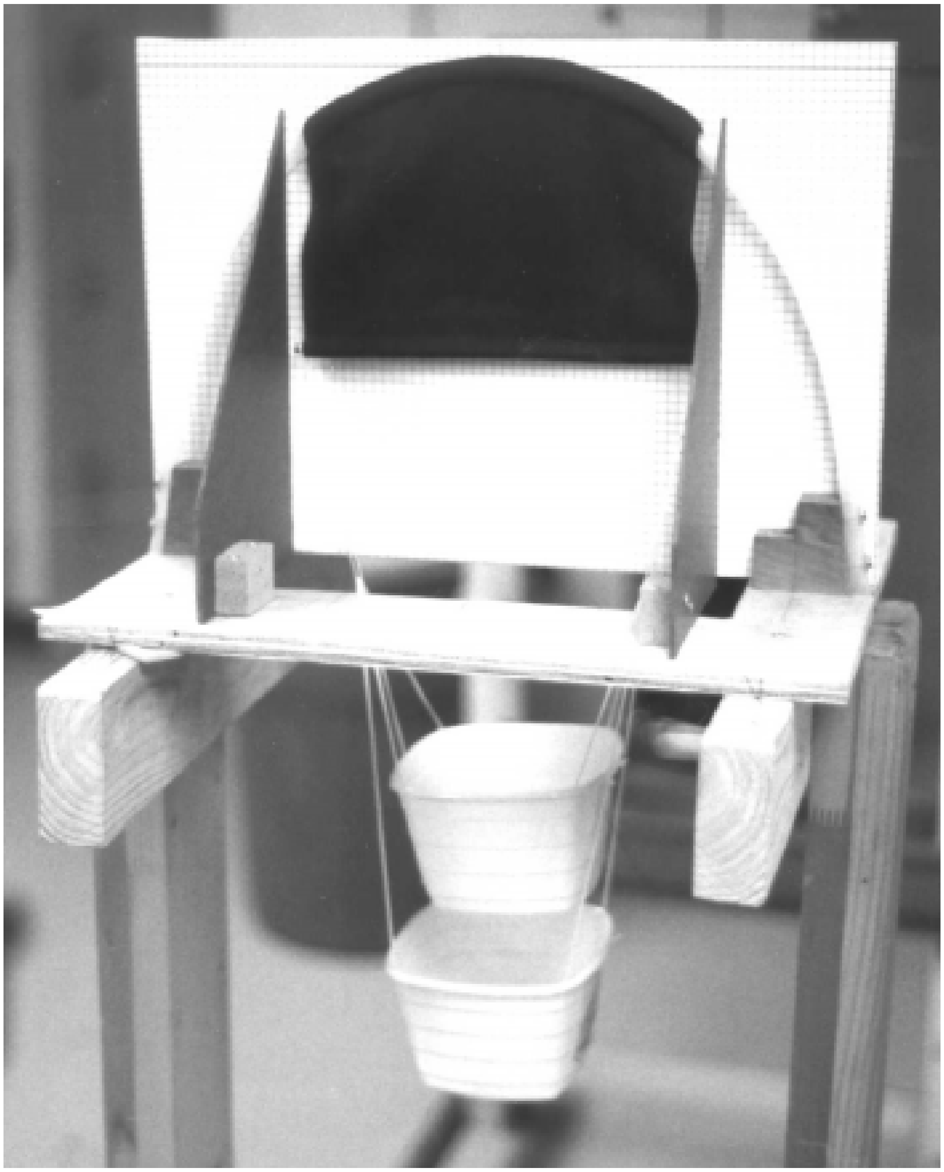

Figure 3.12: 1:50 Scale Single Arch Model with Loading Apparatus

Chapter 4. Results

4.1 Introduction

Results from the wind and snow load tests for the three different models are tabulated in Tables 4.1 - 4.23. The tables are grouped into sets based on the different types of models used and testing performed. The tables include readings taken from instrumentation at the time of the tests, load increments, qualitative comments on the visual observations of the behavior of the models during the tests, and additional calculations useful for interpreting the observed and measured data. Comments regarding the observations made during the testing and clarifications of the notations used in the tables are provided following each set of tables. Photographs and diagrams of the various models used and tests conducted are presented following each set of tables.

4.2 1:100 Scale Model

4.2.1 Wind Tunnel Testing

The results of the wind tunnel testing for the 1:100 scale model were primarily qualitative, obtained by visual observation. Results describe model behavior under varying wind velocities across five different trials. These data are shown in Tables 4.1 - 4.5.

Manometer tare readings indicate the pressure recorded from the differential manometer just prior to testing. The density of air was determined using the following equation:

Table 4.1: 1:100 Scale Model Wind Tunnel Testing Data Table: Trial 1

TRIAL 1: LONG SIDE OF MODEL 90° TO WIND DIRECTION

January 6, 1998
Manometer tare: 0.090 in. water
Temperature: 25.8 °C
Start time: 9:22 a.m.
Barometric Pressure: 27.975 in. mercury (94723 N/m^2)
Air Density: 1.104 kg/m^3

RPM	Manometer Reading (in. water)	Pressure (N/m^2)	Velocity (ft/sec)	Velocity (mph)	Reynolds Number	Froude Number	Comments	Video Frame
100	0.14	12.45	15.6	10.6	173742	1.9		
150	0.24	37.36	27.0	18.4	300930	3.4		
200	0.40	75.97	38.5	26.2	429111	4.8		
250	0.59	124.5	49.3	33.6	549421	6.1	begin slight flutter on leeward side	
275	0.70	150.7	54.2	37.0	604363	6.8		
300	0.82	181.8	59.5	40.6	663868	7.4		
325	0.93	208.0	63.7	43.4	710008	7.9		
350	1.06	241.6	68.6	46.8	765255	8.6		
375	1.21	279.0	73.8	50.3	822298	9.2	significant deflections	
400	1.34	311.4	77.9	53.1	868711	9.7		
425	1.52	356.2	83.3	56.8	929155	10.4	(photo taken)	
450	1.68	394.8	87.7	59.8	978216	10.9		
475	1.86	440.9	92.7	63.2	1033729	11.6		612
500	2.04	484.5	97.2	66.3	1083627	12.1	very little flutter of membrane	
525	2.22	529.3	102	69.3	1132660	12.7		
550	2.51	602.8	108	73.9	1208726	13.5		

Table 4.2: 1:100 Scale Model Wind Tunnel Testing Data Table: Trial 2

TRIAL 2: LONG SIDE OF MODEL 45^o TO WIND DIRECTION

January 6, 1998
Manometer tare: 0.065 in. water
Temperature: 25.9 ^oC
Start time: 10:19 a.m.
Barometric Pressure: 27.975 in. mercury (94723 N/m^2)
Air Density: 1.104 kg/m^3

RPM	Manometer Reading (in. water)	Pressure ((N/m^2)	Velocity (ft/sec)	Velocity (mph)	Reynolds Number	Froude Number	Comments	Video Frame
50	0.09	6.23	11.02	7.51	122854	1.4		
100	0.14	18.68	19.09	13.0	212790	2.4		
150	0.24	43.59	29.16	19.9	325042	3.6		
175	0.31	61.03	34.50	23.5	384595	4.3		
200	0.39	80.95	39.73	27.1	442957	5.0	small deflections, very slight flutter	
250	0.57	125.79	49.53	33.8	552161	6.2		
275	0.67	150.70	54.21	37.0	604363	6.8		
300	0.82	188.06	60.56	41.3	675140	7.5		
325	0.93	215.46	64.82	44.2	722650	8.1		
350	1.06	247.84	69.52	47.4	775054	8.7		591
375	1.21	285.20	74.58	50.8	831425	9.3	significant deflections noted	629
400	1.38	327.54	79.92	54.5	891011	10.0	vibration on leeward end	776
425	1.57	374.87	85.50	58.3	953210	10.7	slight flutter noted	822
450	1.74	417.21	90.20	61.5	1005605	11.2		
475	1.89	454.58	94.15	64.2	1049667	11.7		
500	2.11	509.38	99.67	68.0	1111135	12.4		
525	2.28	551.72	103.7	70.7	1156397	12.9		
550	2.55	618.97	109.9	74.9	1224851	13.7	end vibration, severe deflections	1064

Table 4.3: 1:100 Scale Model Wind Tunnel Testing Data Table: Trial 3

TRIAL 3: LONG SIDE OF MODEL PARALLEL TO WIND DIRECTION

January 6, 1998
Manometer tare: 0.070 in. water
Temperature: 26.2 ^{o}C
Start time: 11:01 a.m.
Barometric Pressure: 27.975 in. mercury (94723 N/m^2)
Air Density: 1.102 kg/m^3

RPM	Manometer Reading (in. water)	Pressure (N/m^2)	Velocity (ft/sec)	Velocity (mph)	Reynolds Number	Froude Number	Comments	Video Frame
50	0.09	4.98	9.87	6.73	109984	1.2		112
100	0.15	19.93	19.7	13.5	219968	2.5	(measurements shown in video)	181
150	0.26	47.33	30.4	20.7	338993	3.8		
200	0.41	84.69	40.7	27.7	453475	5.1		
225	0.49	104.6	45.2	30.8	504009	5.6		
250	0.62	137.0	51.7	35.3	576760	6.4		330
275	0.73	164.4	56.7	38.6	631809	7.1	deflections noted, no flutter	
300	0.85	194.3	61.6	42.0	686849	7.7	slight flutter at leeward end	
325	1.00	231.6	67.3	45.9	749990	8.4		
350	1.16	271.5	72.8	49.7	811946	9.1	flutter near second vertical arch	482
375	1.30	306.4	77.4	52.8	862515	9.6	significant deflections noted	
400	1.49	353.7	83.1	56.7	926740	10.4		
425	1.68	401.0	88.5	60.4	986795	11.0		
450	1.89	453.3	94.1	64.2	1049179	11.7		
475	2.09	503.1	99.1	67.6	1105324	12.4		733
500	2.29	553.0	104	70.9	1158752	13.0	wavering rippling at top and middle	
525	2.55	617.7	110	74.9	1224728	13.7	same rippling	
550	2.75	667.5	114	77.9	1273155	14.2	same rippling	

Table 4.4: 1:100 Scale Model Wind Tunnel Testing Data Table: Trial 4

TRIAL 4: LONG SIDE OF MODEL 30^{o} TO WIND DIRECTION

January 6, 1998
Manometer tare: 0.060 in. water
Temperature: 25.7 ^{o}C
Start time: 12:07 p.m.
Barometric Pressure: 27.975 in. mercury (94723 N/m^2)
Air Density: 1.104 kg/m^3

RPM	Manometer Reading (in. water)	Pressure (N/m^2)	Velocity (ft/sec)	Velocity (mph)	Reynolds Number	Froude Number	Comments	Video Frame
50	0.09	7.47	12.1	8.23	134580	1.5		
100	0.14	19.93	19.7	13.4	219768	2.5		
150	0.23	42.34	28.7	19.6	320365	3.6		140
200	0.38	79.71	39.4	26.9	439537	4.9	deflections noted, slight flutter	
225	0.45	97.14	43.5	29.7	485235	5.4		218
250	0.54	119.6	48.3	32.9	538320	6.0	slight flutter on leeward side	
275	0.64	144.5	53.1	36.2	591744	6.6		
300	0.77	176.8	58.7	40.0	654711	7.3	slight flutter at leeward end, near bottom	350
325	0.88	204.2	63.1	43.0	703602	7.9	same	370
350	1.01	235.4	67.8	46.2	755329	8.4		440
375	1.17	276.5	73.4	50.1	818619	9.2	slight flutter on end cap	
400	1.31	311.4	77.9	53.1	868711	9.7		529
425	1.47	351.2	82.8	56.4	922635	10.3		550
450	1.62	388.6	87.1	59.4	970471	10.8		
475	1.79	430.9	91.7	62.5	1021982	11.4		
500	1.98	478.2	96.6	65.8	1076641	12.0	severe deflections	
525	2.17	525.6	101	69.0	1128656	12.6		
550	2.45	595.3	108	73.5	1201211	13.4		

Table 4.5: 1:100 Scale Model Wind Tunnel Testing Data Table: Trial 5

TRIAL 5: LONG SIDE OF MODEL 60° TO WIND DIRECTION

January 6, 1998
Manometer tare: 0.060 in. water
Temperature: 25.6 °C
Start time: 12:45 p.m.
Barometric Pressure: 27.975 in. mercury (94723 N/m²)
Air Density: 1.105 kg/m³

RPM	Manometer Reading (in. water)	Pressure (N/m²)	Velocity (ft/sec)	Velocity (mph)	Reynolds Number	Froude Number	Comments	Video Frame
50	0.08	4.98	9.85	6.72	109834	1.2		
100	0.15	22.42	20.9	14.2	232994	2.6		50
150	0.25	47.33	30.4	20.7	338533	3.8		80
200	0.41	87.18	41.2	28.1	459470	5.1		120
225	0.49	107.11	45.7	31.1	509281	5.7	slight deflections	160
250	0.59	132.01	50.7	34.6	565407	6.3	very slight flutter	200
275	0.70	159.41	55.7	38.0	621317	6.9		240
300	0.83	191.79	61.1	41.7	681505	7.6	bulging on leeward side	270
325	0.97	226.67	66.5	45.3	740874	8.3		
350	1.11	261.54	71.4	48.7	795826	8.9	[a]	
375	1.27	301.39	76.6	52.2	854312	9.5		360
400	1.43	341.24	81.5	55.6	909042	10.2	[b]	460
425	1.61	386.08	86.7	59.1	966918	10.8	[c]	500
450	1.80	433.41	91.9	62.7	1024468	11.5	[d]	530
475	1.94	468.28	95.5	65.1	1064885	11.9		560
500	2.19	530.55	102	69.3	1133479	12.7	[e]	
525	2.45	595.31	108	73.4	1200667	13.4	[f]	640
550	2.75	670.03	114	77.9	1273796	14.2	[g]	720

[a] slight rippling on leeward side near the bottom, near end cap
[b] slight rippling on windward end, near cap towards bottom
[c] slight rippling on windward side at the top of the end cap
[d] slight rippling on windward side at the top of the end cap
[e] rippling creeping around to leeward side
[f] rippling r between last arches on windward end cap
[g] rippling between last arches on windward end cap

$$\rho = \frac{P}{RT}$$

where:

ρ = air density (kg/m^3)

P = barometric pressure (N/m^2)

R = universal gas constant = 287.05 N-m/kg-K

T = temperature (K).

Differential manometer readings taken during the testing were converted to velocities using Bernoulli's equation for fluids, the temperature for each trial, and the barometric pressure. Calculated velocities ranged from 0 to 77.9 miles per hour. Reynolds numbers and Froude numbers were also calculated for all of the trials and velocities.

Certain model responses were similar across the five trials. Slight membrane flutter, defined as an oscillation of some portion of the membrane, began between 200 and 300 revolutions per minute during all trials. Flutter decreased when the deformations of the membrane became severe enough to put tension in the membrane. In all trials, the regions of pressure and suction as a result of wind velocity pressure were easily identifiable. No damage was caused to the membrane or the model as a result of fluttering, pressure, or suction.

During some trials, the model responded to wind conditions in a noteworthy manner. During Trials 3 and 5, where the long side of the model was at 0° and 60°, respectively to the wind flow, some erratic rippling of the membrane was noted. For Trial 3 this occurred along the ridge of the model between the two windward-most vertical arches. For Trial 5 this occurred on the windward end between the horizontal end arch and the first angled arch, which was angled 30° with respect to horizontal. This rippling did not cause any damage to the membrane or the model.

All of the trials, except for Trial 3, resulted in pressure on approximately 80% of the windward side up from the bottom of the arches, as shown in Figure 4.1. The remainder of the membrane bulged outward in suction. These trends varied slightly on the ends of the model, depending on the angle of orientation with respect to the wind. However, Trial 3 resulted in alternating regions of pressure and suction that occurred in each vertical bay, as shown in Figure 4.2.

Observations indicated that the membrane was the only portion of the model that deflected during the testing; the arches remained stationary. Throughout all of the trials, no portion of the model was damaged, and the membrane did not rupture.

Since no damage was inflicted upon the membrane or the arches during the wind tunnel testing, the same model was used, without modification, for the snow load testing.

4.2.2 Snow Load Testing

Both quantitative and qualitative results were obtained from the snow load testing. The qualitative results were obtained from observations made of the behavior of the model as the loads were increased to failure. Measurements were taken from 27 nodes located in the membrane as the membrane deflected under the loading. Results are shown in Tables 4.6, 4.7a, and 4.7b. The deflections recorded in Tables 4.7a and 4.7b are the total deflections from the unloaded state of the model. The placement of the nodes on the membrane is shown in Figure 4.3.

Figure 4.1: 1:100 Scale Model Wind Tunnel Test Trial 4

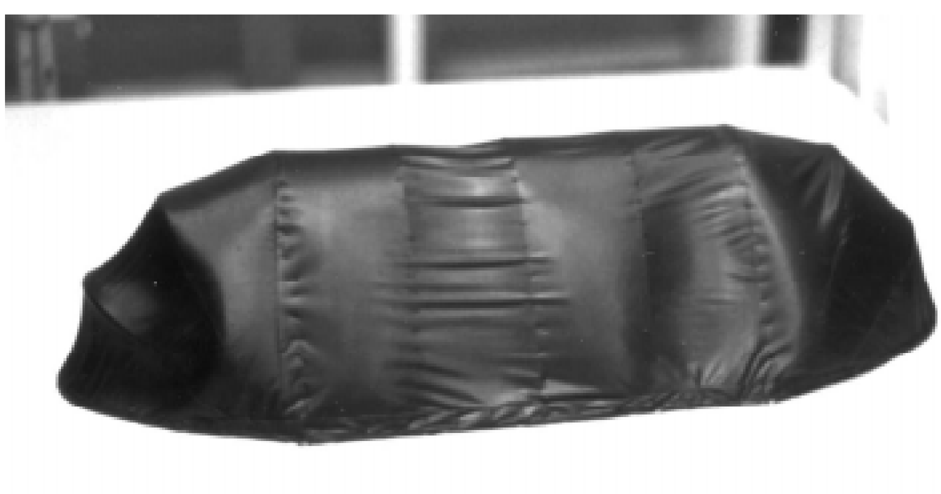

Figure 4.2: 1:100 Scale Model Wind Tunnel Test Trial 3

Table 4.6: 1:100 Scale Model Snow Load Testing Data Table

Increment Number	# of Load Strips in Each End Bay	# of Load Strips in Each Middle Bay	Weight per Strip (pounds)	Weight on Membrane (pounds)	Load on Membrane (pounds/ft^2)
0	0	0	0	0	0
1	4	3	0.06	1.20	4.80
2	3	3	0.10	3.00	12.00
3	3	3	0.10	4.80	19.20
4	3	3	0.10	6.60	26.40
5	3	3	0.10	8.40	33.60
6	3	3	0.10	10.20	40.80
7	3	3	0.10	12.00	48.00
8	1	1	0.20	13.20	52.80
9	1	1	0.20	14.40	57.60
10	1	1	0.20	15.60	62.40
11	1	1	0.20	16.80	67.20
12	1	1	0.20	18.00	72.00
13	1	1	0.20	19.20	76.80
14	1	1	0.20	20.40	81.60
15	1	1	0.20	21.60	86.40
16	1	1	0.20	22.80	91.20
17	1	1	0.20	24.00	96.00
18	1	1	0.20	25.20	100.80

Increment Number	Comments
0	black mark made on all markers
1	single sided lead impregnated putty tape used, photo taken, black mark made on all markers
2	double sided lead impregnated putty tape used until noted, black marks made on all markers
3	photo taken, black marks made on bay AB and the center markers in bays BC and CD
4	white mark made on center markers of bays as well as markers 25, 26, and 27
5	2 photos taken, no marks made
6	black marks made on all markers
7	no marks made
8	lead impregnated duct tape used for remaining increments, no marks made, photo taken
9	white marks made on bay AB markers
10	no marks made
11	no marks made, close-up photo taken
12	no marks made
13	black marks made on all markers, end photo taken
14	no marks made
15	no marks made
16	no marks made
17	failure, fabric torn in bays DE and EF, load on bay BC toppled and replaced
18	attempted additional loads in bays AB, BC and CD, the loads were very unstable, end of experiment

Table 4.7a: 1:100 Scale Model Snow Load Testing Deflection Table (in.)

		Increment Numbers								
	Node	1	2	3	4	5	6	7	8	9
Bay AB	1	0.15	0.21	0.30	0.35	N/A	0.45	N/A	N/A	0.58
	2	0.18	0.26	0.31	0.35	N/A	0.43	N/A	N/A	0.60
	3	0.11	0.19	0.25	0.29	N/A	0.35	N/A	N/A	0.51
	4	0.21	0.30	0.41	0.46	N/A	0.57	N/A	N/A	0.71
	5	0.26	0.35	0.45	0.50	N/A	0.60	N/A	N/A	0.73
	6	0.22	0.31	0.36	0.44	N/A	0.50	N/A	N/A	0.63
	7	0.17	0.22	0.29	0.32	N/A	0.40	N/A	N/A	0.48
	8	0.21	0.24	0.32	0.36	N/A	0.42	N/A	N/A	0.50
	9	0.16	0.20	0.25	0.31	N/A	0.35	N/A	N/A	0.42
Bay BC	10	0.08	0.19	N/A	N/A	N/A	0.25	N/A	N/A	N/A
	11	0.08	0.19	N/A	N/A	N/A	0.24	N/A	N/A	N/A
	12	0.12	0.20	N/A	N/A	N/A	0.24	N/A	N/A	N/A
	13	0.14	0.27	0.32	0.37	N/A	0.44	N/A	N/A	N/A
	14	0.13	0.28	0.32	0.36	N/A	0.42	N/A	N/A	N/A
	15	0.11	0.18	0.21	0.24	N/A	0.30	N/A	N/A	N/A
	16	0.12	N/A	N/A	N/A	N/A	0.23	N/A	N/A	N/A
	17	0.15	0.17	N/A	N/A	N/A	0.28	N/A	N/A	N/A
	18	0.10	0.16	N/A	N/A	N/A	0.25	N/A	N/A	N/A
Bay CD	19	0.06	0.17	N/A	N/A	N/A	N/A	N/A	N/A	N/A
	20	0.09	0.22	N/A	N/A	N/A	N/A	N/A	N/A	N/A
	21	0.10	0.25	N/A	N/A	N/A	N/A	N/A	N/A	N/A
	22	0.09	0.19	0.30	0.37	N/A	0.42	N/A	N/A	N/A
	23	0.12	0.23	0.27	0.32	N/A	0.39	N/A	N/A	N/A
	24	0.13	0.22	0.28	0.34	N/A	0.39	N/A	N/A	N/A
	25	0.08	0.16	N/A	0.24	N/A	0.29	N/A	N/A	N/A
	26	0.04	0.12	N/A	0.21	N/A	0.25	N/A	N/A	N/A
	27	0.06	0.12	N/A	0.18	N/A	0.21	N/A	N/A	N/A

Table 4.7b: 1:100 Scale Model Snow Load Testing Deflection Table (in.)

		Increment Number								
	Node	10	11	12	13	14	15	16	17	18
Bay AB	1	N/A	N/A	N/A	0.68	N/A	N/A	N/A	0.72	N/A
	2	N/A	N/A	N/A	0.69	N/A	N/A	N/A	0.72	N/A
	3	N/A	N/A	N/A	0.56	N/A	N/A	N/A	0.72	N/A
	4	N/A	N/A	N/A	0.80	N/A	N/A	N/A	0.95	N/A
	5	N/A	N/A	N/A	0.81	N/A	N/A	N/A	0.96	N/A
	6	N/A	N/A	N/A	0.71	N/A	N/A	N/A	0.88	N/A
	7	N/A	N/A	N/A	0.53	N/A	N/A	N/A	0.68	N/A
	8	N/A	N/A	N/A	0.56	N/A	N/A	N/A	0.69	N/A
	9	N/A	N/A	N/A	0.46	N/A	N/A	N/A	0.62	N/A
Bay BC	10	N/A	N/A	N/A	0.34	N/A	N/A	N/A	N/A	N/A
	11	N/A	N/A	N/A	0.32	N/A	N/A	N/A	N/A	N/A
	12	N/A	N/A	N/A	0.30	N/A	N/A	N/A	0.35	N/A
	13	N/A	N/A	N/A	0.52	N/A	N/A	N/A	0.54	N/A
	14	N/A	N/A	N/A	0.51	N/A	N/A	N/A	0.57	N/A
	15	N/A	N/A	N/A	0.38	N/A	N/A	N/A	0.47	N/A
	16	N/A	N/A	N/A	0.33	N/A	N/A	N/A	0.36	N/A
	17	N/A	N/A	N/A	0.30	N/A	N/A	N/A	0.39	N/A
	18	N/A	N/A	N/A	0.30	N/A	N/A	N/A	0.36	N/A
Bay CD	19	N/A	N/A	N/A	N/A	N/A	N/A	N/A	0.34	N/A
	20	N/A	N/A	N/A	N/A	N/A	N/A	N/A	0.45	N/A
	21	N/A	N/A	N/A	0.30	N/A	N/A	N/A	0.40	N/A
	22	N/A	N/A	N/A	0.48	N/A	N/A	N/A	0.84	N/A
	23	N/A	N/A	N/A	0.47	N/A	N/A	N/A	0.75	N/A
	24	N/A	N/A	N/A	N/A	N/A	N/A	N/A	0.69	N/A
	25	N/A	N/A	N/A	0.37	N/A	N/A	N/A	0.61	N/A
	26	N/A	N/A	N/A	0.33	N/A	N/A	N/A	0.55	N/A
	27	N/A	N/A	N/A	0.26	N/A	N/A	N/A	0.44	N/A

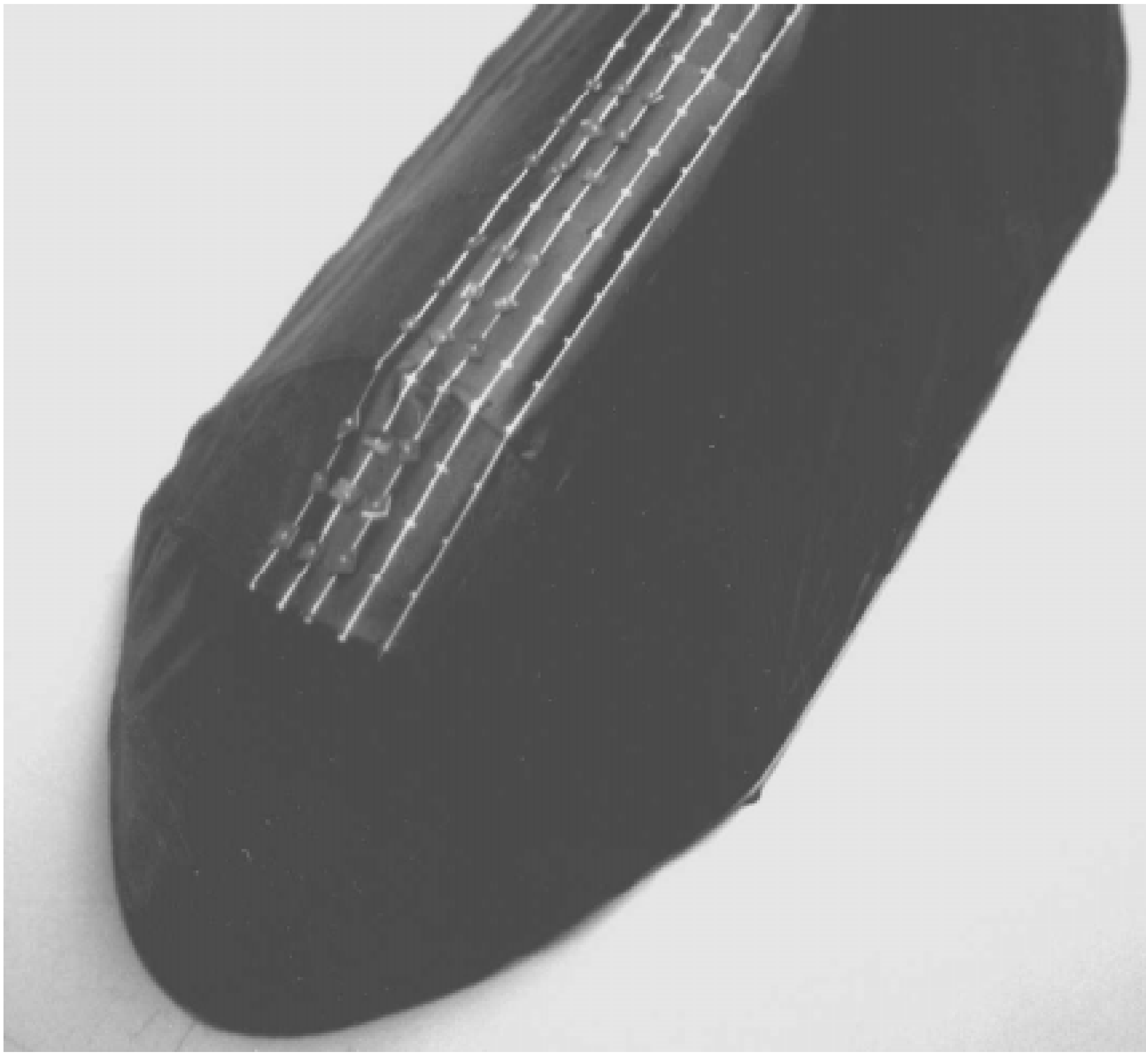

Figure 4.3: 1:100 Scale Model Node Layout

Figures 4.4, 4.5, and 4.6 present the deflected shapes of the membrane at load increments 0, 1, 6, 13, and 17, at three cross sections of the model. These increments were used because they provided the most complete sets of measurements during the testing.

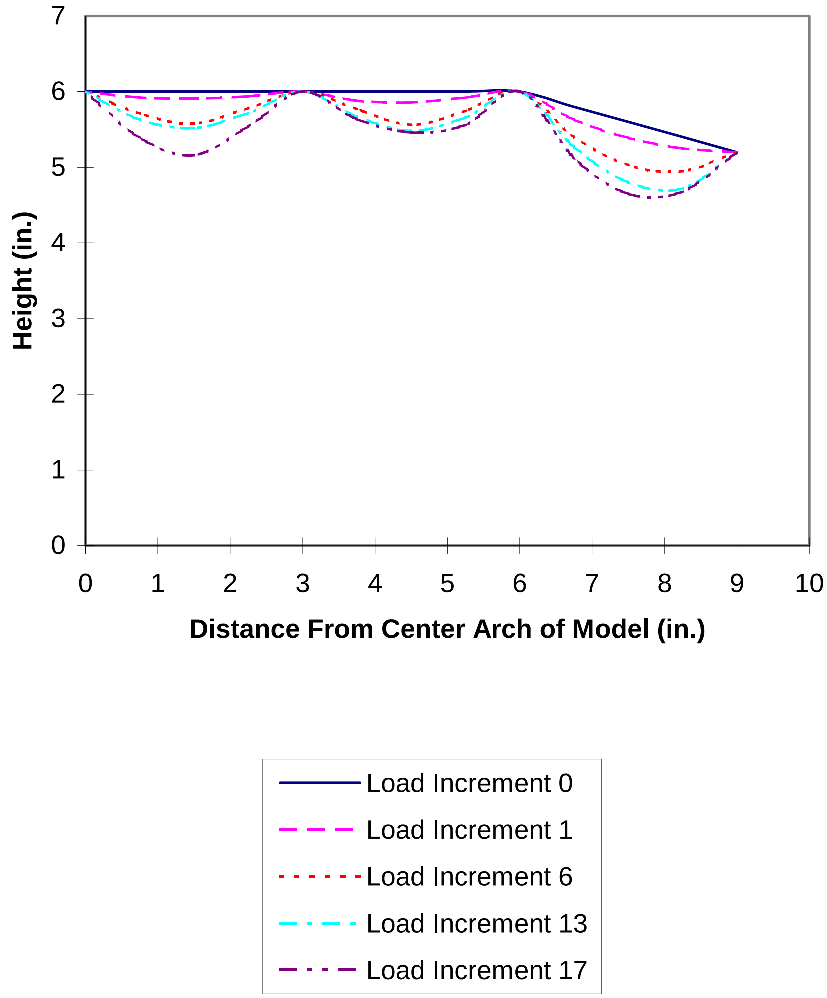

Figure 4.4: 1:100 Scale Model Membrane Deflections at Load Increments 0, 1, 6, 13, and 17 Between Nodes 1 and 25

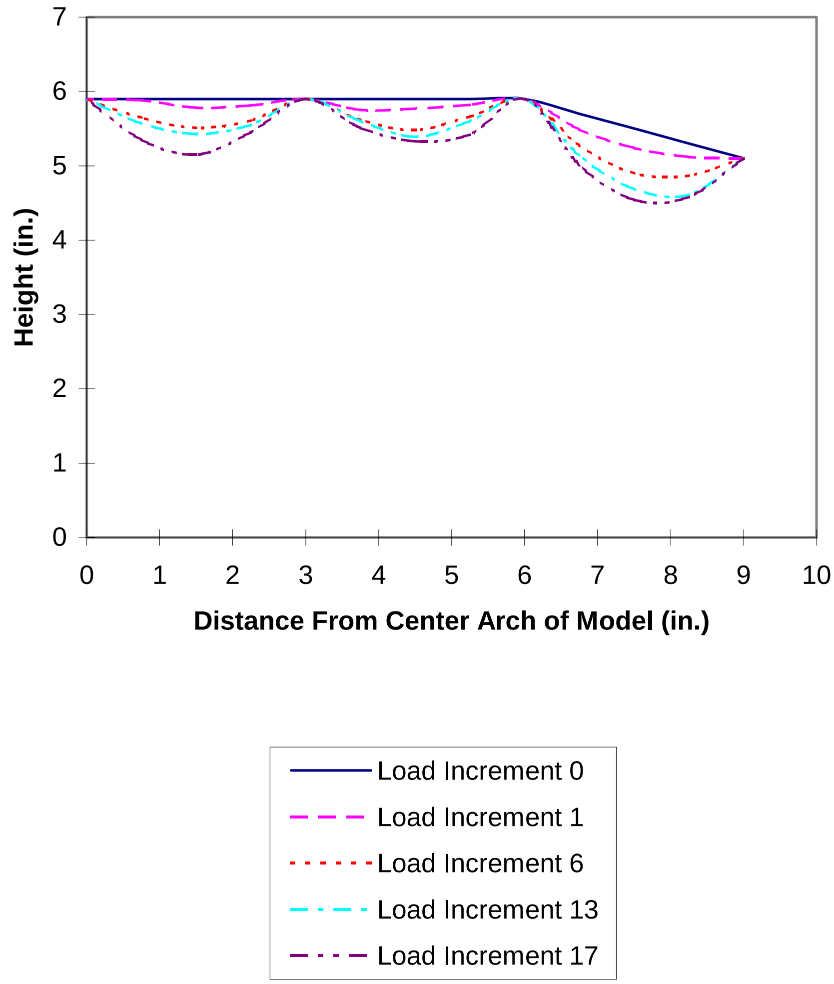

Figure 4.5: 1:100 Scale Model Membrane Deflections at Load Increments 0, 1, 6, 13, and 17 Between Nodes 2 and 26

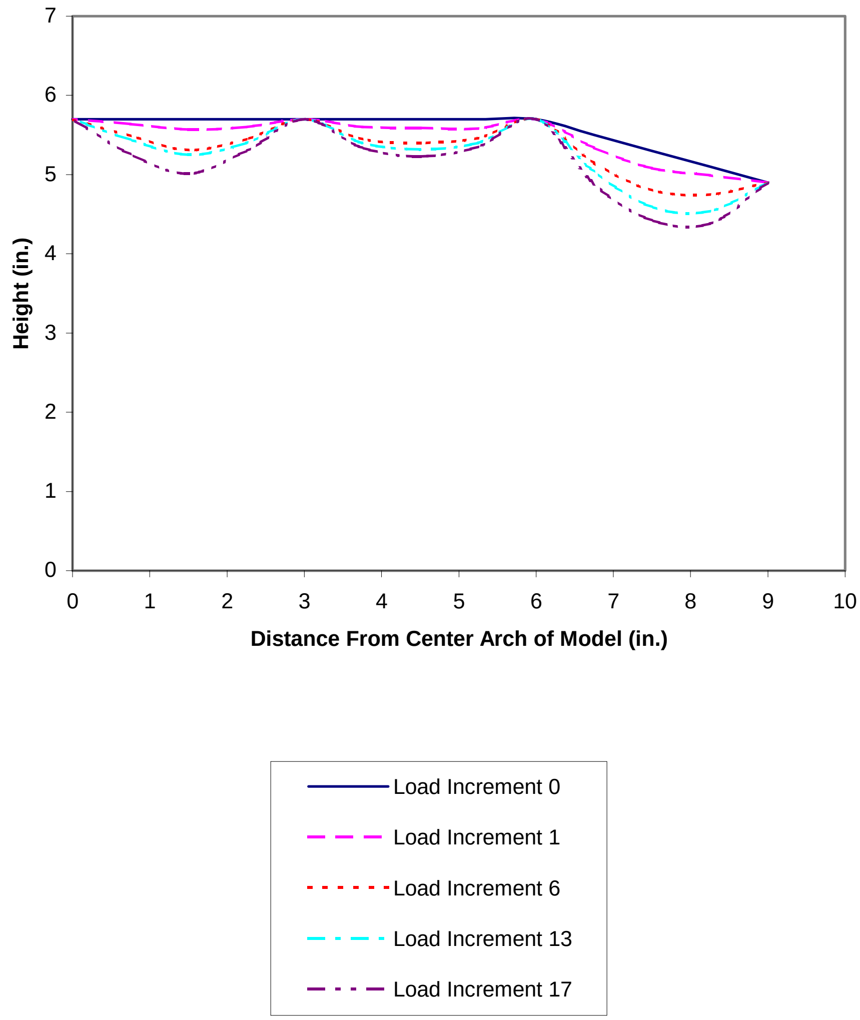

Figure 4.6: 1:100 Scale Model Membrane Deflections at Load Increments 0, 1, 6, 13, and 17 Between Nodes 3 and 27

Observations made during the testing provided information about the behavior of the model during snow load testing. It was observed that the thin loading area on the model and the flexibility of the membrane resulted in instability and toppling of the loads. The toppling of the loads began occurring after the application of load increment 8, and occurred again at load increments 9 and 16. When the loads toppled, they were replaced on the model until stability at that load increment was obtained. The toppling occurred at the end bays, AB and FG. It was observed that bays AB and FG did not deflect equally; bay AB had greater deflections than bay FG. The four central bays, BC, CD, DE, and EF, were observed to deform similarly. These deformations can be seen for load increment 5 in Figure 4.7. However, the membrane curvature was observed to flatten on top as the loads were added, thus increasing the potential loading area. Load increment 9 remained on the model for 3.5 hours, and monofilament strand markings indicated that no additional deflections occurred during the 3.5 hour sustained loading period. Results of monofilament strand markings indicate that no measurable arch deflections occurred during the experiment.

Structural failure occurred after the addition of load increment 17. The mode of failure was a tearing of the membrane at arches E and F, along the edges of the arches closest to the center of the model, as shown in Figure 4.8. Deflection measurements were recorded after load increment 17 was added and before the failure occurred. Measurements taken from monofilament strand markings indicated that no additional deflections occurred after failure. After failure, bays AB, BC, and CD were loaded but

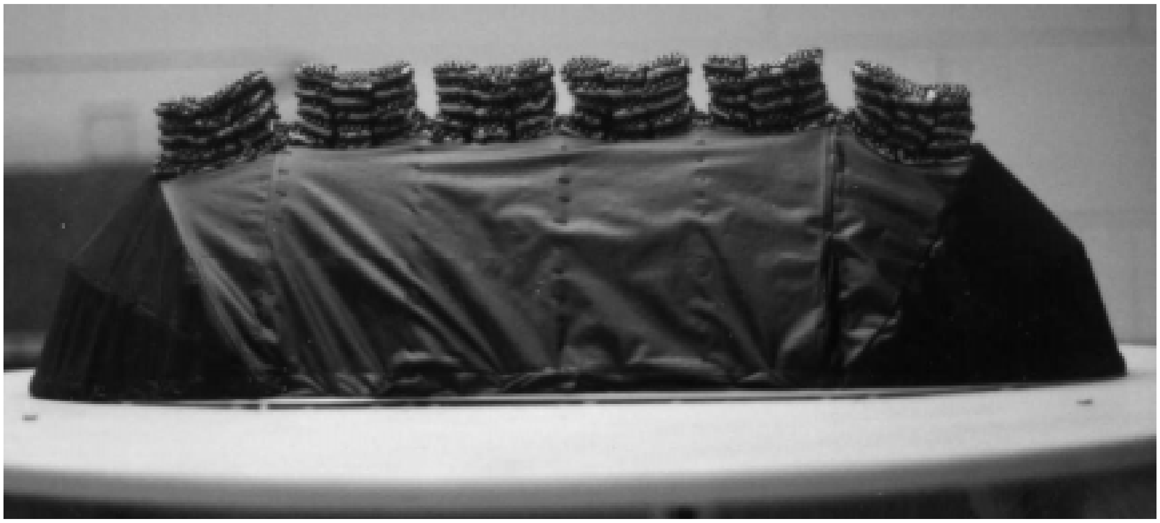

Figure 4.7: 1:100 Scale Model Snow Load Testing at Load Increment 5

Figure 4.8: 1:100 Scale Model Snow Load Testing After Failure

the weights were very unstable on the model and no further loading or deflection measurement was possible.

4.3 1:50 Scale Model

4.3.1 Wind Tunnel Testing

Results of the wind tunnel testing for the 1:50 scale model were primarily qualitative. Visual observations were made of the behavior of the model as the wind velocities were increased. In addition, observations were recorded on the flow of the stream of smoke produced by the smoke generating devices. The frequency of the fans in the tunnel, the speeds of the wind as determined from an established chart of velocity versus frequency, and comments made during the testing have been tabulated in Tables 4.8 - 4.12.

Observations made during the testing indicated that the stream of smoke from the smoke generator was thin and its flow was turbulent before reaching the model. The smoke was clearly observed up to wind speeds of 5 miles per hour. Beyond that velocity, the stream was observed with difficulty. Observations made from the fogging machine indicated that a denser smoke was produced, but the flow became turbulent before reaching the model and observations were made with difficulty when wind speeds were increased above 5 miles per hour. Results from visual observations provided an indication of the wind flow around the model and can be seen in the videotape of the wind tunnel testing.

Table 4.8: 1:50 Scale Model Wind Tunnel Testing Data Table: Trial 1

TRIAL 1: LONG SIDE OF MODEL 90^{o} TO WIND DIRECTION March 19, 1998 Smoke outflow nozzle located 6 in. from top of work surface, aligned with central arch of model					
Frequency (Hz)	Velocity (feet/sec)	Velocity (mph)	Smoke (on or off)	Comments	Video Frame
0	0.00	0.00	on		0
10	1.5	1.1	on	photo taken	
20	3.5	2.4	on		
25	4.5	3.0	on		
30	6.3	4.3	on	smoke very thin	
35	7.5	5.0	on		
40	8.8	6.0	on		
50	10.6	7.3	on		
60	12.5	8.5	on		
70	13.9	9.5	on		
80	15.2	10.4	on	photo taken	

Table 4.9: 1:50 Scale Model Wind Tunnel Testing Data Table: Trial 2

TRIAL 2: LONG SIDE OF MODEL 45^{o} TO WIND DIRECTION March 19, 1998 Smoke outflow nozzle located 6 in. from top of work surface, aligned with central arch of model					
Frequency (Hz)	Velocity (feet/sec)	Velocity (mph)	Smoke (on or off)	Comments	Video Frame
0	0.00	0.00	on		1555
10	1.5	1.1	on		
20	3.5	2.4	on		
25	4.5	3.0	on		
30	6.3	4.3	on	photo taken	
35	7.5	5.0	on	photo taken	
40	8.8	6.0	on		
50	10.6	7.3	on		
60	12.5	8.5	on		
70	13.9	9.5	on		
80	15.2	10.4	on	photo taken	2879

Table 4.10: 1:50 Scale Model Wind Tunnel Testing Data Table: Trial 3

TRIAL 3: LONG SIDE OF MODEL 0° TO WIND DIRECTION March 19,1998 Smoke outflow nozzle located 8.5 in. from top of work surface, aligned with central arch of model					
Frequency (Hz)	Velocity (feet/sec)	Velocity (mph)	Smoke (on or off)	Comments	Video Frame
0	0.00	0.00	on		2879
10	1.5	1.1	on		
20	3.5	2.4	on		
25	4.5	3.0	off		
30	6.3	4.3	off		
35	7.5	5.0	on	photo taken	
40	8.8	6.0	off		
50	10.6	7.3	off		
60	12.5	8.5	on		
70	13.9	9.5	off		
80	15.2	10.4	off		3151

Table 4.11: 1:50 Scale Model Wind Tunnel Testing Data Table: Trial 4

TRIAL 4: LONG SIDE OF MODEL 30° TO WIND DIRECTION March 19, 1998 Smoke outflow nozzle located 8.5 in. from top of work surface, aligned with central arch of model					
Frequency (Hz)	Velocity (feet/sec)	Velocity (mph)	Smoke (on or off)	Comments	Video Frame
0	0.00	0.00	on		3151
10	1.5	1.1	on		
20	3.5	2.4	on	photo taken	
25	4.5	3.0	off		
30	6.3	4.3	off		
35	7.5	5.0	on		
40	8.8	6.0	off		
50	10.6	7.3	off		
60	12.5	8.5	on		
70	13.9	9.5	off		
80	15.2	10.4	off		

Table 4.12: 1:50 Scale Model Wind Tunnel Testing Data Table: Trial 5

TRIAL 5: LONG SIDE OF MODEL 60^o TO WIND DIRECTION March 19, 1998 Smoke outflow nozzle located 6 in. from top of work surface, aligned with central arch of model					
Frequency (Hz)	Velocity (feet/sec)	Velocity (mph)	Smoke (on or off)	Comments	Video Frame
0	0.00	0.00	on		
10	1.5	1.1	on	photo taken	
20	3.5	2.4	on		
25	4.5	3.0	on		
30	6.3	4.3	on	smoke very thin	
35	7.5	5.0	on		
40	8.8	6.0	on		
50	10.6	7.3	on		
60	12.5	8.5	on		
70	13.9	9.5	on		
80	15.2	10.4	on	photo taken	

Results indicated that the wind velocities of the wind tunnel did not cause any noticeable deflection of the membrane or arches. The only motion of the membrane was a slight flapping at the juncture of the two leaning arches and the final vertical arch on the leeward side of the model. No Reynolds numbers or Froude numbers were determined for this testing because of the lack of structural responses observed.

Since no damage was inflicted upon the membrane or the arches during the wind tunnel testing, the same model was used, without modification, for the snow load testing.

4.3.2 Snow Load Testing

Both quantitative and qualitative results were obtained from the snow load testing. The qualitative results were obtained from observations made of the behavior of the model as the loads were increased to failure. Measurements were taken at 44 nodes located in the membrane as the membrane deflected under each load increment. Results have been tabulated in Tables 4.13, 4.14a, and 4.14b. The deflections recorded in Tables 4.14a and 4.14b are the total deflections from the unloaded state of the model. Figures 4.9, 4.10, and 4.11 provide the deflected shapes of the membrane at three cross sections of the model for each of the three load increments. Load increment 2b on these figures represents the deflections due to sustained loading. Figure 4.12 shows a plot of load versus downward deflection of the apex of arches B, C, D, and E.

Table 4.13: 1:50 Scale Model Snow Load Testing Data Table

March 22, 1998					
Increment Number	Load Strips in Each Bay	Weight Added	Weight per Strip	Total Weight	Comments
		(lb)	(lb)	(lb)	
0	0	0	0	0	black mark made on all strands
1	3	15.94	0.89	15.94	white mark made on all strands
2	3	11.04	0.61	26.98	black mark made on all strands, [a]
3	3	7.12	0.40	34.10	black mark made on all strands, failure

[a] an additional white mark was made on all strands between increments 2 and 3 to measure creep

Table 4.14a: 1:50 Scale Model Snow Load Testing Deflection Table (in.)

		Load Increment Numbers					
	Node	1	2	Creep	3	End of Strand	Creep Deflection
Arch A	3	-0.08	0.04	0.07	4.13	N/A	0.03
Bay AB	4	1.00	1.65	1.95	5.02	10.42	0.30
	5	0.61	1.22	1.50	8.58	9.98	0.28
	6	0.22	0.68	0.85	6.00	9.11	0.17
	7	1.21	2.16	2.51	10.04	10.80	0.35
	8	1.12	1.96	2.28	9.12	10.50	0.32
	9	0.47	0.96	1.16	6.15	9.50	0.20
	10	0.72	1.84	2.31	10.38	11.22	0.47
	11	0.92	1.88	2.24	9.52	10.98	0.36
	12	0.48	0.97	1.16	6.40	9.92	0.19

Table 4.14b: 1:50 Scale Model Snow Load Testing Deflection Table (in.)

		Load Increment Numbers					
	Node	1	2	Creep	3	End of Strand	Creep Deflection
Arch B	13	0.80	2.01	2.52	11.07	12.36	0.51
	14	0.61	1.58	2.02	9.88	11.92	0.44
	15	0.20	0.68	0.94	6.27	10.70	0.26
Bay BC	16	1.08	2.50	3.06	11.12	11.86	0.56
	17	0.88	2.07	2.55	10.14	11.40	0.48
	18	0.46	1.20	1.51	6.88	10.33	0.31
	19	1.30	2.82	3.41	11.18	11.76	0.59
	20	1.12	2.43	2.99	10.20	11.40	0.56
	21	0.58	1.43	1.79	6.92	10.24	0.36
	22	1.02	2.53	3.17	11.05	11.82	0.64
	23	0.85	2.16	2.73	10.11	11.43	0.57
	24	0.38	1.13	1.47	6.75	10.28	0.34
Arch C	25	0.72	2.20	2.84	11.39	12.19	0.64
	26	0.54	1.80	2.32	10.03	11.81	0.52
	27	0.13	0.69	1.01	6.39	10.57	0.32
Bay CD	28	1.11	2.64	2.67	11.22	11.83	0.03
	29	0.84	2.19	2.72	10.16	11.42	0.53
	30	0.39	1.25	1.60	6.85	10.32	0.35
	31	1.20	2.77	3.39	10.56	11.83	0.62
	32	1.02	2.42	2.96	10.20	11.41	0.54
	33	0.57	1.48	1.82	6.88	10.28	0.34
	34	1.02	2.57	3.13	10.76	11.92	0.56
	35	0.86	2.17	2.68	10.18	11.41	0.51
	36	0.48	1.24	1.61	6.82	10.30	0.37
Arch D	37	0.35	1.73	2.29	11.18	12.18	0.56
	38	0.51	1.70	2.16	9.95	11.63	0.46
	39	0.20	0.72	0.97	6.41	10.39	0.25
	45	-0.20	0.05	0.21	5.23	10.68	0.16
	46	0.23	1.34	1.74	9.42	11.90	0.40
Arch E	40	0.08	0.41	0.56	5.81	10.65	0.15
	41	0.50	1.46	1.81	9.84	11.84	0.35
	42	0.73	1.98	2.43	11.30	12.12	0.45
	43	0.54	1.58	1.94	10.00	11.68	0.36
	44	0.14	0.59	0.78	6.45	10.51	0.19

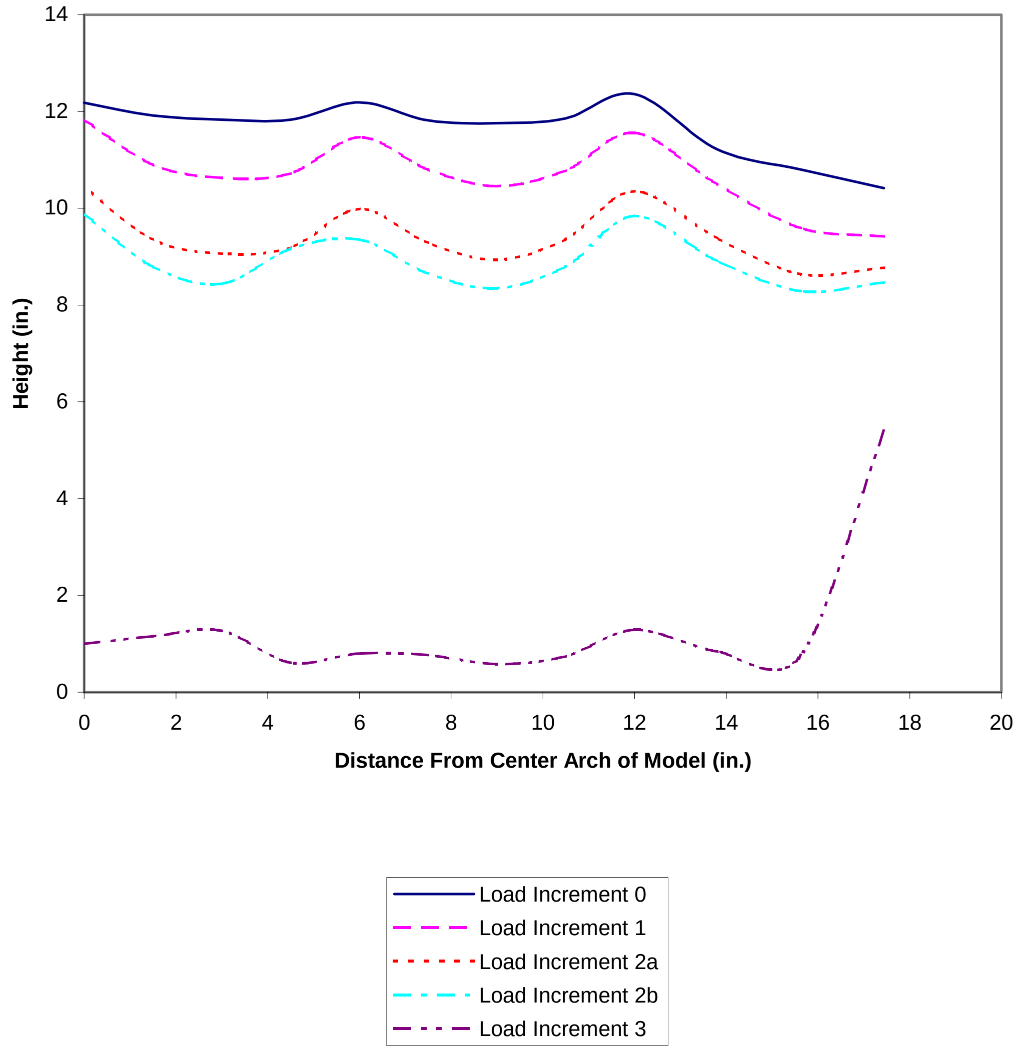

Figure 4.9: 1:50 Scale Model Membrane Deflections at Load Increments 0, 1, 2a, 2b, and 3 Between Nodes 4 and 37

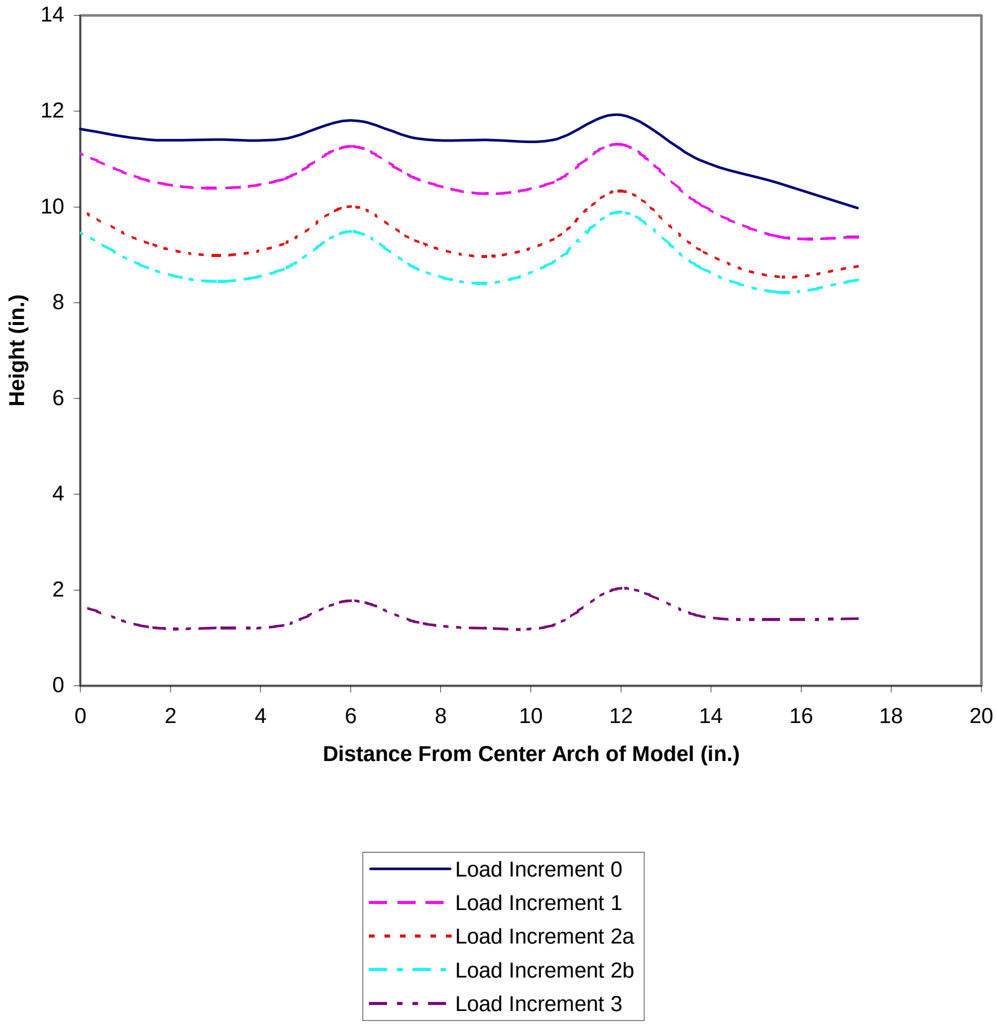

Figure 4.10: 1:50 Scale Model Deflections at Load Increments 0, 1, 2a, 2b, and 3 Between Nodes 5 and 38

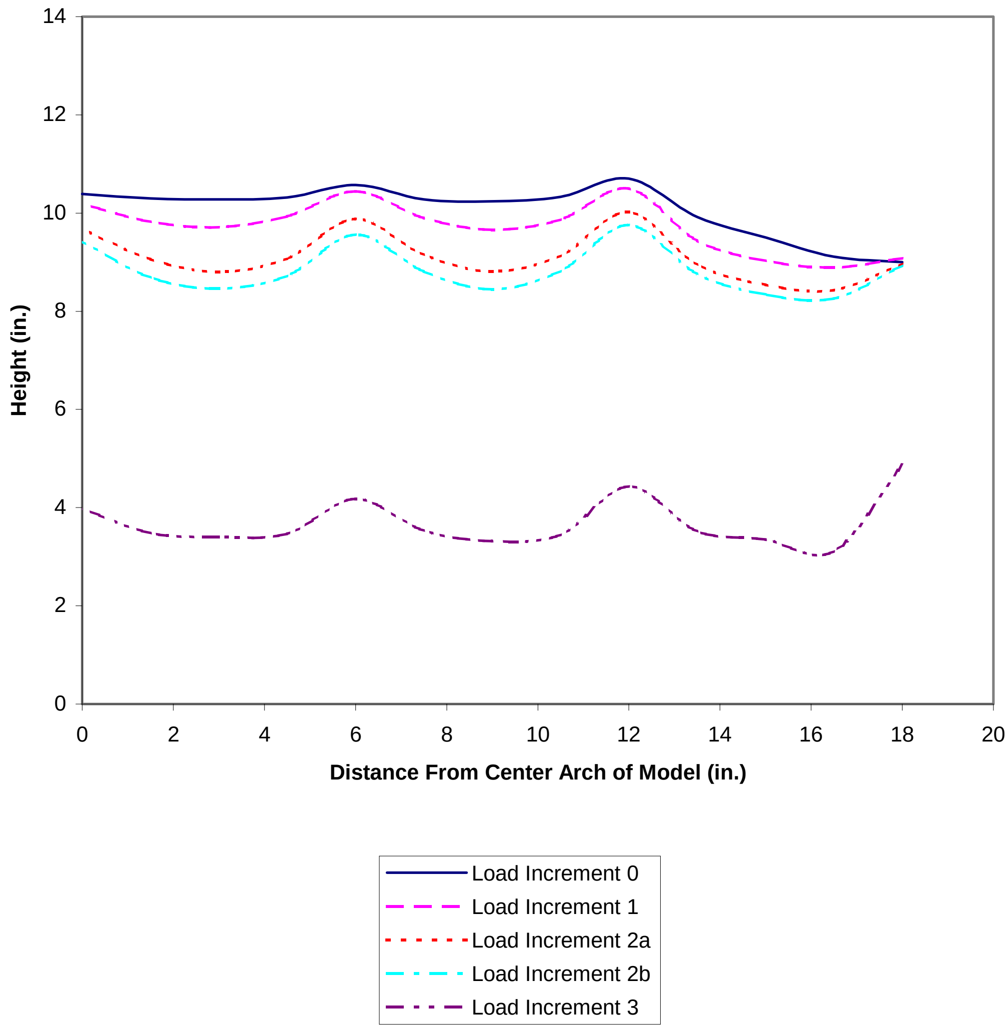

Figure 4.11: 1:50 Scale Model Deflections at Load Increments 0, 1, 2a, 2b, and 3 Between Nodes 3 and 39

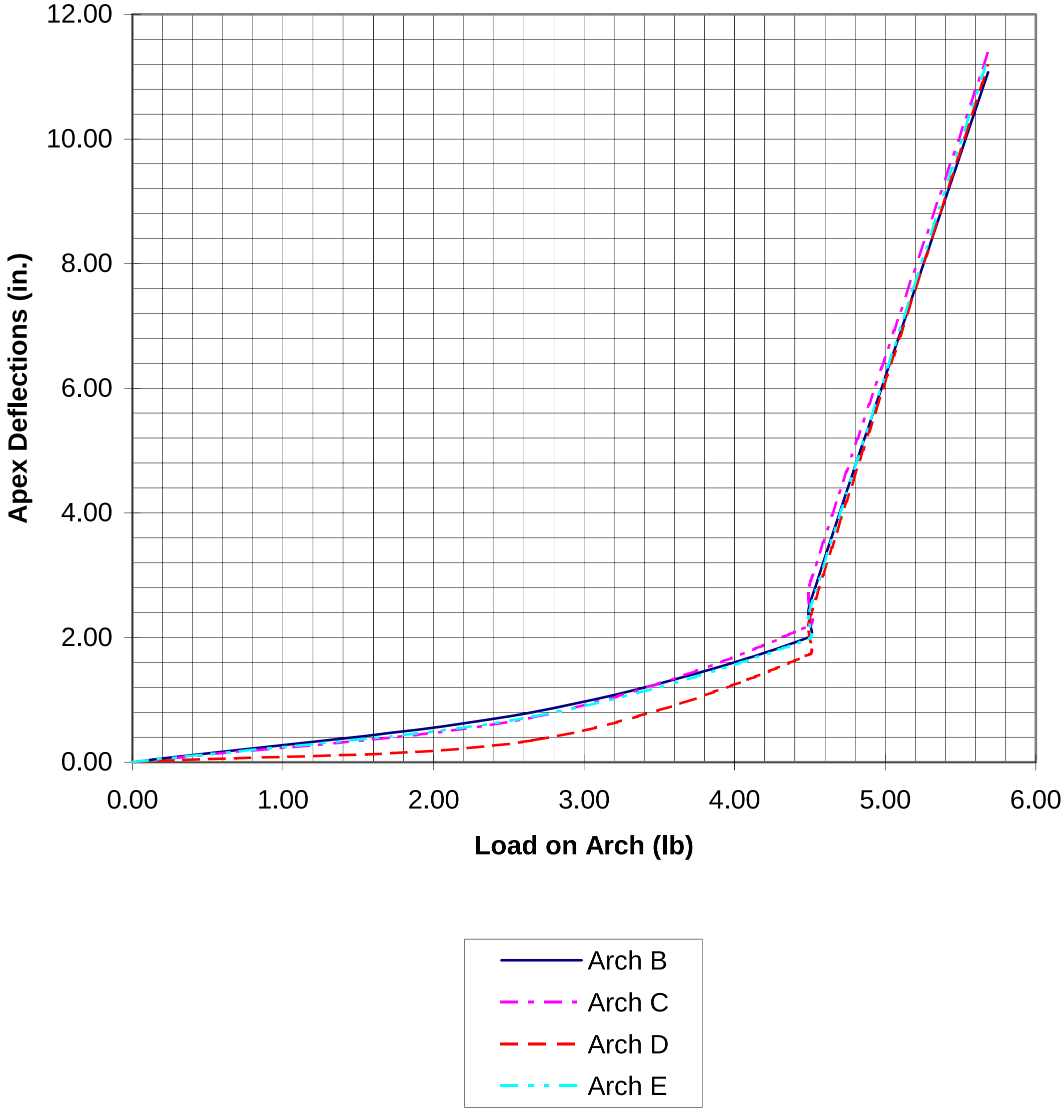

Figure 4.12: 1: 50 Scale Model Load Vs. Arch Apex Deflections for Arches B, C, D, and E

Results were obtained by recording measurements between the load increments. Between the second and third load increments, two measurements were recorded. The first measurement was made immediately after the load was applied. The second was made approximately 2 hours after the application of the second load and immediately before the third load increment was added. The second measurement obtained the additional deflections, or creep, that occurred after sustained loading of the model during the 2-hour interim. The third load increment was added slowly to the model, and as the last strip of weight was added, the structure began to collapse and rapidly failed. The failed model is shown in Figures 4.13 and 4.14. Final deflection measurements were recorded on the shape of the failed model.

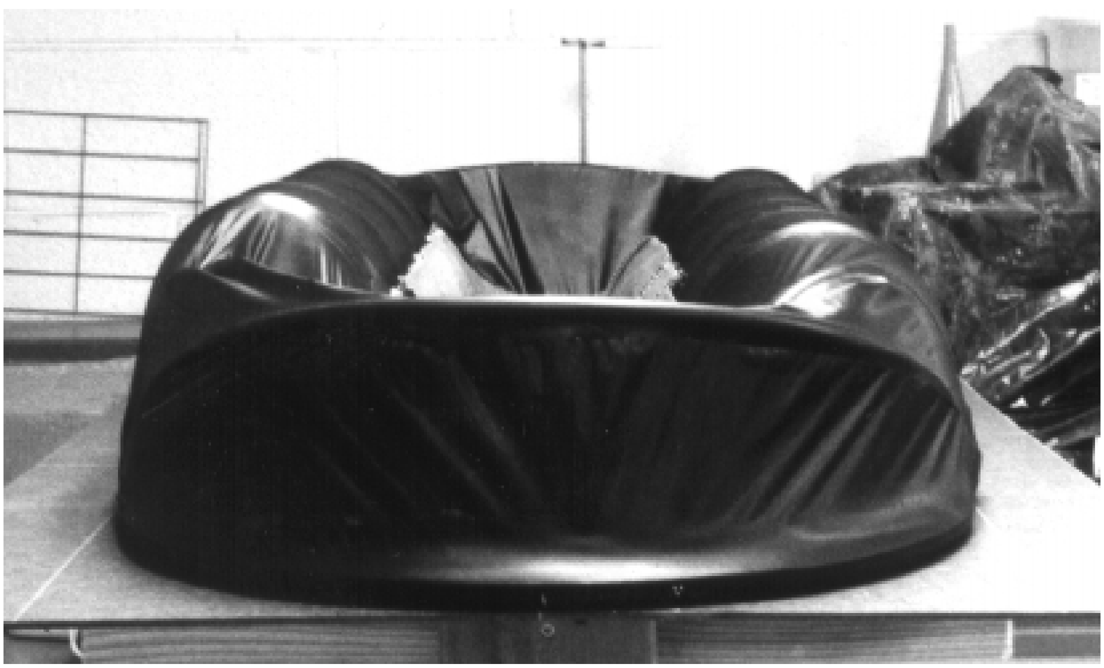

Figure 4.13: 1:50 Scale Model Snow Load Testing After Failure (End View)

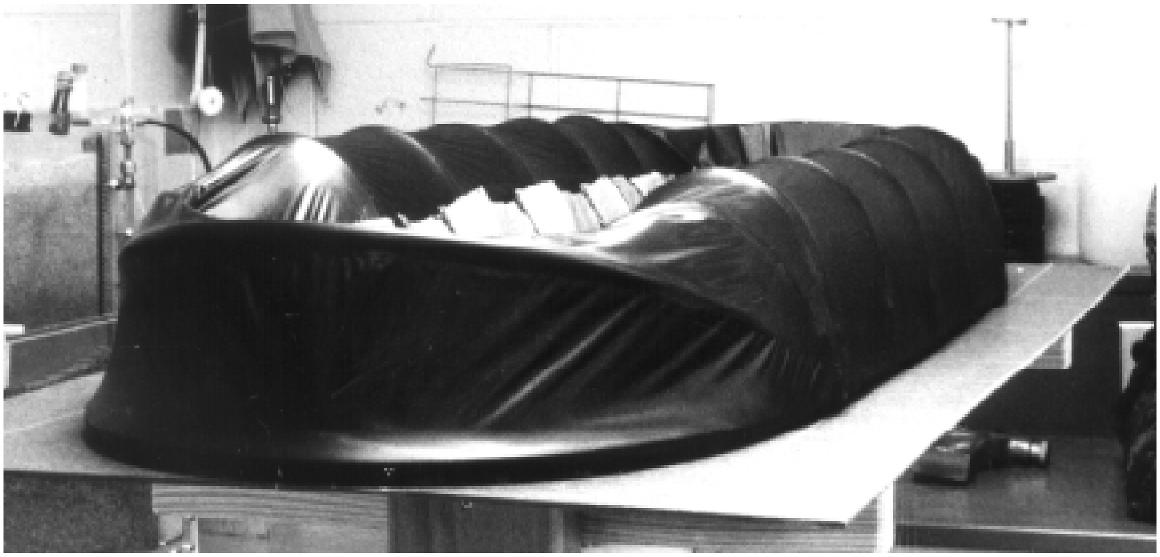

Figure 4.14: 1:50 Scale Model Snow Load Testing After Failure

Failure of the model occurred suddenly and symmetrically due to simultaneous snap-through of the central portion of all the arches. After failure, all of the five vertical arches were resting on the sheet of masonite that covered the underside of the model. No additional weights were added after failure.

It was recorded that nodes 3 and 45 underwent slightly negative (i.e. upward) deflections after the first load increment was added and then went into positive deflection for the remaining load additions. Observations and deflection measurements indicated that the deformation of the model was not symmetric. As loads were added, the tops of the arches flattened out, thus affecting the proposed load area. After the addition of load increment 2 it was observed that arches B and F leaned slightly towards the center of the model. After the model was unloaded all of the arches sprang up, and had returned nearly to their original shape after several hours. However, the arches appeared to maintain an asymmetric curvature with a slightly flattened area at the tops of the arches.

4.4 1:50 Scale Single Arch Model

4.4.1 Snow Load Testing

Both quantitative and qualitative results were obtained from the snow load testing of the 1:50 scale single arch model. The qualitative results were obtained from observations made of the behavior of the model as the loads were increased to failure. The weight increments, the conversion of these weights into loads on the arches, and observations noted during the experiments were tabulated and are presented in Tables 4.15 - 4.22. The digitized deformations of the loaded arches are shown in Figures 4.15 - 4.20. Some portions of the deformed shapes could not be documented due to the size of the scribing surface that was used. The deformations for Trials 5 and 8 are not presented because only the initial shape of these arches was recorded due to lateral deflections.

Each trial began by scribing the shape of the arch while it was loaded only with the buckets, the string, the brass tube, and the fabric sleeve. The combined weight of these items is given by the tare referred to in Tables 4.15 - 4.22. Various load combinations were recorded in Tables 4.15 - 4.22. The model was loaded in each trial until the arch collapsed, as seen in Figure 4.21, or until some part of the hanging apparatus inhibited continued deflections of the arch, as seen in Figure 4.22.

Failure of the arches occurred suddenly and asymmetrically upon reaching the critical load. Table 4.23 summarizes the failure loads for the eight trials and includes the

Table 4.15: 1:50 Scale Single Arch Snow Load Testing: Trial 1

Trial 1: Full Distributed Snow Load, Laterally Restrained March 1, 1998 Tare for two buckets, brass rod, and string: 0.15 pounds				
Increment Number	Weight Increment (lb)	Total Weight (lb)	Total Load (lb/ft)	Comments
0	0.00	0.15	0.18	line 0 scribed, photo taken
1	1.00	1.15	1.38	line 1 scribed
2	1.00	2.15	2.58	no line
3	1.00	3.15	3.78	line 3 scribed
4	1.00	4.15	4.98	no line, photo taken
5	1.00	5.15	6.18	line 5 scribed
6	1.00	6.15	7.38	no line, arch began leaning to left of center
7	1.00	7.15	8.58	line 7 scribed, photo taken
8	1.00	8.15	9.78	line 8 scribed, photo taken, failure

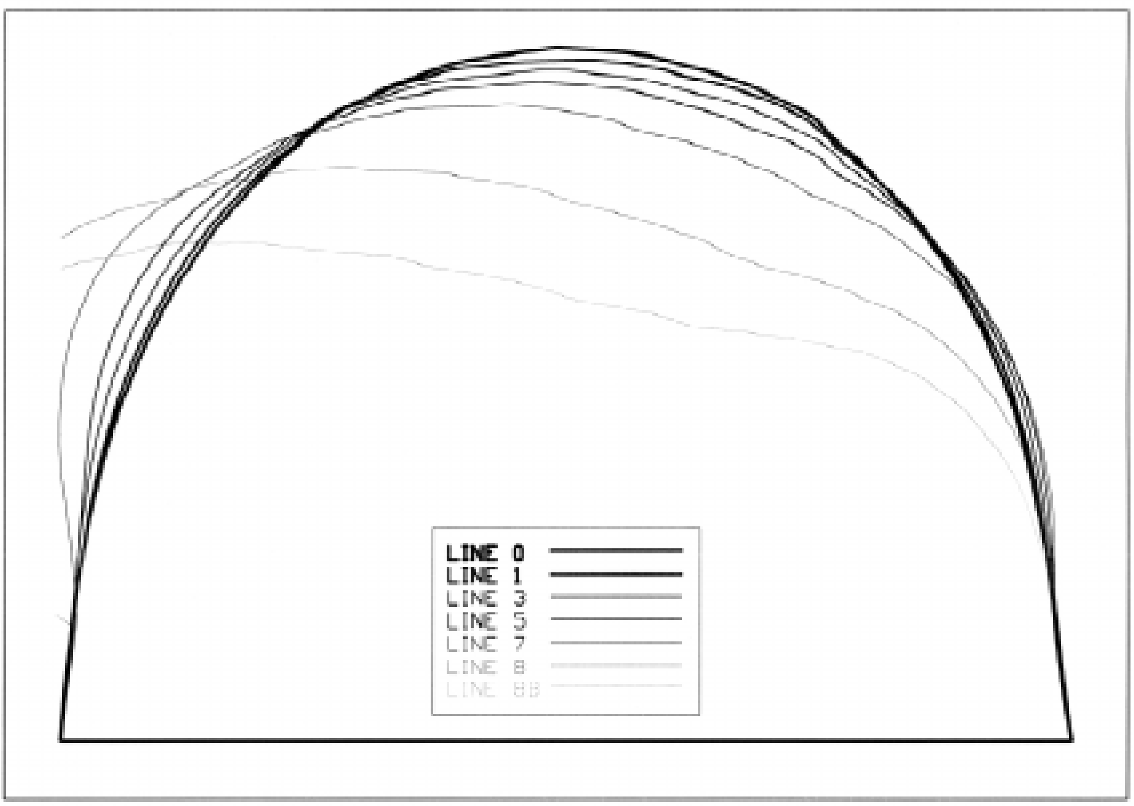

Figure 4.15: 1:50 Scale Single Arch Model Snow Load Deflected Shapes: Trial 1

Table 4.16: 1:50 Scale Single Arch Snow Load Testing: Trial 2

Trial 2: Full Distributed Snow Load, Laterally Restrained March 1, 1998 Tare for two buckets, brass rod and string: 0.15 pounds				
Increment Number	Weight Increment (lb)	Total Weight (lb)	Total Load (lb/ft)	Comments
0	0.00	0.15	0.18	line 0 scribed, photo taken
1	1.00	1.15	1.38	no line
2	1.00	2.15	2.58	line 2 scribed, photo taken
3	1.00	3.15	3.78	no line
4	1.00	4.15	4.98	line 4 scribed, arch bearing on restraints
5	1.00	5.15	6.18	no line, more symmetric than for trial 1
6	1.00	6.15	7.38	line 6 scribed, photo taken
7	1.00	7.15	8.58	no line
8	0.50	7.65	9.18	line 7 scribed, slight lean to right of center
9	0.25	7.90	9.48	no line, severe lean to right, photo taken
10	0.25	8.15	9.78	line 8 scribed, photo taken, failure

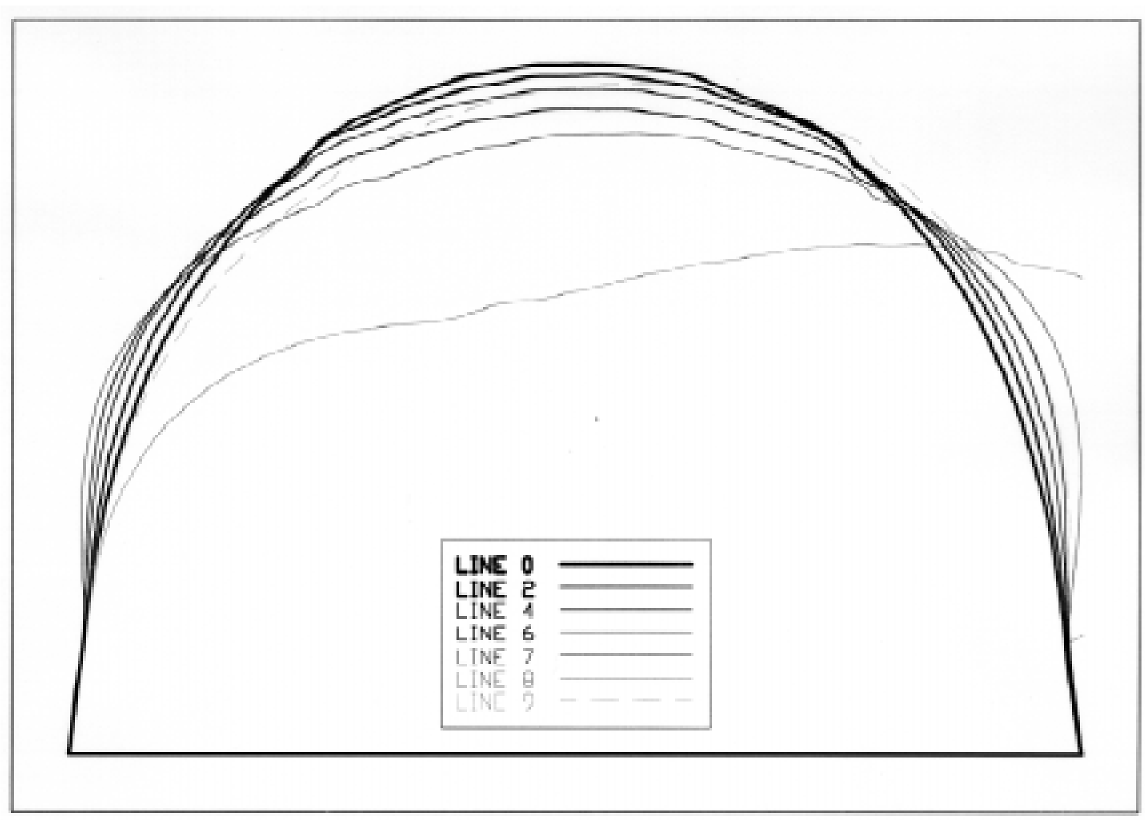

Figure 4.16: 1:50 Scale Single Arch Model Snow Load Deflected Shapes: Trial 2

Table 4.17: 1:50 Scale Single Arch Snow Load Testing: Trial 3

Trial 3: Full Distributed Snow Load, Laterally Restrained March 1, 1998 Tare for two buckets, brass rod and string: 0.15 pounds				
Increment Number	Weight Increment (lb)	Total Weight (lb)	Total Load (lb/ft)	Comments
0	0.00	0.15	0.18	line 0 scribed, photo taken
1	1.00	1.15	1.38	no line
2	1.00	2.15	2.58	line 2 scribed, photo taken
3	1.00	3.15	3.78	no line
4	1.00	4.15	4.98	line 4 scribed, arch bearing on left restraint
5	1.00	5.15	6.18	no line
6	1.00	6.15	7.38	line 6 scribed
7	0.50	6.65	7.98	no line, slight lean to right
8	0.50	7.15	8.58	line 7 scribed, more lean to right, photo
9	0.25	7.40	8.88	no line, continued lean to right observed
10	0.25	7.65	9.18	line 8 scribed, photo of side taken
11	0.25	7.90	9.48	line 9 scribed
12	0.25	8.15	9.78	line 10 scribed, failure

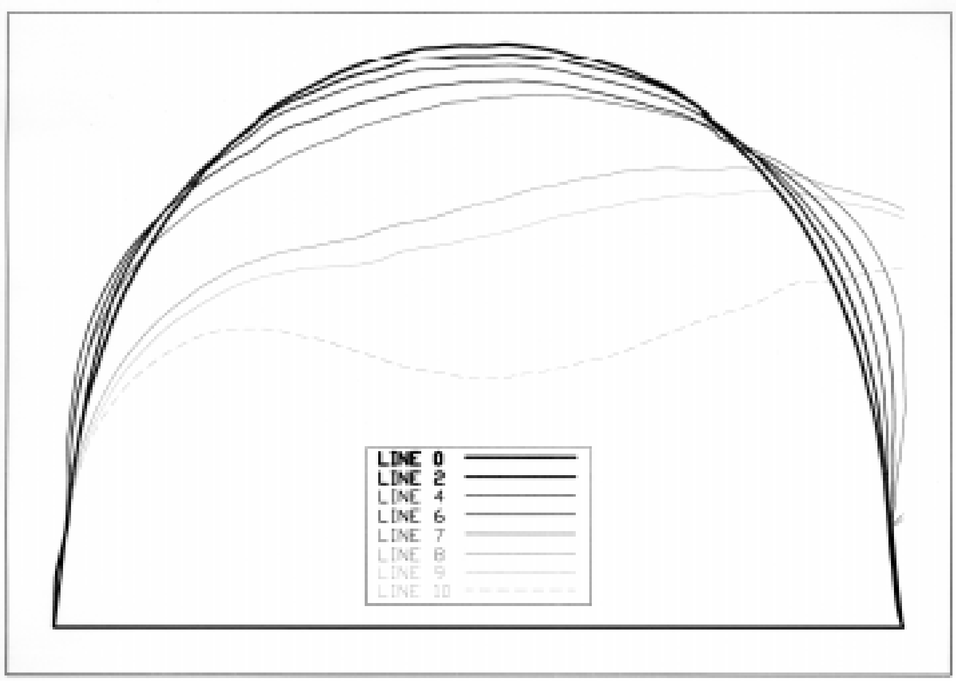

Figure 4.17: 1:50 Scale Single Arch Model Snow Load Deflected Shapes: Trial 3

Table 4.18: 1:50 Scale Single Arch Snow Load Testing: Trial 4

Trial 4: Full Distributed Snow Load, Laterally Unrestrained

March 2, 1998
Tare for two buckets, brass rod and string: 0.15 pounds

Increment Number	Weight Increment (lb)	Total Weight (lb)	Total Load (lb/ft)	Comments
0	0.00	0.15	0.18	line 0 scribed, photo taken
1	0.50	0.65	0.78	no line
2	0.50	1.15	1.38	no line, arch was still vertical in the plane of the arch
3	0.50	1.65	1.98	line 1 scribed, slight lean away from grid
4	0.25	1.90	2.28	severe lean away from grid, front and side photos taken
5	0.25	2.15	2.58	no line
6	0.50	2.65	3.18	no line, front and side photos taken, failure

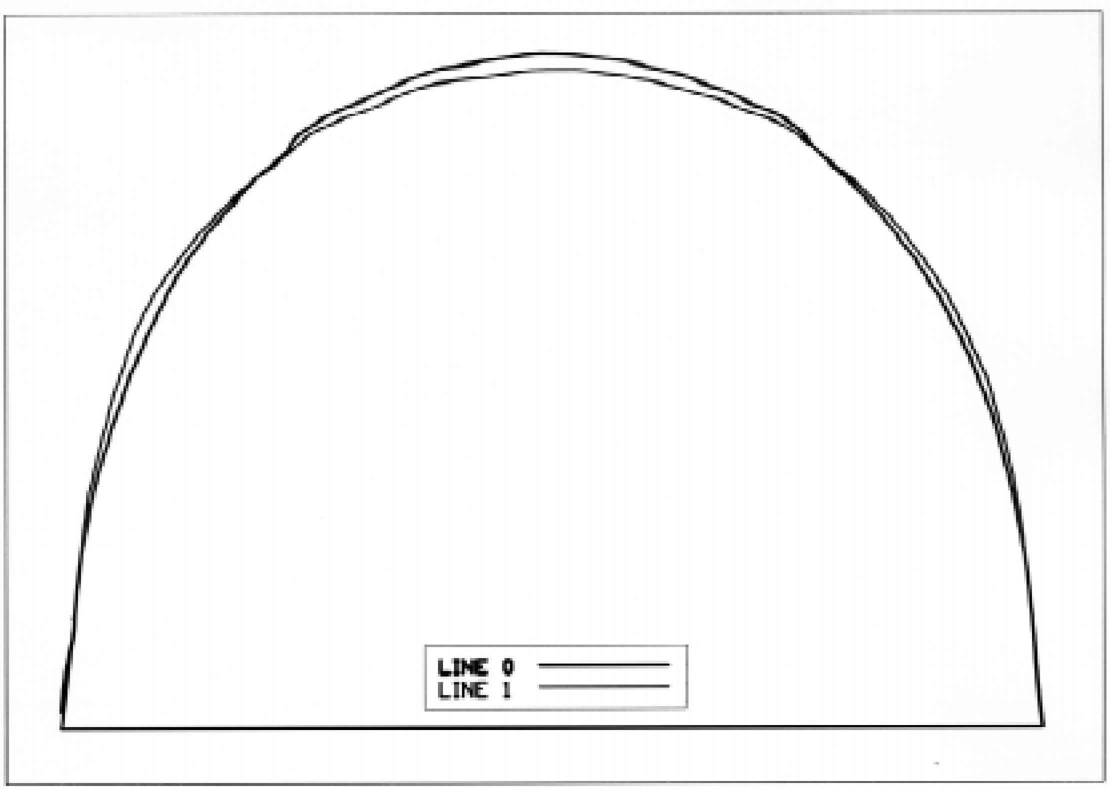

Figure 4.18: 1:50 Scale Single Arch Model Snow Load Deflected Shapes: Trial 4

Table 4.19: 1:50 Scale Single Arch Snow Load Testing: Trial 6

Trial 6: Partially Distributed Snow Load on Right Side of Arch, Laterally Restrained March 7, 1998 Tare for two buckets, brass rod and string: 0.13 pounds				
Increment Number	Weight Increment (lb)	Total Weight (lb)	Total Load (lb/ft)	Comments
0	0.00	0.13	0.31	line 0 scribed, photo taken
1	0.50	0.63	1.51	no line
2	0.50	1.13	2.71	no line, arch touching right restraint
3	0.50	1.63	3.91	line 1 scribed
4	0.50	2.13	5.11	no line, arch touching both restraints, photo
5	0.50	2.63	6.31	line 2 scribed
5	0.50	3.13	7.51	no line
6	0.50	3.63	8.71	line 3 scribed
7	0.50	4.13	9.91	failure, snap-through, line 4 scribed, photo

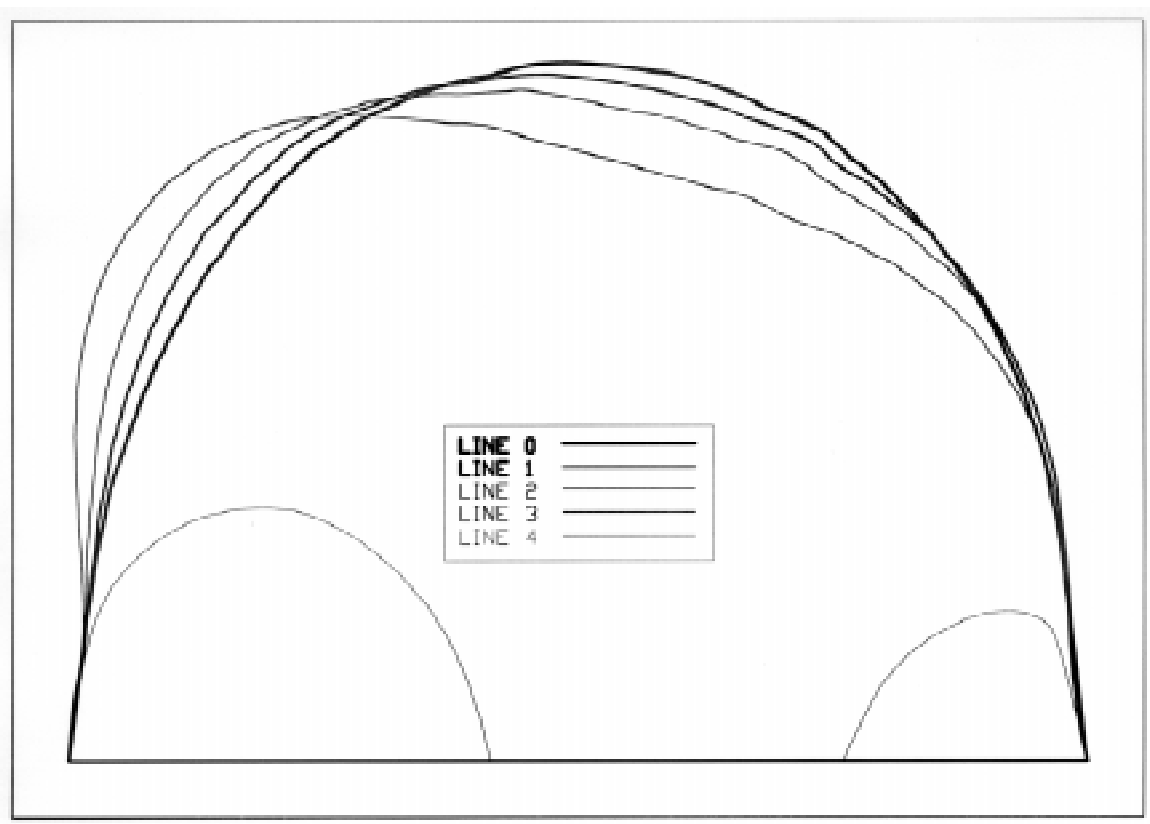

Figure 4.19: 1:50 Scale Single Arch Model Snow Load Deflected Shapes: Trial 6

Table 4.20: 1:50 Scale Single Arch Snow Load Testing: Trial 7

Trial 7: Partially Distributed Snow Load on Left Side of Arch, Laterally Restrained				
March 7, 1998				
Tare for two buckets, brass rod and string: 0.13 pounds				
Increment Number	Weight Increment (lb)	Total Weight (lb)	Total Load (lb/ft)	Comments
0	0.00	0.13	0.31	line 0 scribed, photo taken
1	0.50	0.63	1.51	no line, arch touching both restraints
2	0.50	1.13	2.71	line 1 scribed
3	0.50	1.63	3.91	no line
4	0.50	2.13	5.11	line 2 scribed, photo taken
5	0.50	2.63	6.31	line 3 scribed
5	0.25	2.88	6.91	no line
6	0.25	3.13	7.51	line 4 scribed
7	0.25	3.38	8.11	line 5 scribed, photo taken
8	0.25	3.63	8.71	no line
9	0.25	3.88	9.31	line 6 scribed
10	0.05	3.93	9.43	no line
11	0.10	4.03	9.67	line 7 scribed, failure

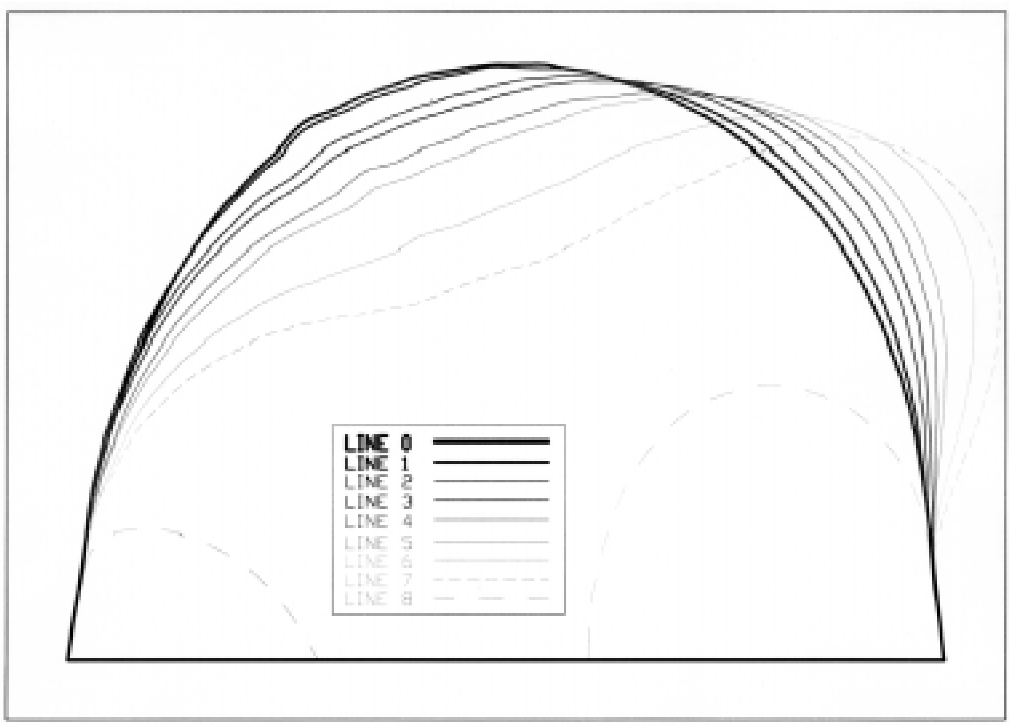

Figure 4.20: 1:50 Scale Single Arch Model Snow Load Deflected Shapes: Trial 7

Table 4.21: 1:50 Scale Single Arch Snow Load Testing: Trial 5

Trial 5: Full Distributed Snow Load, Laterally Unrestrained

March 2, 1998
Tare for two buckets, brass rod and string: 0.15 pounds

Increment Number	Weight Increment (lb)	Total Weight (lb)	Total Load (lb/ft)	Deflection of Arch Center (in.)	Comments
0	0.00	0.15	0.18	not recorded	line 0 scribed, photo taken
1	0.50	0.65	0.78	not recorded	no line, arch was still vertical in arch plane
2	0.50	1.15	1.38	not recorded	no line
3	0.25	1.40	1.68	1.50	no line, lean away from grid noted
4	0.25	1.65	1.98	4.63	no line, lean away from grid, two photos
5	0.25	1.90	2.28	5.50	no line
5	0.25	2.15	2.58	6.31	no line
6	0.50	2.65	3.18	7.63	no line
7	0.25	2.90	3.48	8.25	no line, front and side photos taken, failure

Table 4.22: 1:50 Scale Single Arch Snow Load Testing: Trial 8

Trial 8: Partially Distributed Snow Load on Right Side of Arch, Laterally Unrestrained

March 7, 1998
Tare for two buckets, brass rod and string: 0.13 pounds

Increment Number	Weight Increment (lb)	Total Weight (lb)	Total Load (lb/ft)	Deflection of Arch Center (inches)	Comments
0	0.00	0.13	0.31	1.06	line 0 scribed, photo taken
1	0.25	0.38	0.91	1.19	no line
2	0.25	0.63	1.51	1.38	no line
3	0.25	0.88	2.11	1.69	no line
4	0.25	1.13	2.71	2.75	no line, front and side photos taken
5	0.25	1.38	3.31	4.56	no line, arch beginning to lean right
5	0.25	1.63	3.91	not recorded	no line, front and side photos taken
6	0.25	1.88	4.51	6.38	no line
7	0.25	2.13	5.11	7.13	no line, front and side photos taken
8	0.25	2.38	5.71	7.88	no line, front and side photos taken
9	1.00	3.38	8.11	8.50	no line, front and side photos taken, failure

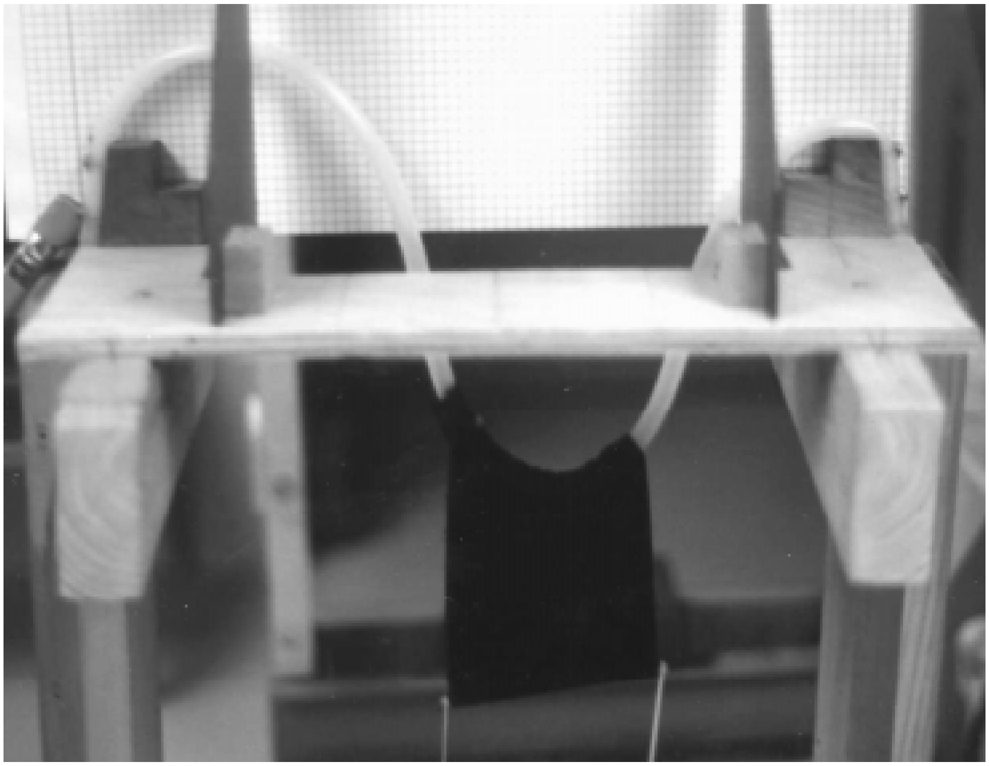

Figure 4.21: 1:50 Scale Single Arch Model After Failure: Trial 7

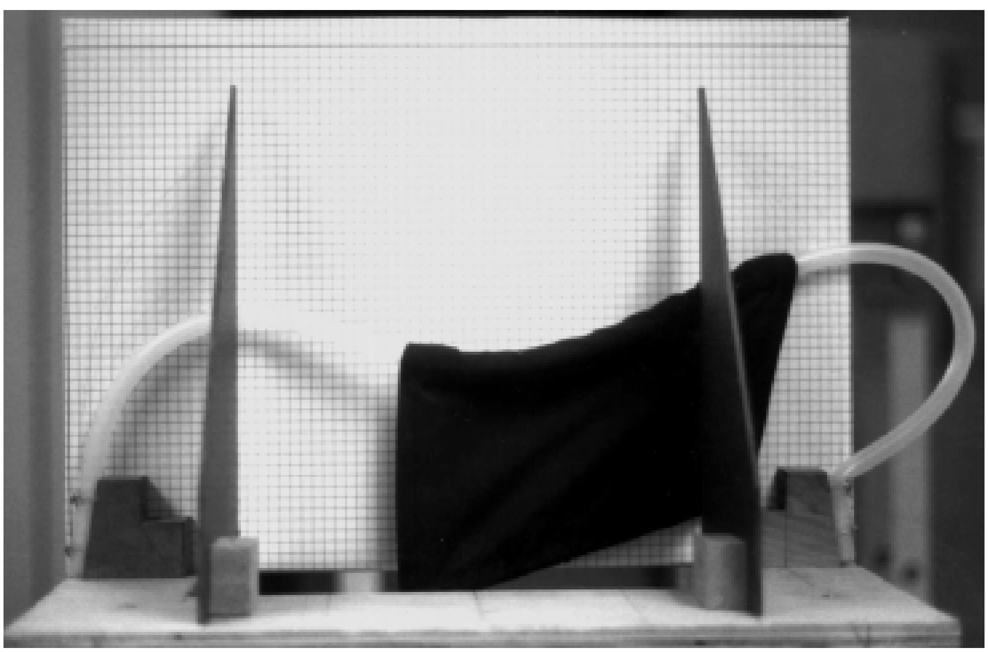

Figure 4.22: 1:50 Scale Single Arch Model After Failure: Trial 3

Table 4.23: 1:50 Scale Model and Single Arch Model Failure Loads

Trial #	Failure Weight (lb)	Failure Load (lb/ft)
1	8.15	9.78
2	8.15	9.78
3	8.15	9.78
4	2.56	3.18
5	2.9	3.48
6	4.13	9.91
7	4.03	9.67
8	3.38	8.5
1:50 Scale Model	5.68	6.28

failure load for the 1:50 scale model as a comparison. An outline of the final, failed arch was recorded for each of the laterally restrained trials. It was impossible to scribe lines beyond the third load increment for any of the laterally unrestrained trials due to the distances between the deformed arches and the scribing surface, as shown in Figure 4.23. Figure 4.24 provides a plot of the load versus the horizontal deflections for Trial 8. Figures 4.25 and 4.26 show plots of the load versus arch apex deflections for Trials 3 and 7. For Trials 1 and 2, the arches were unloaded and the unloaded shapes were outlined.

Results indicated that none of the arches deflected symmetrically, and some of the arches twisted as they were loaded, as seen in Figure 4.27, where the portion of the arch in the foreground is bearing on the restraint on the right, while the portion of the arch farther away is bearing on the scribing surface on the left. Observations indicated that at certain times during the trials the sleeve that supported the buckets buckled and acted as two concentrated point loads on each end of the sleeve rather than a fully distributed load.

Figure 4.23: 1:50 Scale Single Arch Model: Trial 4

None of the unloaded arches fully returned to their original shapes.

During Trial 8, the loading apparatus was moved to the outside of the model base after it had begun bearing on the inside of the opening in the model base and halting further deformation. Moving the loading apparatus allowed the top of the arch to continue deflecting to a point below the fixed ends of the arches, as shown in Figure 4.28.

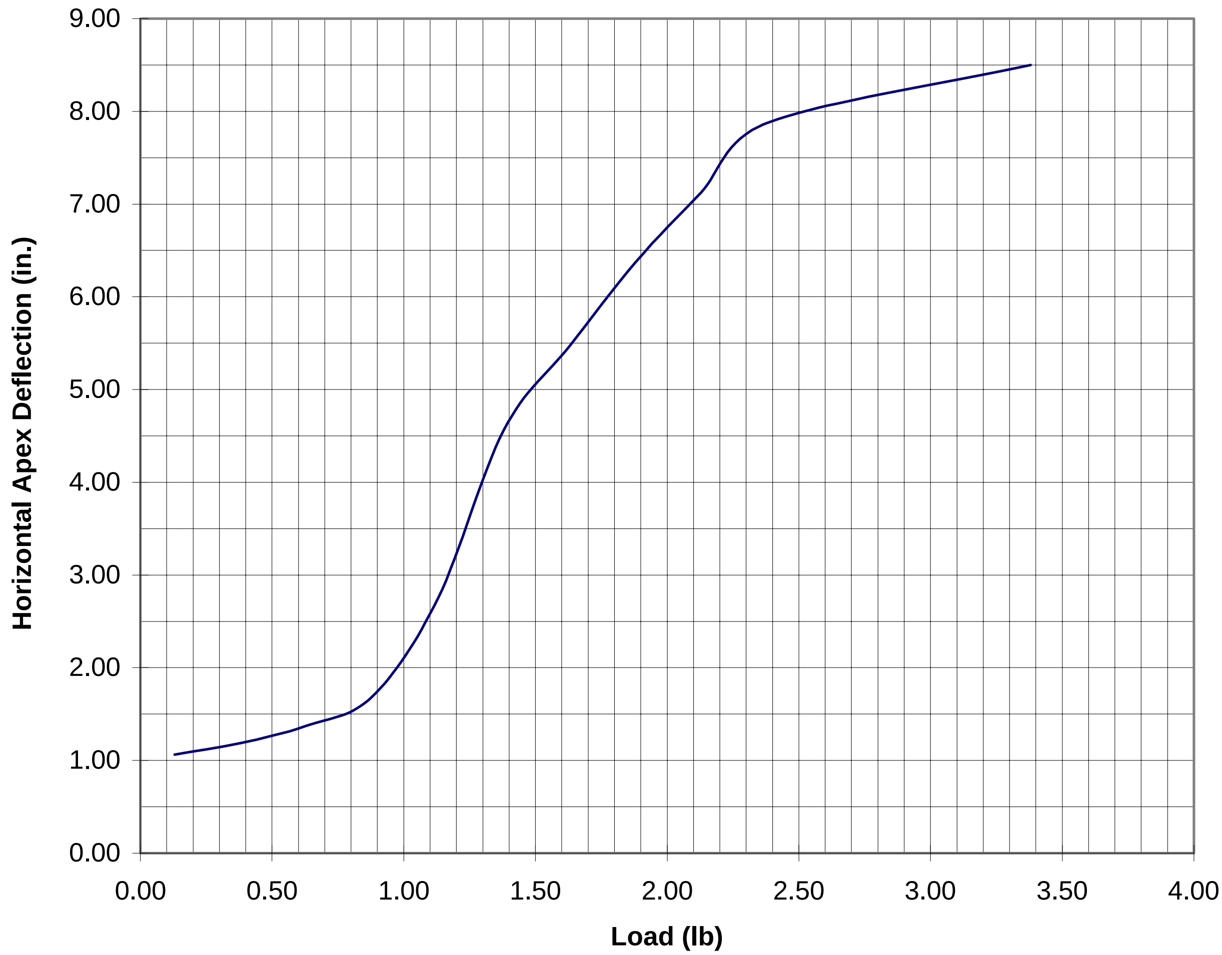

Figure 4.24: Load Vs. Horizontal Arch Apex Deflection For Trial 8

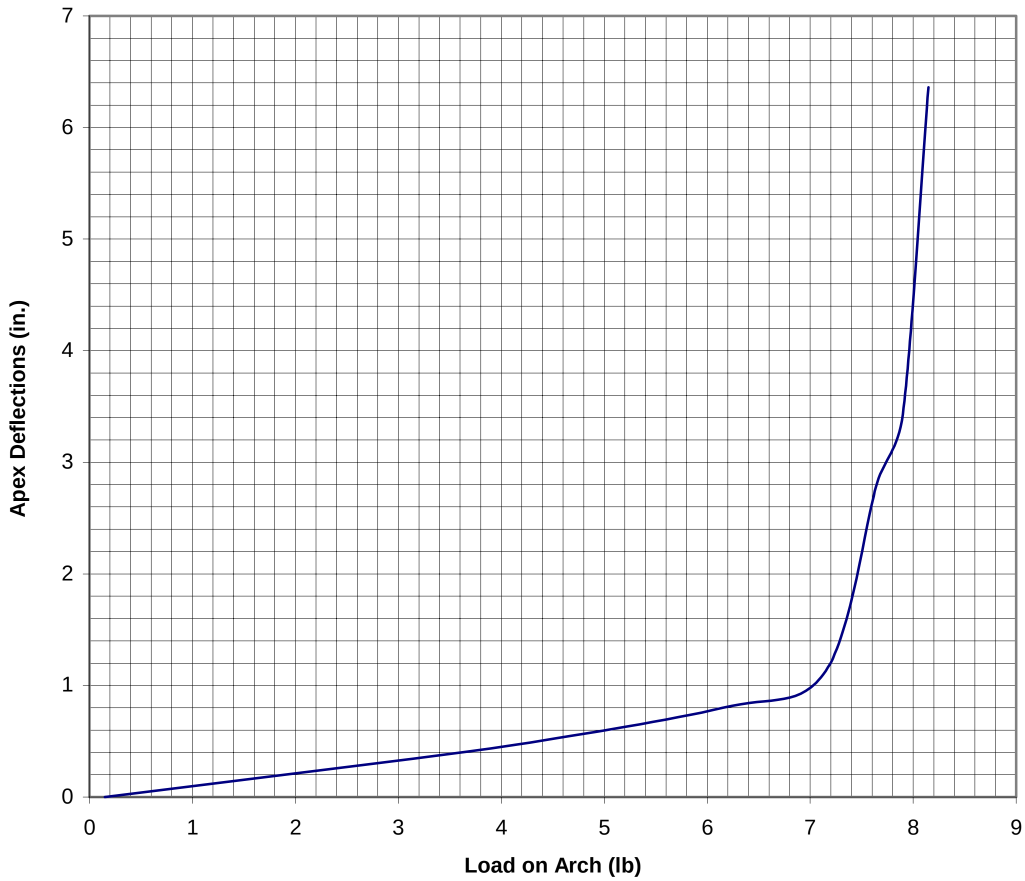

Figure 4.25: 1:50 Scale Single Arch Model Load Vs. Arch Apex Deflections: Trial 3

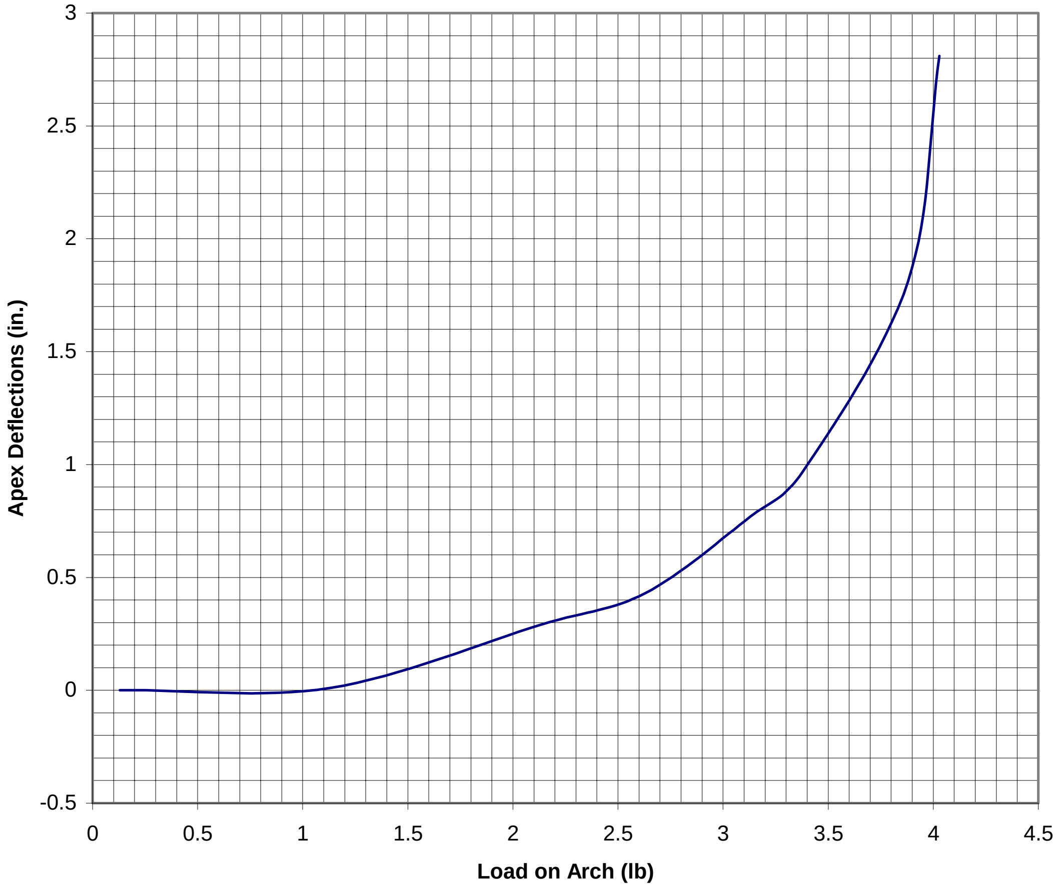

Figure 4.26: 1:50 Scale Single Arch Model Load Vs. Arch Apex Deflections: Trial 7

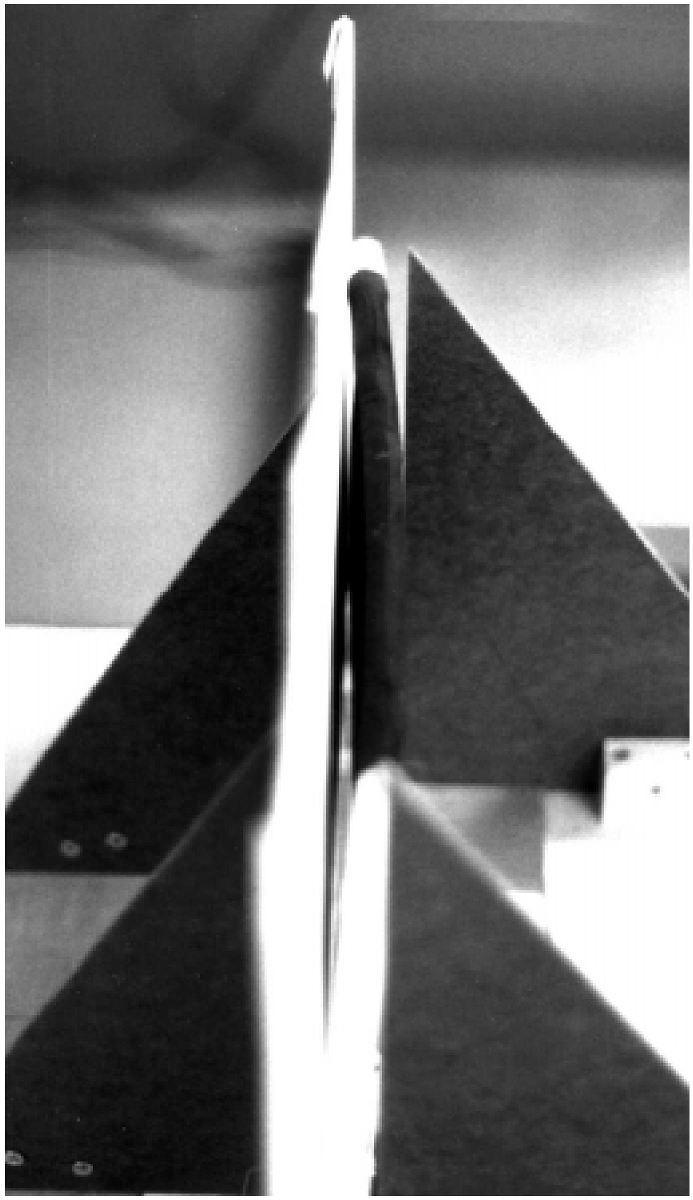

Figure 4.27: 1:50 Scale Single Arch Model With Twist: Trial 3

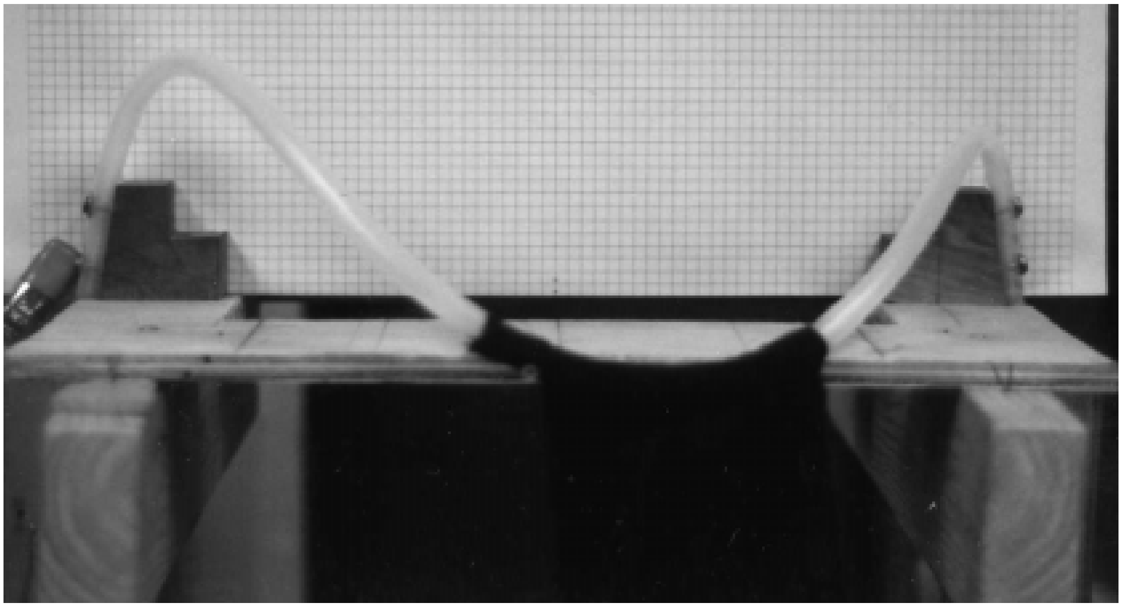

Figure 4.28: 1:50 Scale Single Arch Model After Shifting Load Apparatus: Trial 8

Chapter 5. Conclusions

5.1 Introduction

Three scale models were constructed, and wind and snow load testing of these models led to a number of observations regarding the behavior of these arch-supported membrane structural scale models. The conclusions drawn from these observations will be summarized below, along with recommendations for future research.

5.2   1:100 Scale Model

5.2.1 Wind Tunnel Testing

The visual observations from the wind tunnel testing indicated that the general nature of the pressure and suction distributions on the model were similar to those of semi-cylindrical structural models. It was useful to find that no damaging flutter of the membrane occurred during the testing. The experiment was limited in that the copper tubing used to form the arches was very stiff and was therefore not very representative of the pressurized arches used in actual arch-supported membrane structures. It is recommended that a more flexible material be used for the arches in future wind tunnel studies.

5.2.2 Snow Load Testing

It was observed that as the model was loaded, the initial curvature of the membrane flattened out under the loaded area. This flattening increased the portion of the membrane that created a 30º angle with the horizontal. Under actual snow conditions, this would allow for an increase in surface area upon which snow could accumulate. Therefore it is recommended that the snow loading be done in an iterative manner, in which additional weight is added to each consecutive load increment to account for the increased area of possible snow accumulation.

The load on the membrane was calculated to be 100.80 psf at the time of failure. This is equivalent to a linear load of 25.20 lb/ft (2.10 lb/in.) on each vertical arch and 12.60 lb/ft (1.05 lb/in) on each leaning arch at the end of the loaded area. The failure mode was the tearing of the membrane. There were no measurable deflections of the arches, attributed to the rigidity of the copper tubing. Because the holes created in the membrane by stitching it to the arches may have created a weakness in the membrane, it is recommended that a different method of attachment be used so as not to contribute to the initiation of tearing.

5.3 1:50 Scale Model

5.3.1 Wind Tunnel Testing

The low-speed wind tunnel testing observations provided only a rough representation of the flow around the model. It is recommended that future studies be conducted with a smoke generator that could provide more distinct information about the wind flow patterns around the structure. No deflections of the membrane or arches were observed and no flutter of the membrane occurred during the testing. It is recommended that a wind tunnel capable of higher speeds be used in future studies. In this manner, an understanding of these structures in more adverse conditions could be obtained.

5.3.2 Snow Load Testing

As the loads were applied, the initial curvature of the membrane flattened out under the loaded area of the membrane. Because the arches were flexible and deflected with the membrane, the flattened area was increased to a greater extent than for the 1:100 scale model. It was useful to note that the portion of the membrane that created a 30º angle with the horizontal was increased with each load increment. Therefore it can be concluded that under actual snow load conditions, an increase in the surface area upon which snow could accumulate would result. It is recommended that future snow load testing be done in an iterative manner, in which additional weight is added to each consecutive load increment to account for the increased area of accumulation possible in actual snow load conditions.

The load on the membrane was calculated to be 13.64 psf at the time of failure. This is equivalent to a linear load of 6.82 lb/ft (0.57 lb/in.) on each vertical arch and 3.42 lb/ft (0.29 lb/in) on each leaning arch at the end of the loaded area. The failure mode was the simultaneous snap-through of the center portions of the loaded arches. It was found that the critical loads of the arches had been reached or exceeded by the final load increment. The flexible arches provided a much better approximation of the pressurized arches used in the actual structures represented by the models. Therefore it may be concluded that in actual snow load conditions, a critical snap-through of the center portions of the arches would be the mode of failure.

Figure 4.12, in Chapter 4, is a plot of load versus arch apex deflections for arches B, C, D, and E, and shows an apparent softening of the arches as the load was increased to failure. The plots at 4.50 lb show the two deflections that were recorded between load increments 2 and 3. The difference in the two measurements was the result of deflection due to sustained loading, or creep. It can be concluded that softening and creep are important considerations to note when evaluating snow load response.

5.4 1:50 Scale Single Arch Model

The failure loads for each of the eight trials are given in Table 4.23. The failure mode for Trials 6 and 7 was the sudden snap-through of the arches. The failure mode for Trials 1 - 5 and Trial 8 was the excessive deflections limited only by the fact that the arches could only deflect to the point where the loading apparatus was bearing on some part of the model. Figures 4.25 and 4.26 provide plots of the load on the arches versus the downward deflections at the apex of the arches for Trials 3 and 7. Figure 4.24 provides a plot of load versus the horizontal deflection of the apex of the arch for Trial 8.

Figures 4.25 and 4.26 show a softening of the arches as the loads were increased to failure. Figure 4.24 shows a region of increased softening from 0.80 lb to 1.25 lb. It was found that compared to the 1:50 scale model, the single arch model had a greater load capacity before the critical load was reached, as shown in Table 5.1. This may have been the result of the arch shape maintaining characteristics of the load-distributing sleeve used for testing. It is recommended that to more fully understand the behavior of single arches under loading, a less restrictive sleeve should be used.

5.5 General Conclusions and Recommendations

It was found during the snow load testing that for the 1:100 scale model the mode of failure was the tearing of the membrane. This was in contrast to the mode of failure in the 1:50 scale model, which was the snap-through of the flexible arches. It may be concluded that the relative stiffness of the arches and strength of the membrane need to be considered when designing these types of structures. In addition, an understanding of the combined responses between the arches and membrane is needed when calculating the capacities of the structural components and the entire structure.

The scale model investigations that have been conducted indicate that additional research of this type needs to be executed in order to obtain a more complete understanding of pressurized arch-supported membrane structures. One aspect that future research should address is the interactive effects of combined wind and snow loading. Wind tunnel studies should be performed using a rigid model having the same shape as the proposed structures so that the pressure distribution for the structure could be determined, for use with numerical and computer analyses. Wind tunnel tests on a flexible model, where the deflections of the arches and membrane can be recorded, should also be performed. A thorough understanding of the materials that will be used to construct the final structures would be fundamental for being able to extrapolate the scale model testing results into applicable design criteria.

Bibliography

Beger, G. and Macher, E. (1967). "Results of Wind Tunnel Tests on Some Pneumatic Structures." *Proc., 1st Colloq. on Pneumatic Structures*, Stuttgart, Germany, 142-146.

Berger, H. (1996). *Light Structures - Structures of Light: The Art and Engineering of Tensile Architecture,* Birkhaüser, Switzerland.

Blackmore, P. (1997). "The Role of Wind Tunnel Testing in the Design of Building Structures." *Proc. Instn. Civ. Engrs. Structs. & Bldgs,* 122, 253-265.

Bohme, F. and Rontsch, G. (1967). "Model Analysis of a Semi-Cylindrical Air-Supported Hull." *Proc., 1st Colloq. on Pneumatic Structures*, Stuttgart, Germany, 147-150.

Daw, D. and Davenport, A. (1989). "Aerodynamic Damping and Stiffness of a Semi-Circular Roof in Turbulent Wind." *Journal of Wind Engineering and Industrial Aerodynamics*, 32, 83-92.

Dietz, A., Proffitt, R., Chabot, R., and Moak, E. (1969). “Wind Tunnel Tests and Analyses for Ground Mounted, Air-Supported Structures (Revised).” *Technical Report 70-7-GP,* United States Army, United States Army Natick Laboratory, Natick, Massachusetts, U. S. A.

Fukao, Y., Iwasa, Y., Mataki, Y., and Okada, A. (1986). “Experimental Test and Simulation Analyses of the Dynamic Behavior of Low - Profile, Cable - Reinforced, Air - Supported Structures.” *Shells, Membranes, and Space - Frames, Proceedings from the IASS Symposium*, Osaka, Japan, 149-155.

Hajek, M. and Holub, Z. (1967). “Some Problems Concerning the Testing of Materials for Pneumatic Structures.” *Proc., 1st Colloq. on Pneumatic Structures*, Stuttgart, Germany, 159-162.

Han, P. and Olson, M. (1987). “Interactive Analysis of Wind - Loaded Pneumatic Membrane Structures.” *Computers & Structures*, 25, 699-712.

Ikemoto, N., Mizoguchi, Y., Fujikake, M., Kojima, O., and Hirota, M. (1986). “Development of a Design System for Fabric Tension Structures.” *Shells, Membranes, and Space - Frames, Proceedings from the IASS Symposium*, Osaka, Japan, 341-348.

Kalstrom, J. (1997). "Pumped Up, A Study of New Air Structures." *Fabrics & Architecture*, 9(3), 40-44.

Kassem, M. and Novak, M (1992). "Wind-Induced Response of Hemispherical Air-Supported Structures." *Journal of Wind Engineering and Industrial Aerodynamics*, 41, 177-178.

Kawaguchi, M., Chin, Y., Tanaka, A., Baba, T., Hosogaya, T., Oki, H., and Mochizuki, T. (1972). "Engineering Problems of Pneumatic Structures." *Proc., 1971 IASS Symposium Part II on Tension Structures and Space Frames*, Tokyo and Kyoto, 449-460.

Kawamura, S. and Kiuchi, T. (1986a). "An Experimental Study of a One - Membrane Type Pneumatic Structure - Wind Load and Response." *Journal of Wind Engineering and Industrial Aerodynamics*, 23, 127-140.

Kawamura, S. and Kiuchi, T. (1986b). "Wind Design Method of Air Supported Structures." *Shells, Membranes, and Space - Frames, Proceedings from the IASS Symposium*, Osaka, Japan, 233-240.

Kronenburg, R. (1995). "Tensile Architecture." *Architectural Design*, 65, 8-15.

Kronenburg, R. (1996). *Portable Structures*, Architectural Press, Oxford, England.

Kunieda, H. (1975). "Flutter of Hanging Roofs and Curved Membrane Roofs." *Int. J. Solids Structures*, 11, 477-492.

Lukasiewicz, S. and Balas, L. (1988). "Stability and Large Deformation Behavior of Self - Standing Inflatable Membranes." *Proceedings of the International Symposium on Innovative Application of Shells and Spatial Forms*, Bangalore, India, 371-381.

Moran, P. and Robertson, A. P. (1986). "Comparisons of Full-Scale and Wind Tunnel Measurements of Wind Loads on a Free-Standing Canopy Roof Structure." *Journal of Wind Engineering and Industrial Aerodynamics*, 23, 113- 125.

Newman, B. and Goland, D. (1982). "Two-Dimensional Inflated Buildings in a Cross Wind." *Journal of Fluid Mechanics*, 117, 507-530.

Oiger, K. and Parts, A. (1988). "An Analysis of Work and Calculation of Tent Roofs." *Proceedings of the International Symposium on Innovative Application of Shells and Spatial Forms*, Bangalore, India, 611-621.

Reffell, B. (1967). "High Pressure Structures." *Proc., 1st Colloq. on Pneumatic Structures*, Stuttgart, Germany, 64-67.

Rudolf, F. (1967). "A Contribution to the Design of Air-Supported Structures." *Proc.,1st Colloq. on Pneumatic Structures,* Stuttgart, Germany, 128-133.

Shugar, T., Brittan, M., and Hsu, M. (1985). "Nonlinear Structural Analysis of a Large Tensioned Fabric Hangar." *Proc. Structural Engineering Congress '85, Session #12, Design, Fabrication, and Erections of Fabric Structures,* 1-27.

Spinelli, P. (1983). "Dynamic Response Under Wind of a Cylindrical Air Supported Structure." *Journal of Wind Engineering and Industrial Aerodynamics*, 11, 213-224.

Srivastava, N. K., Turkkan, N., and Dickey, R. (1984). "Wind Tunnel Study of a Flexible Membrane Structure." *Proc., 3rd Int. Conf. on Space Structures*, 785-790.

Srivastava, N. K., Turkkan, N., Dickey, R., and Bakarat, D. (1983). "Study of Air Supported Spherical Structures Subjected to an Experimentally Obtained Wind Pressure Distribution." *Proc., Int. Sym. on Shell and Spatial Structures*, Rio de Janeiro, Brazil.

Steeves, E. (1975a). "A Linear Analysis of the Deformation of Pressure Stabilized Beams." *Technical Report 75-47 AMEL*, United States Army, Natick Laboratory, Natick, Massachusetts, U. S. A., January.

Steeves, E. (1975b). "Behavior of Pressure Stabilized Beams Under Load." *Technical Report 75-82 AMEL*, United States Army, Natick Development Center, Natick, Massachusetts, U. S. A., May.

Steeves, E. (1978a). "Structural Behavior of Pressure Stabilized Arches." *Technical Report Natick/TR-78/018*, United States Army, Natick Research & Development Command, Natick, Massachusetts, U. S. A., June.

Steeves, E. (1978b). "Pressure Stabilized Beam Finite Element." *Technical Report Natick/TR-79/002*, United States Army Natick Research & Development Command, Natick, Massachusetts, U. S. A., December.

Steeves, E. (1979). "Optimum Design of Pressure Stabilized Beams." *Technical Report Natick/TR-79/019*, United States Army, Natick Research & Development Command, Natick, Massachusetts, U. S. A., August.

Swami, B., Seetharamulu, K., and Chaudhary, K. (1988). "Wind Pressures on a Shell Roof Model – A Case Study." *Proceedings of the International Symposium on Innovative Application of Shells and Spatial Forms*, Bangalore, India, 845-854.

Sygulski, R. (1996). "Dynamic Stability of Pneumatic Structures in Wind: Theory and Experiment." *Journal of Fluids and Structures*, 10, 945-963.

Sykes, D. (1994). "Windloading Tests on Models of Two Tension Structures for EXPO'92, Seville." *Journal of Wind Engineering and Industrial Aerodynamics*, 52, 371-385.

Uemura, M. (1972). "Membrane Tension and Deformation in Cylindrical Pneumatic Structures Subject to Wind Loads." *Proc., 1971 IASS Symposium Part II on Tension Structures and Space Frames*, Tokyo and Kyoto, 199-210.

Appendix A

Samples of the material that were used for the membranes for the 1:100 and 1:50 scale models were tension tested in the Engineering Science and Mechanics Laboratory to obtain a value for the modulus of elasticity. Three samples, each having a test size of 6 in. long, 1.06 in. wide, and 0.004 in. thick, were tested. The data collection system utilized for the testing recorded the load (lb) and the corresponding displacement (in.) for each data point, as the sample was loaded. Test 1 recorded 815 data points with a peak load of 1.428 lb and a peak displacement of 0.706 in. Test 2 recorded 484 data points with a peak load of 2.132 lb and peak displacement of 4.038 in. Test 3 recorded 289 data points with a peak load of 2.250 lb and a peak displacement of 3.331 in. The load and displacement data were converted to stresses and strains at each data point, and plots of the stress versus strain were created for each test. These plots are shown in Figures A.1, A.2, and A.3. From these three plots, an average value for the modulus of elasticity was calculated to be 3.6 ksi.

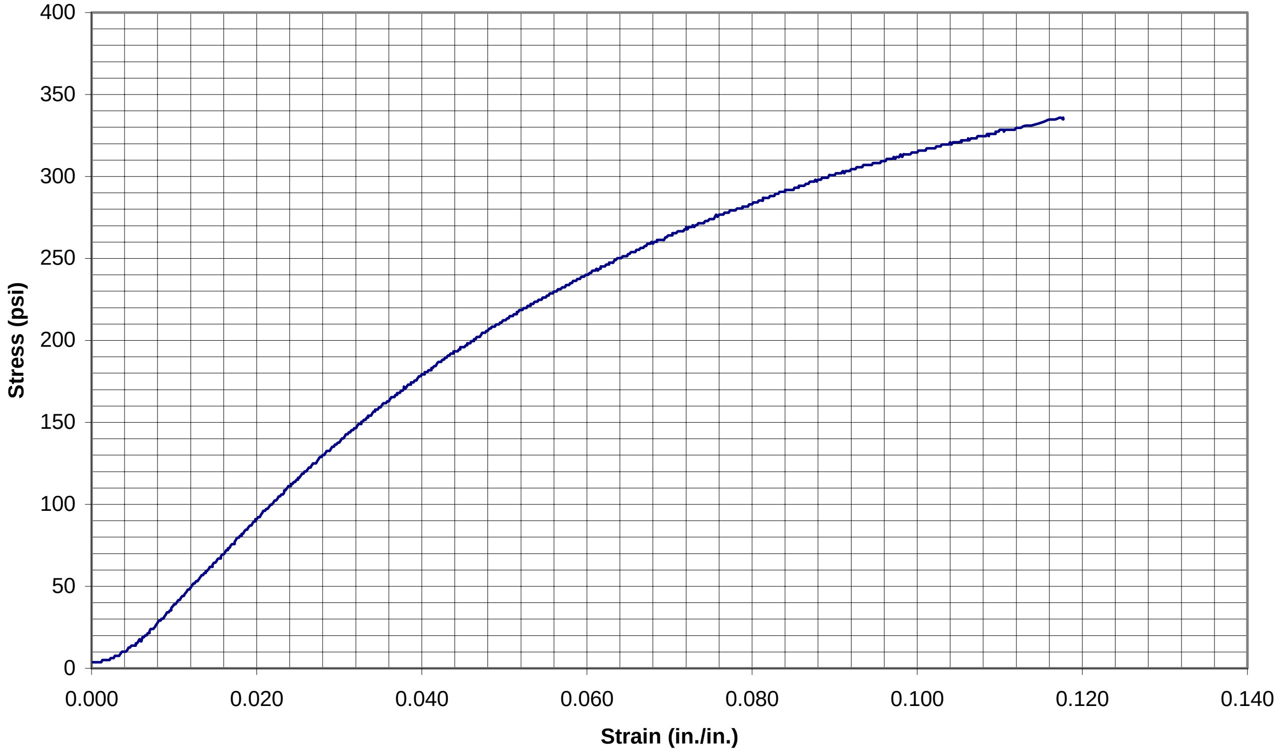

Figure A.1: Stress vs. Strain: Test 1

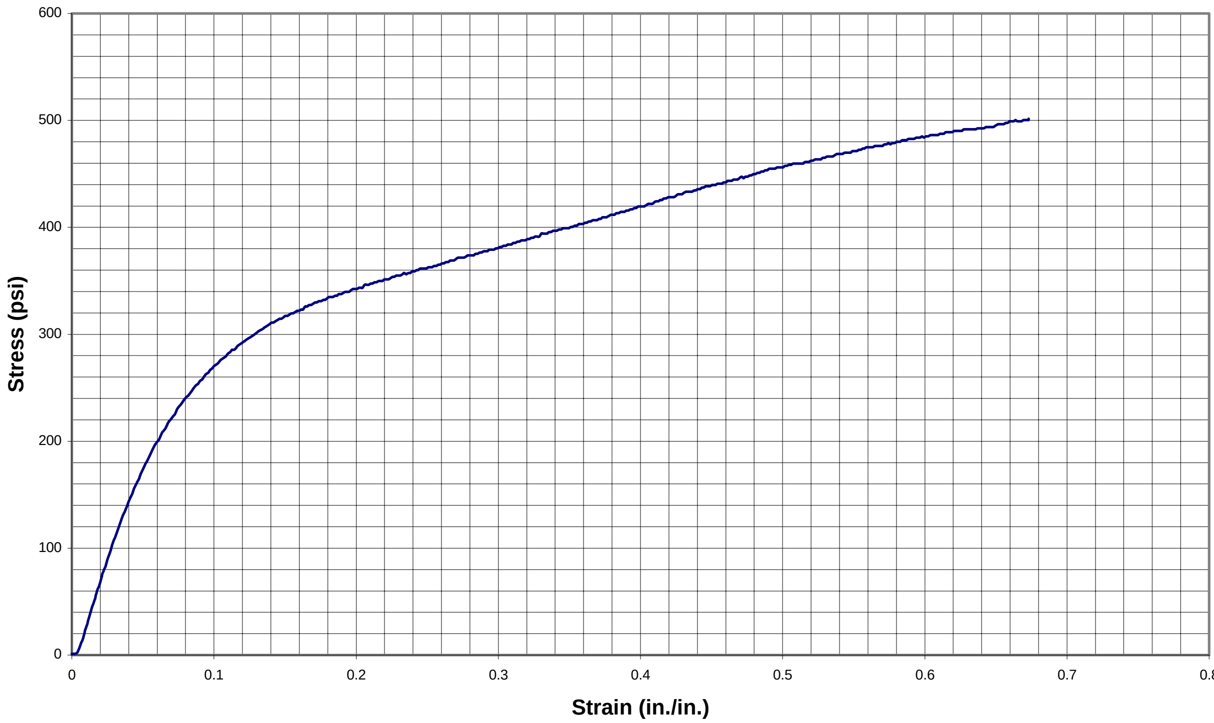

Figure A.2: Stress vs. Strain: Test 2

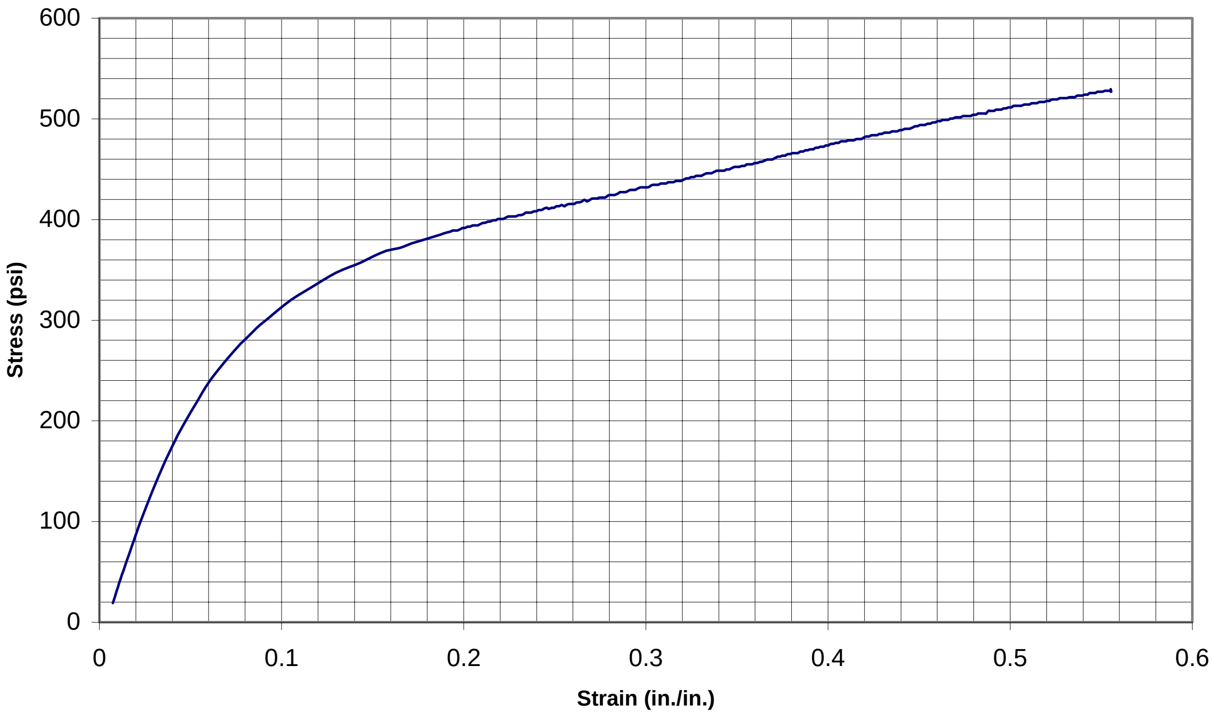

Figure A.3: Stress vs. Strain: Test 3

Vita

David Marc Carradine was born on August 17, 1970 in Washington, D. C. He received his Bachelor of Architecture degree from Virginia Tech in May, 1994. He married his wife, Ann Haruko Carradine, on May 28, 1994. After working as a timber-framer for two years he returned to Virginia Tech in June, 1996, to pursue a Master of Science degree in Civil Engineering, specializing in structures. In August, 1998 the author will begin working towards a Doctorate of Philosophy in Biological Systems Engineering at Virginia Tech, focusing on wood and wood structures.